



U.S. Department
of Transportation
**Federal Railroad
Administration**

Development of Safety Criteria for Evaluating Concrete Tie Track in the Northeast Corridor

Office of Research and
Development
Washington, D.C. 20590

Volume I Remedial Projects Assessment

DOT/FRA/ORD-86/08.1

June 1986
Final Report

This document is available to
the U.S. public through the
National Technical Information
Service, Springfield, Virginia 22161.

NOTICE

The United States Government does not endorse products or manufacturers. Trade or manufacturers' names appear herein solely because they are considered essential to the object of this report.

NOTICE

This document is disseminated under the sponsorship of the Department of Transportation in the interest of information exchange. The United States Government assumes no liability for its contents or use thereof.

Technical Report Documentation Page

1. Report No. ② FRA/ORD-86/08.1	2. Government Accession No.	3. Recipient's Catalog No.	
4. Title and Subtitle DEVELOPMENT OF SAFETY CRITERIA FOR EVALUATING CONCRETE TIE TRACK IN THE NORTHEAST CORRIDOR VOLUME 1. REMEDIAL PROJECTS ASSESSMENT		5. Report Date June 1986	
7. Author(s) Donald R. Ahlbeck, James M. Tuten, Jeffrey A. Hadden and Harold D. Harrison		6. Performing Organization Code	
9. Performing Organization Name and Address Battelle's Columbus Laboratories 505 King Avenue, Columbus, Ohio 43201 * Salient Systems, Inc., Worthington, Ohio 43085		8. Performing Organization Report No.	
12. Sponsoring Agency Name and Address U. S. Department of Transportation Federal Railroad Administration 400 7th Street, S.W., Washington, D.C. 20590		10. Work Unit No. (TRAIS)	
		11. Contract or Grant No. DTFR53-83-C-00009	
		13. Type of Report and Period Covered Final Report April 1983-December 1984	
		14. Sponsoring Agency Code RRS-31	
15. Supplementary Notes			
16. Abstract <p>Minor problems with the performance of some track components have been noted in Northeast Corridor concrete-tie track. Performance-related events have been caused primarily by short-duration impact loads due to wheel tread or rail running surface roughness. To reduce these occurrences, remedial projects were initiated by Amtrak. These included the development of a wheel impact load detector (WILD) to identify specific impact load-producing wheelsets, field tests of more resilient tie pads, use of a different rail clip design, repair of engine burns, etc. This report provides an assessment of these remedial projects.</p> <p>Four test sites were chosen for detailed track walker surveys to define the condition of NEC concrete-tie track. Four surveys on six-month intervals were conducted over each of the sites, a total of 19 miles of track. Component event codes from the surveys were stored in a data management system that allowed analysis of performance issues and correlation with rail anomalies (joints, battered welds, etc.). Little tendency toward clustering of events was found, and the track was generally in excellent condition.</p> <p>The WILD detector system was used both to develop wheel load statistics and to identify passing Amtrak wheelsets developing high impact loads. A wheel truing program was initiated by Amtrak, using the WILD as an inspection tool, that quickly eliminated extreme loads and reduced rough tread conditions. Measured loads and wheel profiles were used to develop and validate a vehicle/track dynamics model. Laboratory and in-track tests were conducted to investigate track component dynamic response to impact loads using a calibrated drop hammer.</p>			
17. Key Words Concrete tie track, wheel/rail impact loads, wheel tread profiles, track dynamic response, track performance		18. Distribution Statement Document available through National Technical Information Service 5285 Port Royal Road Springfield, VA 22161	
19. Security Classif. (of this report) Unclassified	20. Security Classif. (of this page) Unclassified	21. No. of Pages 105	22. Price



Digitized by the Internet Archive
in 2012 with funding from
University of Illinois Urbana-Champaign

<http://archive.org/details/developmentofsaf86081ahlb>

TABLE OF CONTENTS

	<u>Page</u>
PREFACE	viii
1.0 SUMMARY	1
2.0 BACKGROUND	6
3.0 TRACK CONDITION ASSESSMENT	8
3.1 Survey Data Processing	8
3.2 Results of Track Surveys	14
3.3 Summary of Track Condition Assessment	32
4.0 REMEDIAL PROJECTS ASSESSMENT	34
4.1 Wheel Impact Load Detector	34
4.1.1 Dynamic Wheel Load Characterization	34
4.1.2 Description of Detector	35
4.1.3 Detector System Development	42
4.1.4 Applications of the Detector	43
4.2 Passenger Wheel Profile Conditions	46
4.2.1 Experiments on the Northeast Corridor	46
4.2.2 Computer Simulation Development	59
4.2.3 Energy Loss Considerations	66
4.3 Rail Running Surface Profiles	70
4.3.1 Rail Profile Measurements	70
4.3.2 Impact Detector Site Tests	74
5.0 TRACK COMPONENT DYNAMIC PERFORMANCE	86
5.1 Track Structure Performance Experiments	88
5.1.1 Impact Simulation With Drop Hammer	88
5.1.2 Laboratory Simulation of Track Impact Dynamics	91
5.2 Results of Experiments	93
5.2.1 Tie/Tie Pad Performance	96
5.2.2 Rail Fastener Performance	98
5.2.3 Shoulder/Insert Performance	105
5.3 Conclusions	108
REFERENCES	109

LIST OF TABLES

Page

Table 3-1.	Description of Detailed Track Component Survey Test Sites	9
Table 3-2.	Description of Track Component Survey Event Codes.	11
Table 3-3.	Summary of Track Component Performance for Site 1	17
Table 3-4.	Summary of Track Component Performance for Site 2	18
Table 3-5.	Summary of Track Component Performance for Site 3	19
Table 3-6.	Summary of Track Component Performance for Site 5	20
Table 3-7.	Occurrences of Fastener Incidents in Vicinity of Weld or Rail Joint Anomalies--Sites 1, 2 and 3	21
Table 3-8.	Occurrences of Fastener Incidents in Vicinity of Engine Burn Anomalies--Site 1	21
Table 3-9.	Comparison of Fastener Safety Evaluation Criteria Site 1, Survey 1 Trackwalker Results	25
Table 3-10.	Fastener Event Patterns in Test Sites--Fasteners Out on One Side of Rail	26
Table 3-11.	Fastener Event Patterns Within Test Sites--Fasteners Moving or Out on Both Sides of Rail	27
Table 3-12.	Insulator Events (Broken or Missing) in Test Sites--One Side of Rail	28
Table 4-1.	Correlation of Wheel Impact Loads at Edgewood Detector Site With Specific Types of Freight Traffic-- Data From 4-2-84 to 4-30-84, 6-29-84 to 7-6-84.	43
Table 4-2.	Energy Dissipated by Typical Rough Wheel Profiles	69
Table 4-3.	Comparison of Measured and Predicted Peak Vertical Loads Over Edgewood Rail Surface Anomaly	84

LIST OF ILLUSTRATIONS

Figure 3-1.	Examples of Track Survey Component Events.	10
Figure 3-2.	Example of Track Diagram for Track Walker Field Notes.	12
Figure 3-3.	Flow Chart for Detailed Track Survey Data Reduction and Management	13
Figure 3-4.	Example of Track Survey Data Storage Format in Basis Data Management Program.	15

LIST OF ILLUSTRATIONS
(Continued)

	<u>Page</u>
Figure 3-5. Example of Fastener Fault Clustering on Rail Opposite a Rail Joint or Battered Weld	22
Figure 3-6. Example of Fastener Fault Clustering on Same Rail as Battered Engine Burn	23
Figure 3-7. Extensive Track Component Fault Pattern Noted in Survey of Test Site #5	30
Figure 4-1. Example Time Histories of Tie Bending Moments and Vertical Wheel Loads Under Adjacent Trucks of Freight Cars on Concrete Tie Track	36
Figure 4-2. Cumulative Probability Curves of Static and Dynamic Vertical Wheel Loads on Northeast Corridor Concrete Tie Track (All Traffic)	37
Figure 4-3. Examples of Typical Impact Load Detector Circuit Outputs	39
Figure 4-4. Wheel Impact Load Detector Block Diagram	40
Figure 4-5. Three Examples of Wheel Exception Reports	41
Figure 4-6. Effect of Wheel Truing Program on Passenger Wheel Extreme Load Statistics	45
Figure 4-7. Examples of Wheel Vertical Load Statistics: Event Counts in Different Speed and Load Bands in Three Different Ballast Temperature Ranges	47
Figure 4-8. Example of Wheel Vertical Loads Through Impact Detector Site Under Amtrak Test Train	50
Figure 4-9. Comparison of Test Train Wheel Load Statistics With Revenue Freight and Passenger Traffic	52
Figure 4-10. Peak Vertical Wheel Load Measurements Versus Speed for Amcoach Wheels on Impact Test Train	53
Figure 4-11. Peak Vertical Wheel Load Measurements Versus Speed For Heritage Wheelsets on Impact Test Train	54
Figure 4-12. Measured Circumferential Wheel Profiles (Runout) of Amtrak Test Train Wheels	56
Figure 4-13. Peak Vertical Wheel Load Measurements Versus Speed for Heritage Car Wheelset, Axle 22, of Impact Test Train	58
Figure 4-14. Peak Vertical Wheel Load Measurements Versus Speed Under Freshly-Turned Heritable Car Wheels	60
Figure 4-15. Concrete Tie Track Response to Drop-Hammer Impact Load	63
Figure 4-16. Shapes of Concrete Tie Transverse Bending Modes . . .	64

LIST OF ILLUSTRATIONS
(Continued)

	Page
Figure 4-17. Comparison of Wheel Impact Load Simulation With and Without Concrete Tie Bending Modes	65
Figure 4-18. Comparison of Predicted and Measured Load Tie-Histories for Heritage Car Wheel Tread Anomaly	67
Figure 4-19. Comparison of Predicted and Measured Peak Loads for Axle 19 of Impact Test Train Over Speed Range	68
Figure 4-20. Rail Longitudinal Running-Surface Profilometer	71
Figure 4-21. Measured` Rail Running-Surface Profile Near Engine Burn, M.P. 67.00, Site 1, Section 1, Tie 72, E. Rail	73
Figure 4-22. Measured Rail Running-Surface Profile Near Engine Burn, M.P. 67, Site 1, Section 4, Tie 8, W. Rail	75
Figure 4-23. Measured Rail Running-Surface Profile Near Engine Burn, M.P. 66, Site 1, Section 1, Ties 121/122, W. Rail	76
Figure 4-24. Predicted Dynamic Vertical Wheel Load at Battered Engine Burn Under High-Speed Passenger Car	77
Figure 4-25. Measured Rail Running-Surface Profile at Engine Burn, Edgewood Impact Detector Circuit #3	79
Figure 4-26. Example of Loads From Impact Detector Site Under High-Speed Passenger Train	80
Figure 4-27. Comparison of Vertical Loads Over Smooth Track (Circuit #1) and Engine Burn (Circuit #2)--Amcoach Axle #11, Newly-Turned Wheel Profiles	81
Figure 4-28. Comparison of Vertical Loads Over Smooth Track (Circuit #1) and Engine Burn (Circuit #3)--Heritage Car Axle #17, Newly-Turned Wheels	82
Figure 4-29. Predicted Vertical Wheel Loads for Simulated High-Speed Passenger Car Over Measured Rail Surface Anomaly at Edgewood Impact Detector Circuit #3	83
Figure 5-1. Relationships of Impact Loads Within the Vehicle and Track Structures	87
Figure 5-2. Sketch of Automated Drop Hammer.	89
Figure 5-3. Comparison of Impact Load Time-Histories for Passenger Car Wheel and Drop Hammer.	90
Figure 5-4. Influence of Wheel Vertical Preload on Rail-Seat Tie Bending Strain	92
Figure 5-5. Comparison of Tie Dynamic Bending Response Beneath Rail Seat, Nec Versus 5-Tie Track.	94
Figure 5-6. Influence of Hammer Drop Height on Peak Tie Bending Moment Under Rail Seat for Different Test Conditions .	95

LIST OF ILLUSTRATIONS
(Continued)

	<u>Page</u>
Figure 5-7. Typical Flexural Cracks Found in Concrete Ties	97
Figure 5-8. Attenuation of Tie Bending Response to Impact Loading With Resilient Rail-Seat Tie Pad	99
Figure 5-9. Tie Bending Response to In-Track Drop Tests With Stiff EVA Pads and Resilient (DAYCO) Tie Pads	100
Figure 5-10. Ground Rod Vertical Acceleration Response to In-Track Drop Tests With Stiff EVA Tie Pads and Resilient (DAYCO) Tie Pads	101
Figure 5-11. Comparison of Clip (Toe) Vertical Displacements With Stiff EVA and Resilient Tie Pads	103
Figure 5-12. Comparison of Clip Longitudinal Displacement at Center Leg for Two Clip Designs	103
Figure 5-13. Comparison of Insert and Tie (Shoulder) Vertical Accelerations From In-Track Drop Hammer Tests (Stiff EVA Pads)	107

PREFACE

This report is a summary of work performed under Contract No. DTFR53-83-C-00009 by Battelle's Columbus Laboratories (BCL), and was sponsored by the U.S. Department of Transportation, Federal Railroad Administration. The program manager for this study was Mr. Howard G. Moody of the Federal Railroad Administration, Office of Research and Development.

The program entitled "Development of Safety Criteria for Evaluation Concrete Tie Track in the Northeast Corridor" had as its basic objective the determination of the "safe capacity" of the track. "Safe capacity" is defined as the ability of the fastener system to retain the rail longitudinally and laterally, to prevent rail or track panel buckling and to maintain track gauge, and the ability of the ties to maintain track gauge and cross level within the limits of track geometry standards. Two aspects of this objective are addressed in the program:

- Safe capacity with rail clip fasteners missing or in a weakened condition,
- Safe capacity with damaged or weakened concrete ties.

An additional program objective was to determine the failure modes of concrete ties and the causes of clip fallout and insert failures.

This program consisted of five tasks: (1) Track load/deflection characterization study and track condition assessment, (2) Remedial projects assessment, (3) Clip performance, (4) Tie integrity, and (5) Track strength characterization. This report provides a comprehensive evaluation of Amtrak's remedial programs, primarily the work conducted under the first three tasks of this study.

Substantial support was provided by the National Railroad Passenger Corporation (Amtrak) during the test phases of the study on the Northeast Corridor track and during the development of the wheel impact load detector system. Technical liaison was provided by Messrs. Dennis Wilcox and Dan Jerman on behalf of Mr. D. F. Sullivan of Amtrak. Mr. Bud Coffey of De Leuw, Cather/Parsons carefully inspected almost 50,000 ties (200,000 fasteners) four

times over the period of the program to provide the track walker survey data for this study. Technical support for the tests conducted by the Association of American Railroads Transportation Test Center (AAR/TTC) at Pueblo, Colorado was provided by Messrs. G. W. Walker, Larry Daniels, Dave Read and others. Coordination with the NECIP was provided by Mr. Ted Ferragut of the FRA Office of Passenger and Freight Services.

Battelle's research program was managed by Mr. Harold D. Harrison, who shared in the development of the wheel impact load detector with Mr. James M. Tuten, Principal Research Scientist at BCL. Field and laboratory tests were conducted by James Tuten and Jeffrey Hadden, while computer simulation studies were conducted by Donald Ahlbeck. Technical assistance was provided by Ken Schueller, Gary Conkel, Chris Corogin and Mark Miller of BCL.

1.0 SUMMARY

An important part of the Northeast Corridor Improvement Project was the installation of more than 400 track-miles of concrete tie track. Since installation, minor problems with track components have been discovered. These problems have included clip fallout, loose inserts, broken insulators and cracked ties.

A cooperative investigation was conducted by Amtrak and DOT/FRA, contracting with Battelle's Columbus Laboratories. The primary cause of tie cracking was determined to be high vertical impact loads caused by a few rough wheel profiles on high-speed passenger cars. To improve track performance, remedial projects were initiated by Amtrak. These included the development of a wayside wheel impact load detector to identify specific impact-producing wheelsets. In addition, field tests of more resilient tie pads and a different rail clip design were begun. Research conducted under the program entitled "Development of Safety Criteria for Evaluating Concrete Tie Track in the Northeast Corridor" included an assessment of these remedial projects.

At the start of this program, four test sites were chosen for detailed track walker surveys at six-month intervals to determine the extent of component problems. Data from the surveys were analyzed, using an interactive computer data management program. Correlations of component performance with rail surface anomalies (rail joints, engine burns, battered welds), as well as correlations of one performance issue with another, were examined. In particular, the clustering of events (clip fallout, etc.) that could weaken the track was analyzed in detail.

Results from the track walker surveys showed that only a very small percentage of components exhibited degraded performance. Track in the four representative test sites was in generally excellent condition. Correlation of clip movement and fallout with rail surface roughness was strongest in the test site with older relay rail, where 32 percent of these events occurred within five ties of a rail anomaly. In the other test sites, less than 11 percent of the clip events occurred within five ties of an anomaly. This

confirmed the belief that vibration induced by wheel (as well as rail) roughness must be an important factor in the clip fallout mechanism. Clustering of clip fallout, insert or insulator events did not appear to be a significant problem. Only one location in the rougher-rail site had four clips missing in a row on one side of the rail, and three locations had three clips missing in a row.

Very few insert failures were noted in the survey data. Because of the particular NEC fastener design, the rail is still supported laterally by the insert when clips and insulators are missing. Even a loosened insert (loss of bond) will provide some lateral restraint. Increasing numbers of temporary mechanical rail joints were noted over the course of the study. This may induce greater numbers of insert failures and clip movement. Rewelding the rail at these locations is recommended to reduce the number of running surface anomalies producing impact loads on the rail.

Under separate contract with Amtrak, a wayside wheel impact load detector (WILD) system was designed, fabricated and installed by Battelle on the Northeast Corridor near Edgewood, MD. The detector measures four short samples of vertical loads under passing wheels, using strain gage patterns installed on the rail web. A microcomputer system calculates the peak load in each sample for each passing wheel. A brief load exception report, citing specific wheelsets exceeding preset load limits, is prepared by the computer and transmitted to one or more remote terminal printers. These reports include time and date, train speed and direction. The detector responds by commercial telephone line to specific commands to provide optional reports, which include the matrix of all loads (each wheel, each measurement site) for the last train by the detector, and accumulated wheel load statistics as axle counts in speed and peak-load bands.

Amtrak first used the WILD system to identify specific wheelsets causing high impact loads. Several of these wheelsets were removed from revenue service and assembled into a test train, which also included a few freshly-turned wheelsets as a control. Tests were then performed over a range of speeds from 25 to 110 mph, and load data were recorded from the detector

transducers. Wheelsets were then removed, and circumferential profiles were measured in the Amtrak wheel shop. Wheel treads were examined for damage corresponding to the load-producing profile errors, and in some cases these wheels would pass visual inspection without condemning-limit exceptions, other than minor tread spalling. Some wheelsets showed evidence of incipient bearing failure, such as loss of grease.

Test results were used to define the impact load versus speed relationships for the different profile errors. In general, peak load increased with speed, tending to level off at 80 to 90 mph; but high loads were recorded at lower speeds, so that a slow-order to control the loads due to these wheelsets would not be practical. Measured load time-histories and wheel profiles were used to develop and validate a vehicle/track simulation model for predicting loads and dynamic vehicle/track response under different conditions.

A wheel truing program was initiated in early 1984 by Amtrak with the installation of a new truing machine in the Ivy City yard. Using the WILD as a maintenance tool, specific wheelsets producing impact loads greater than 60,000 lb were identified and pulled from service. The effect of this program was soon evident in the four-week average of extreme-load statistics collected by the WILD. The percent of total events (load measurements for passing passenger wheelsets) exceeding 60,000 lb fell from 0.14 at the end of February to 0.04 by the end of May. This result was attained by shopping the wheels on 38 cars (about 7 percent of the fleet); and the current statistical level represents about a dozen wheelsets in the car fleet passing the WILD site. With the success of this program, Amtrak has lowered its exception load limit to 55,000 lb. Freight traffic, in the meantime, has remained at a nearly-constant level of 0.14 percent exceeding 60,000 lb. This represents an estimated 1.5 to 2 percent of the passing wheelsets. An estimated 0.5 percent of passing wheelsets generate loads exceeding 75,000 lb, the cracking threshold of the concrete ties. At current traffic levels, roughly 100 wheelsets a week passing the WILD site can initiate a crack.

Profiles of rail running surface anomalies (particularly engine burns) were measured on the Northeast Corridor, using a specially-designed profilometer to simulate a 36-inch diameter Amcoach wheel. These profiles were then used with the vehicle/track dynamics model to predict impact loads. Some of the engine burn profiles were found to resemble battered low joints, with a depth of up to 0.09 inch over a 5-foot wavelength. Peak loads on these profiles tended to increase with train speed, while loads over smaller engine burns tended to be independent of speed.

In-track and laboratory tests were conducted with an instrumented drop hammer to define the dynamic response mechanism involved in track component failures. The transverse vibrational bending modes of concrete ties, particularly the second and third modes at about 330 and 630 Hz, respectively, were found to be important in the tie cracking phenomenon. Because of the phase relationship of response peaks of these two modes at the rail seat, cracks could be initiated at either the top or bottom surfaces of the tie. In addition, the tie end opposite the impact load (opposite a rail joint, for example) could experience higher bending stresses near the rail seat than at the impacted end. The resilient tie pads recommended from laboratory studies [3] act as a low-pass mechanical filter, attenuating the impact load energy into the tie exciting these higher-frequency vibration modes. These resilient pads therefore reduce the probability of crack initiation under high impact loading.

Rail clip movement leading to fallout was not observed either in the field measurements or laboratory tests. However, the current 601A clip exhibited lightly-damped oscillations in the longitudinal direction (along the rail) at about 1000 Hz (a frequency close to the tie fourth bending mode) in response to impact loads. The "e" clip did not show this oscillatory behavior, and to date there have been few (if any) fallout occurrences reported with those "e" clips installed on the NEC. Since the 601A clip is sensitive, particularly, to tie vibrations, the same fallout phenomena would not be expected to occur on more highly damped wood ties. Measurements of 601A clip vertical deflections with stiff EVA pads and the resilient Dayco pads showed about the same peak-to-peak deflection under impact load. In the

clip-spreading (rebound) direction, however, smaller deflections were measured with the resilient pads. This implies lower clip peak stresses, rather than higher, with the resilient pads. Similar trends, but with somewhat smaller deflections were noted with the "e" clip.

Tests were performed to explore the insert bond-failure occurrences observed in the NEC track. A total of about 43,000 hammer drops were made on the laboratory track panel, ranging from 52 to 124 percent of the tie cracking threshold, but insert bond failure was not induced. Tests on individual inserts showed that strong compression-wave oscillations in the longitudinal direction (vertical to the tie) can be set up in the 4 to 8 kHz range in response to impact loading. This may cause a microscopic pulverizing action at the insert/tie interface, eventually resulting in loss of bond. Resilient tie pads are expected to reduce this compression-wave response by reducing tie vibration levels.

2.0 BACKGROUND

A significant part of the Northeast Corridor Improvement Project (NECIP) was the extensive use of concrete tie track. Concrete ties with resilient rail clips, stiff pads and insulators were first installed in 1978, primarily in the Boston Division. This section of the corridor has very little freight traffic. Eight miles of concrete ties were installed during December 1978 in Track 4 near Aberdeen, Maryland, an area of relatively heavy freight traffic. Larger scale installations were begun during 1979 in other parts of the southern section of the corridor, also subjected to heavy freight traffic.

In June 1980, rail seat flexural cracks from one to six inches in length were discovered during an inspection of concrete ties in Track 4 near Aberdeen, MD. These were generally "hairline" cracks, cracks that required a careful examination of the tie face in the crib to find. The cracks were considered important as a sign of a mechanism that could eventually lead to tie failure in bending at the rail seat.

An investigation, sponsored by the Federal Railroad Administration (FRA) and Amtrak, was conducted by Battelle's Columbus Laboratories to identify the cause of the tie crack development and to recommend corrective action to minimize further damage to the track. An analysis of measured vertical wheel loads and tie bending moments from the Northeast Corridor track identified short-duration impact loads from a small percentage of high-speed passenger train wheels as the probable cause of the cracks [1,2]. A preliminary examination of these wheels showed a long-wavelength tread irregularity as well as spalled wheel treads to be the source of high impact loads.

Cracked ties were removed from the track and tested for strength using the Amtrak specification as a standard. In general, ties with cracks less than five inches in length showed no loss of static strength and no failure in five million cycles of repeated load. Ties with cracks longer than five inches, although showing some loss in strength, were apparently still functioning adequately in the track. These ties may have reduced life.

Other types of tie cracks have also occurred at some locations in the Northeast corridor. Flexural cracks at the tie center and cracks at the insert may also be linked to the impact load events that cause rail seat flexural cracks. Longitudinal and torsional cracks, as well as some insert damage, may be caused by derailments or maintenance equipment, both during construction and normal maintenance. These types of cracks have resulted in several ties being removed from the track.

In addition to tie cracking, rail clip fallouts were noted in many locations on the corridor. These fallout locations were at first associated with a rail joint, engine burn or other anomaly on the rail running surface. However, a more random occurrence of clip fallouts was noted that could not be characterized by an obvious rail surface anomaly. In a few instances, the cast iron insert had become loose, with a loss of bond between the insert stem and the tie. The clips could no longer restrain the rail in these cases, and the insert shoulder usually does not provide lateral restraint of the rail when in this loosened condition.

Two corrective measures were proposed. The first was to install a more resilient tie pad to attenuate the peak loads between rail and tie. The second was to identify and remove those wheels causing the large loads. Laboratory and field experiments were conducted to study the effects of tie pad stiffness on reducing the impact loading at the tie [3,4]. A fully-automatic wheel impact load detector was designed for Amtrak [5], and was installed on one high-speed track near Edgewood, MD. This detector has been used both as a research tool to develop wheel load statistics under different types of traffic, and by Amtrak as an inspection tool to screen passing wheelsets for profile roughness producing high impact loads.

3.0 TRACK CONDITION ASSESSMENT

To establish a statistically valid basis for track condition assessment, detailed surveys of fastener and tie conditions were conducted within test zones on the Northeast Corridor concrete tie track. As a result of an Amtrak/FRA inspection in April 1982, five test sites of four to six miles in length were chosen. Four detailed surveys at approximately six-month intervals were eventually made on four of the five sites. (The fifth site was dropped for lack of events and traffic.) Descriptions of the four sites, each containing between 10,475 and 15,450 ties, are given in Table 3-1.

3.1 Survey Data Processing

Detailed surveys were conducted by Mr. Bud Coffey of De Leuw, Cather/Parsons, under contract to FRA, who entered specific fastener and tie conditions by an established code on prepared track diagrams. Some of the specific conditions entered in the track walker data base are sketched in Figure 3-1. Survey event codes are given in Table 3-2. Updated track diagrams were prepared by Battelle prior to each survey and bound in looseleaf report form to facilitate data entry under field conditions. An example track diagram is shown in Figure 3-2. In this diagram, a plain code (see Table 3-2) denoted a new activity, code preceded by an asterisk (*) denoted a repeat activity, and code preceded by a dollar sign (\$) denoted previous activity (a clip once out, but reinstalled, for example). Codes were entered in one of the seven appropriate locations on a given tie, as shown in the sketch in Table 3-2.

Field data from the four surveys were processed at Battelle by the data reduction and management system shown in Figure 3-3. The field data were first entered on a Hewlett Packard HP9845 desktop computer with a user-friendly program that provided prompts of required inputs and instant display of entered data before storage on disk. Data for each site for a given survey were then transferred to a VAX 11-780 mainframe computer and stored. Here a program used the stored data to generate updated track diagrams (see Figure 3-2) on a line printer. Reduced-size copies of these diagrams were then used for subsequent survey field notes.

TABLE 3-1. DESCRIPTION OF DETAILED TRACK COMPONENT SURVEY TEST SITES

Test Site 1 - Bush to Aberdeen, Track 2, MP 69-64 (northbound).
Curves - MP 66.5 to 66.1, $0^{\circ}32'$ LH; MP 65.3 to 64.6, $1^{\circ}00'$ RH.
Installed July 1980, about 5.4 MGT/yr. older relay rail.

Test Site 2 - Davis to Northeast Track 4 (renumbered Track 3, June 1983), MP 44-48 (southbound). Curves - MP 46.8 to 47.3, $1^{\circ}00'$ RH; MP 44.0 to 44.7, $0^{\circ}14'$ RH. Installed August - September 1980, about 7.5 MGT/yr.

Test Site 3 - Davis to Northeast, Track 3, MP 44 - 48 (southbound). Curves - (same as Site 2). Installed August - September 1980, about 16 MGT/yr. Renumbered Track 2, June 1983, switched direction to primarily northbound passenger, about 8 MGT/yr.

Test Site 5 - Grundy to Morris, Track 2, MP 65 - 59 (northbound). Installed April 1982, about 3.4 MGT/yr (primarily passenger). New softer (Trelleborg) pads. Curves - MP 64.7 to 64.3, $0^{\circ}43'$ LH; MP 62.0 to 61.3, $0^{\circ}45'$ RH; MP 60.6 to 60.3, $0^{\circ}25'$ RH.

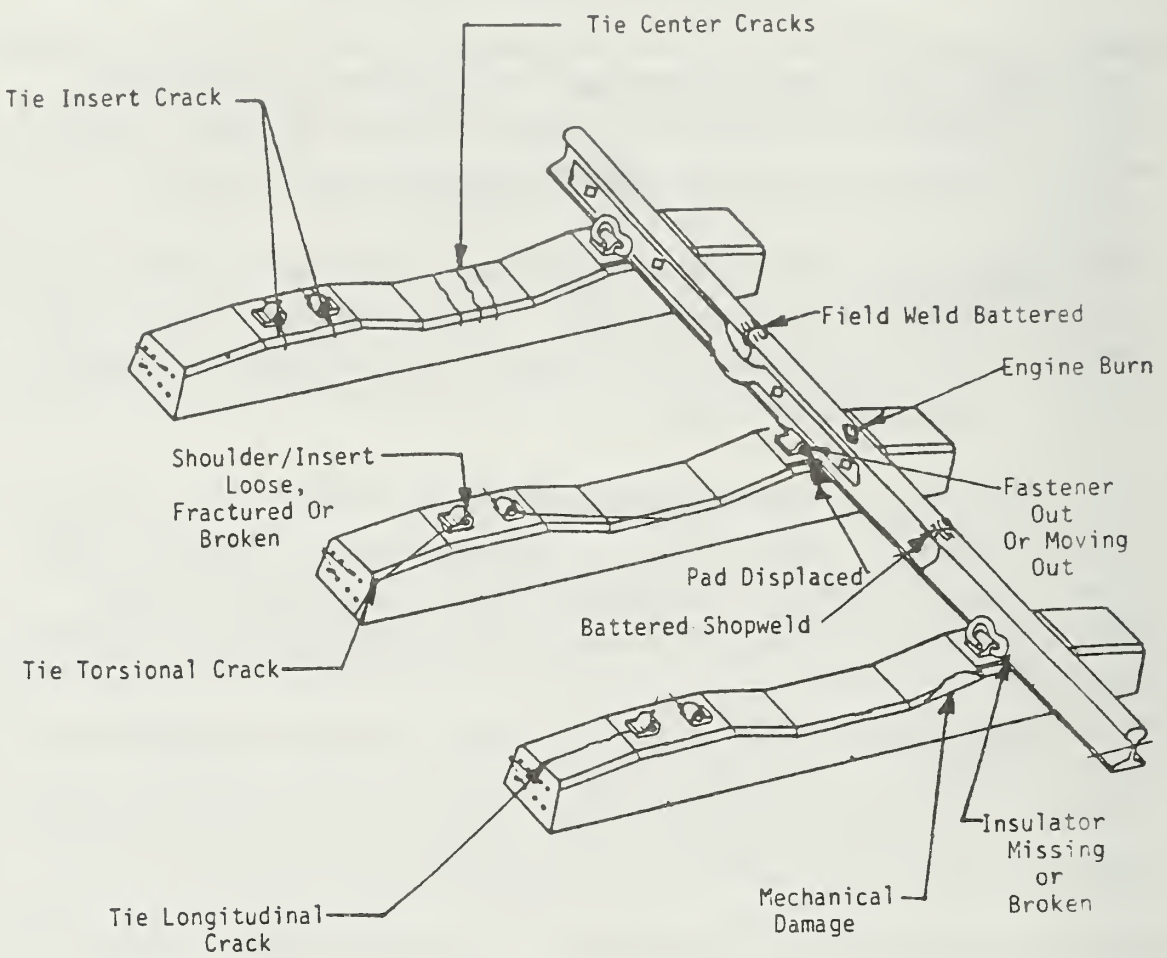


FIGURE 3-1. EXAMPLES OF TRACK SURVEY COMPONENT EVENTS

TABLE 3-2. DESCRIPTION OF TRACK COMPONENT SURVEY EVENT CODES

<u>Code</u>	<u>Description</u>
CT1	Concrete tie center crack
CT2	Concrete tie insert crack
CT3	Concrete tie longitudinal crack
CT4	Concrete tie torsional crack
DT	Damaged tie
EB	Engine burn
EBB	Engine burn, break (in rail)
FI	Fastener improperly installed
FM	Fastener moving ($>\frac{1}{2}$ " inside insert)
FN	Fastener, new
FO	Fastener out
FW	Field weld
FWB	Field weld, battered
FWC	Field weld, crowned
GC	Grade crossing (removed)
IB	Insulator broken
II	Insulator improperly installed
IL	Insulator loose
IM	Insulator missing
IN	Insulator, new
J	Joint
J .	Joint with depth measured
JI	Joint, insulated
JIB	Joint, insulated, battered
JIC	Joint, insulated, crowned
JM	Joint, mechanical
JT	Joint, temporary
PB	Pad, broken
PD	Pad, displaced
PM	Pad missing
S	Skewed tie
SF	Shoulder/insert fractured or broken
SL	Shoulder/insert loose
SM	Shoulder/insert missing
T	Transition, wood to concrete ties
TB	Transition, beginning
TE	Transition, end
LOC	Location

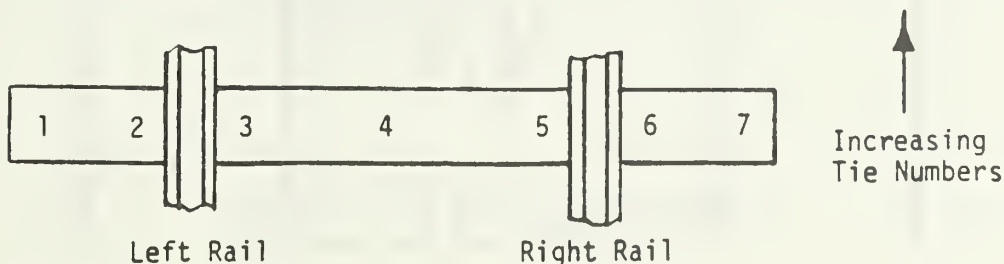
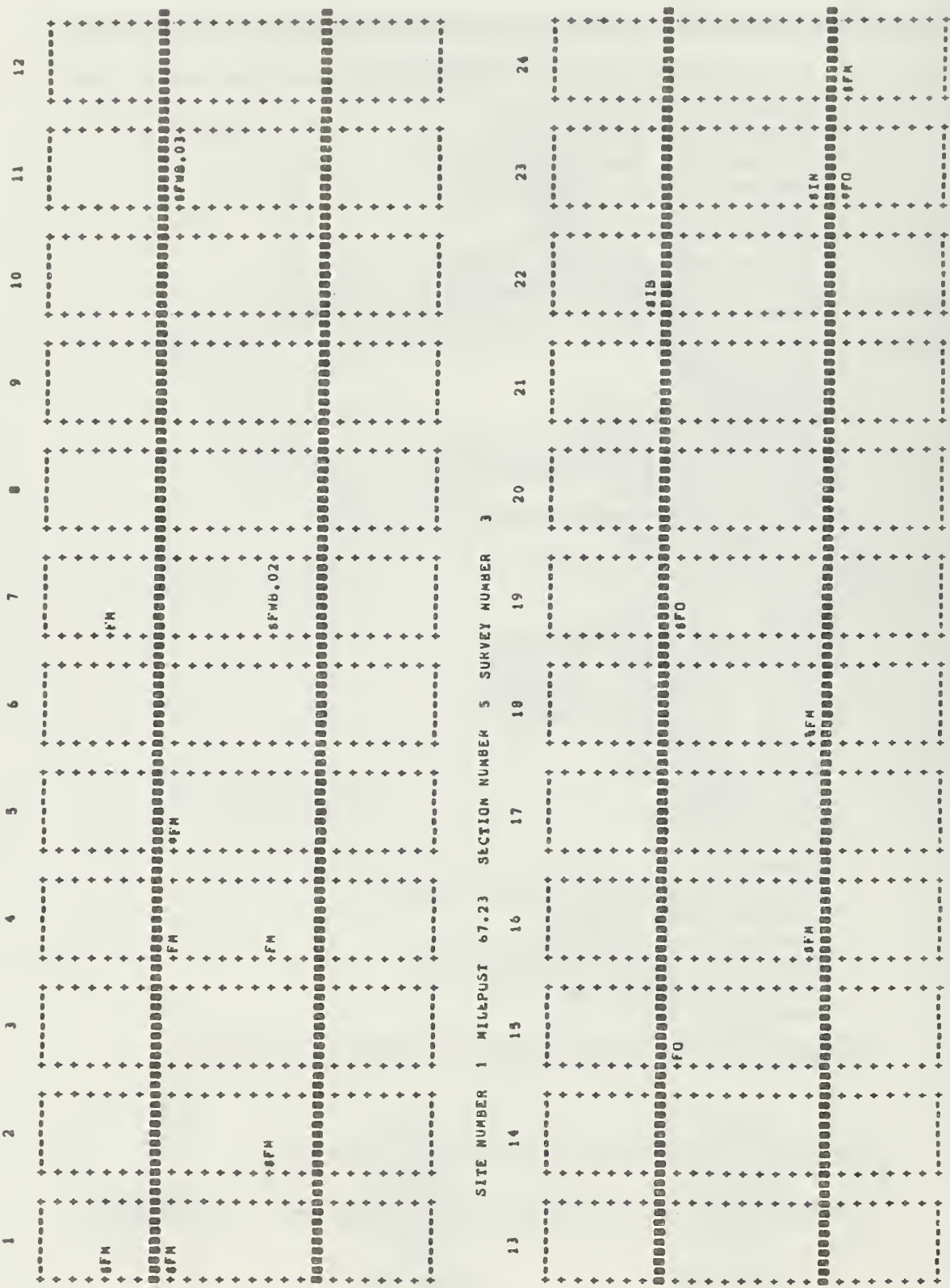


FIGURE 3-2. EXAMPLE OF TRACK DIAGRAM FOR TRACK WALKER FIELD NOTES



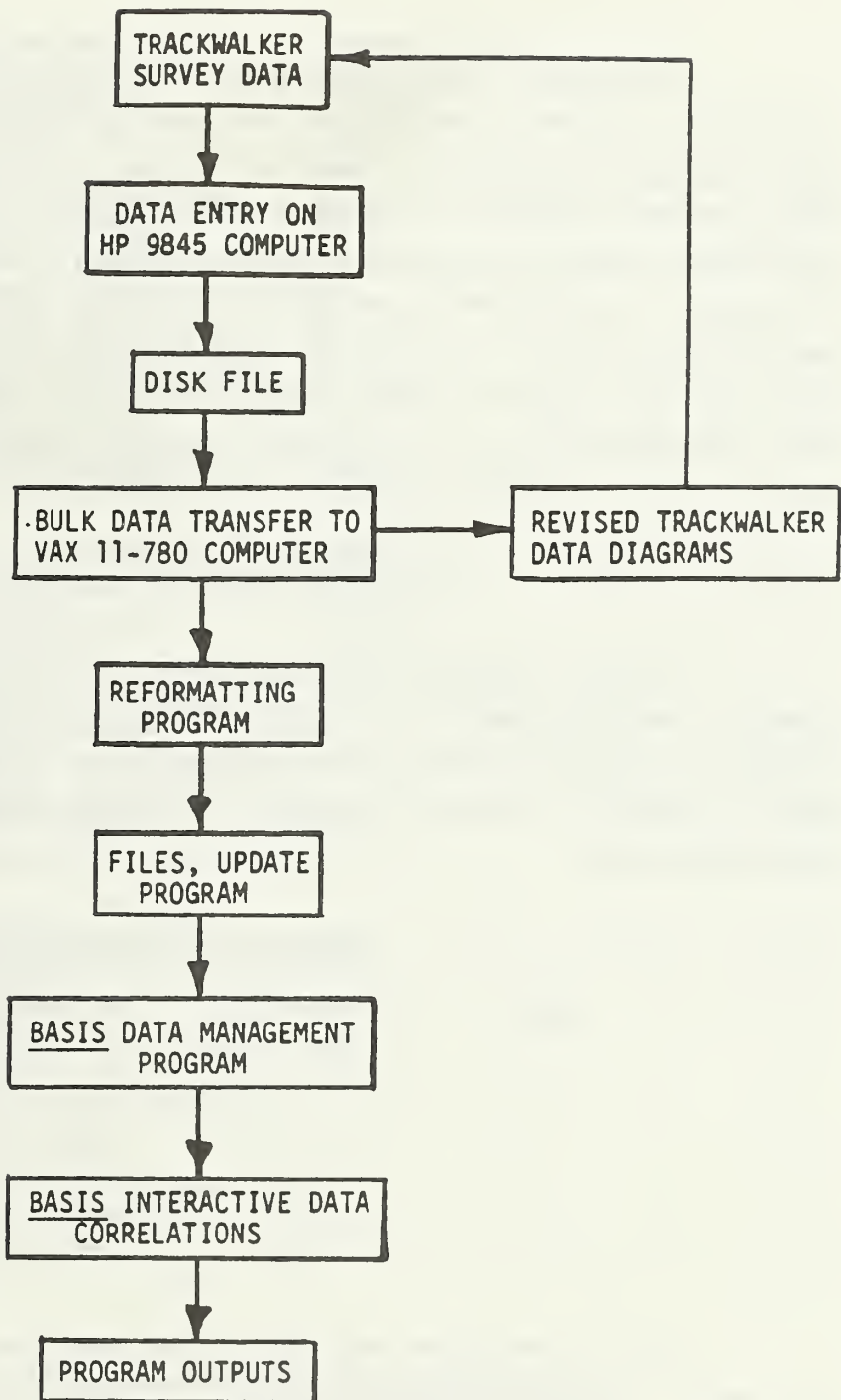


FIGURE 3-3. FLOW CHART FOR DETAILED TRACK SURVEY DATA REDUCTION AND MANAGEMENT

Data stored in the VAX computer were then processed by reformatting and update programs, transferring the data to Battelle's Data Management System, BASIS, which employs a powerful but easy-to-learn query language. The BASIS data base consists of random symbolic keyed files that interrelate via the software system to provide efficient retrieval, manipulation and analysis of the data. Correlation of variables can be performed rapidly with BASIS so that hypotheses on the interrelationships of causes and effects can be tested. An example of the data storage format in BASIS is shown in Figure 3-4 for three successive ties. Each tie has a unique sequence number by which its data are stored in BASIS, as well as a tie number within the site and section.

3.2 Results of Track Surveys

The rail running-surface anomalies within the four test sites consisted of insulated joints (13 or 14 each site), temporary mechanical joints replacing bad welds or flaws, welds (battered or crowned), and engine burns. Over the course of the four surveys, increasing numbers of temporary rail joints were noted:

<u>Temporary Mechanical Joints</u>		
<u>Site</u>	<u>Survey #1</u>	<u>Survey #4</u>
1	2	18
2	2	13
3	2	8
5	8	30

The four test sites had roughly the same number of crowned welds, 40 to 64 each. Site 1, with older relay rail dated 1962, had by far the most engine burns (55) and battered welds (106). Site 5, by contrast, had the next highest number of engine burns (4) and battered welds (75) on rail dating from 1977 to 1981. Smaller numbers of battered welds were found in Site 2 (25) and Site 3 (36), both predominately with newer rail.

0. TIE SEQUENCE NR	9444
2. SITE NR	1
3. MILEPOST NR	67.57
4. SECTION NR	11
5. TIE NR	33
12. DEFECT LOCATION-1	2
13. DEFECT CODE-1	F0
14. SURVEY NR-1	1
16. DEFECT LOCATION-2	3
17. DEFECT CODE-2	F0
18. SURVEY NR-2	1
20. DEFECT LOCATION-3	3
21. DEFECT CODE-3	EB
22. SURVEY NR-3	1
23. DEFECT QUANTITY-3	.050

0. TIE SEQUENCE NR	9445
2. SITE NR	1
3. MILEPOST NR	67.57
4. SECTION NR	11
5. TIE NR	34
12. DEFECT LOCATION-1	2
13. DEFECT CODE-1	F0
14. SURVEY NR-1	1
16. DEFECT LOCATION-2	3
17. DEFECT CODE-2	F0
18. SURVEY NR-2	1

0. TIE SEQUENCE NR	9446
2. SITE NR	1
3. MILEPOST NR	67.57
4. SECTION NR	11
5. TIE NR	35
12. DEFECT LOCATION-1	2
13. DEFECT CODE-1	F0
14. SURVEY NR-1	1
16. DEFECT LOCATION-2	2
17. DEFECT CODE-2	FM
18. SURVEY NR-2	3

FIGURE 3-4. EXAMPLE OF TRACK SURVEY DATA STORAGE
FORMAT IN BASIS DATA MANAGEMENT PROGRAM

Clip, insulator, pad and tie performance over the four surveys is summarized in Tables 3-3 through 3-6. These tables reflect the revised estimates of cumulative tonnage over the test sites which are noted in Table 3-1. In these tables, clip and insulator event numbers represent new occurrences, where maintenance (QC) has been performed between surveys in Sites 1, 2 and 3 to replace clips and broken insulators. Only a partial maintenance was performed within Site 5, between Surveys 2 and 3, so that some cumulative effect is included. Pad, shoulder/insert and tie faults are cumulative in number, since these were not corrected in maintenance.

The BASIS data management system was used to explore some of the characteristics of track component faults, particularly clustering of events and correlations between rail surface anomalies (welds, joints, etc.) and component faults, or between one type of fault and another. Examples of this are given in Tables 3-7 and 3-8, where the numbers of fastener events (fasteners moving or out) associated with specific rail surface anomalies are shown. In the case of welds and joints, which occur predominantly on one rail only, not in pairs, there are significantly more fastener events on the opposite rail within \pm 1 tie of the impact load. An example of this is shown in Figure 3-5, where fasteners are moving on three ties beyond the joint on the opposite rail. This effect is gradually lost 3 to 5 ties away from the rail joint or battered weld. In the case of engine burns, which occur more often in pairs opposite one another, roughly the same number of fastener events were found on the same rail as on the opposite rail within \pm 1 tie. The example in Figure 3-6 shows, in fact, all the fastener action on the same rail as the engine burn. Note that a depth of 0.050 inch indicates some service bending of the rail and subsidence under impact loading at this point.

Site 1 (with older 1962 relay rail) showed 32 percent of the fastener events occurring within \pm 5 ties of a rail running-surface anomaly. The other test sites, however, showed less than 11 percent of the fastener events occurring within \pm 5 ties of an anomaly. This indicates that clip movement and fallout is as much a function of track (particularly tie) vibrations due to passing rough wheels as it is a function of rail running surface roughness.

TABLE 3-3. SUMMARY OF TRACK COMPONENT PERFORMANCE FOR SITE 1

Survey	Total Tonnage (MGT)*	(a) Clip Performance*				% Per MGT	% Per MGT
		Clips Out	%	Per MGT	Clips Moving		
1	10.8	351	0.67	--	287	0.55	--
2	13.1	337	0.65	0.29	1213	2.33	1.01
3	16.7	206	0.40	0.11	1306	2.51	0.70
4	20.3	401	0.77	0.21	1759	3.38	0.97
(b) Insulator# and Pad Performance Pads							
Survey	Total Tonnage (MGT)	Insulators Broken or Missing	%	% Per MGT	Displaced, Broken or Missing	%	Insulators Installed Incorrectly
1	10.8	238	0.46	--	5	0.02	163
2	13.1	235	0.45	0.20	5	0.03	0.001
3	16.7	92	0.18	0.05	12	0.05	0.003
4	20.3	1	< 0.01	< 0.01	14	0.05	0.003
(c) Tie Performance							
Survey	Total Tonnage (MGT)	Shoulder/ Insert Loose, Broken or Missing	%	% Per MGT	Cracked Ties	Damaged Ties	Skewed Ties
1	10.8	7	0.013	0.0012	9	6	0
2	13.1	29	0.056	0.0042	11	6	17
3	16.7	52	0.100	0.0060	15	6	26
4	20.3	78	0.150	0.0074	15	6	39

Total of 13,025 ties in site

* Estimated cumulative since track installed.

Maintenance (QC) performed between surveys.

TABLE 3-4. SUMMARY OF TRACK COMPONENT PERFORMANCE FOR SITE 2

Survey	Total Tonnage (MGT)*	(a) Clip Performance [#]				Clips Moving	%	% Per MGT
		Clips Out	%	Per MGT				
1	14.1	26	0.06	--		206	0.49	--
2	17.8	37	0.09	0.02		311	0.74	0.20
3	23.1	173	0.41	0.08		467	1.11	0.21
4	28.4	152	0.36	0.07		643	1.53	0.29
(b) Insulator [#] and Pad Performance Pads								
Survey	Total Tonnage (MGT)	Insulators Broken or Missing	%	Per MGT	Displaced, Broken or Missing	%	Per MGT	Insulators Installed Incorrectly
1	14.1	40	0.10	--	0	--	--	3
2	17.8	59	0.14	0.04	9	0.04	0.002	0
3	23.1	18	0.04	0.01	32	0.15	0.007	0
4	28.4	0	0	0	38	0.18	0.006	0
(c) Tie Performance								
Survey	Total Tonnage (MGT)	Shoulder/ Insert Loose, Broken or Missing	%	Per MGT	Cracked Ties	Damaged Ties	Skewed Ties	
1	14.1	8	0.019	0.0013	10	5	2	
2	17.8	12	0.029	0.0016	15	8	57	
3	23.1	14	0.033	0.0014	16	8	77	
4	28.4	20	0.047	0.0017	18	8	81	

Total of 10,475 ties in site

* Estimated cumulative since track installed.

Maintenance (QC) performed between surveys.

TABLE 3-5. SUMMARY OF TRACK COMPONENT PERFORMANCE FOR SITE 3

Survey	Total Tonnage (MGT)*	(a) Clip Performance [#]				Clips Moving	%	% Per MGT
		Clips Out	%	% Per MGT	Clips Moving			
1	31.3	157	0.37	--	1462	3.44	--	
2	40.7	127	0.30	0.03	703	1.65	0.18	
3	47.0	147	0.35	0.05	1518	3.57	0.57	
4	51.7	260	0.61	0.13	1300	3.06	0.65	
(b) Insulator [#] and Pad Performance								
Survey	Total Tonnage (MGT)	Insulators Broken or Missing	%	% Per MGT	Displaced, Broken or Missing	%	% Per MGT	Insulators Installed Incorrectly
1	31.3	662	1.56	--	0	0	--	112
2	40.7	102	0.24	0.03	4	0.02	0.0005	0
3	47.0	59	0.14	0.02	15	0.07	0.002	0
4	51.7	0	0	0	21	0.10	0.002	0
(c) Tie Performance								
Survey	Total Tonnage (MGT)	Shoulder/ Insert Loose, Broken or Missing	%	% Per MGT	Cracked Ties	Damaged Ties	Skewed Ties	
1	31.3	7	0.016	0.0005	4	4	0	
2	40.7	13	0.031	0.0008	6	4	23	
3	47.0	20	0.047	0.0010	9	4	44	
4	51.7	23	0.054	0.0010	9	4	55	

Total of 10,625 ties in site

* Estimated cumulative since track installed.

Maintenance (QC) performed between surveys.

TABLE 3-6. SUMMARY OF TRACK COMPONENT PERFORMANCE FOR SITE 5

Survey	Total Tonnage (MGT)*	(a) Clip Performance [#]				Clips Moving	%	% Per MGT
		Clips Out	%	% Per MGT				
1	2.6	399	0.65	--		994	1.61	--
2	4.5	535	0.87	--		1150	1.86	--
3	6.5	438	0.71	--		1484	2.40	--
4	7.8	125	0.20	--		603	0.98	--
(b) Insulator [#] and Pad Performance Pads								
Survey	Total Tonnage (MGT)	Insulators Broken or Missing	%	% Per MGT	Displaced, Broken or Missing	%	% Per MGT	Insulators Installed Incorrectly
1	2.6	888	1.44	--	132	0.43	0.16	15
2	4.5	286	0.46	--	427	1.38	0.31	0
3	6.5	133	0.22	--	575	1.86	0.29	0
4	7.8	0	0	--	605	1.96	0.25	0
(c) Tie Performance								
Survey	Total Tonnage (MGT)	Shoulder/ Insert Loose, Broken or Missing	%	% Per MGT	Cracked Ties	Damaged Ties	Skewed Ties	
1	2.6	2	0.003	0.0012	5	6	61	
2	4.5	3	0.005	0.0011	8	7	72	
3	6.5	6	0.010	0.0015	9	7	90	
4	7.8	13	0.021	0.0027	10	7	94	

Total of 15,450 ties in site

* Estimated cumulative since track installed.

Maintenance (QC) performed between surveys 2 and 3 MP 59-62, only. Percent per MGT cannot be calculated.

TABLE 3-7. OCCURRENCES OF FASTENER INCIDENTS* IN VICINITY
OF WELD OR RAIL JOINT ANOMALIES--
SITES 1, 2 AND 3

<u>Welds, joints</u>		Fasteners Moving or Out						
<u>Location</u> (Rail)	No.	<u>Location</u> (Rail)	Total No. Ties	Total No. Events	Number of Occurrences Within			
					<u>+0 Ties</u>	<u>± 1 Tie</u>	<u>± 3 Ties</u>	<u>± 5 Ties</u>
Right	197	Right	4149	6827	18	120	381	515
Right	197	Left	4377	6721	74	216	422	555
Left	211	Left	4377	6721	11	111	419	582
Left	211	Right	4149	6827	68	175	395	534

* Fasteners out or moving.

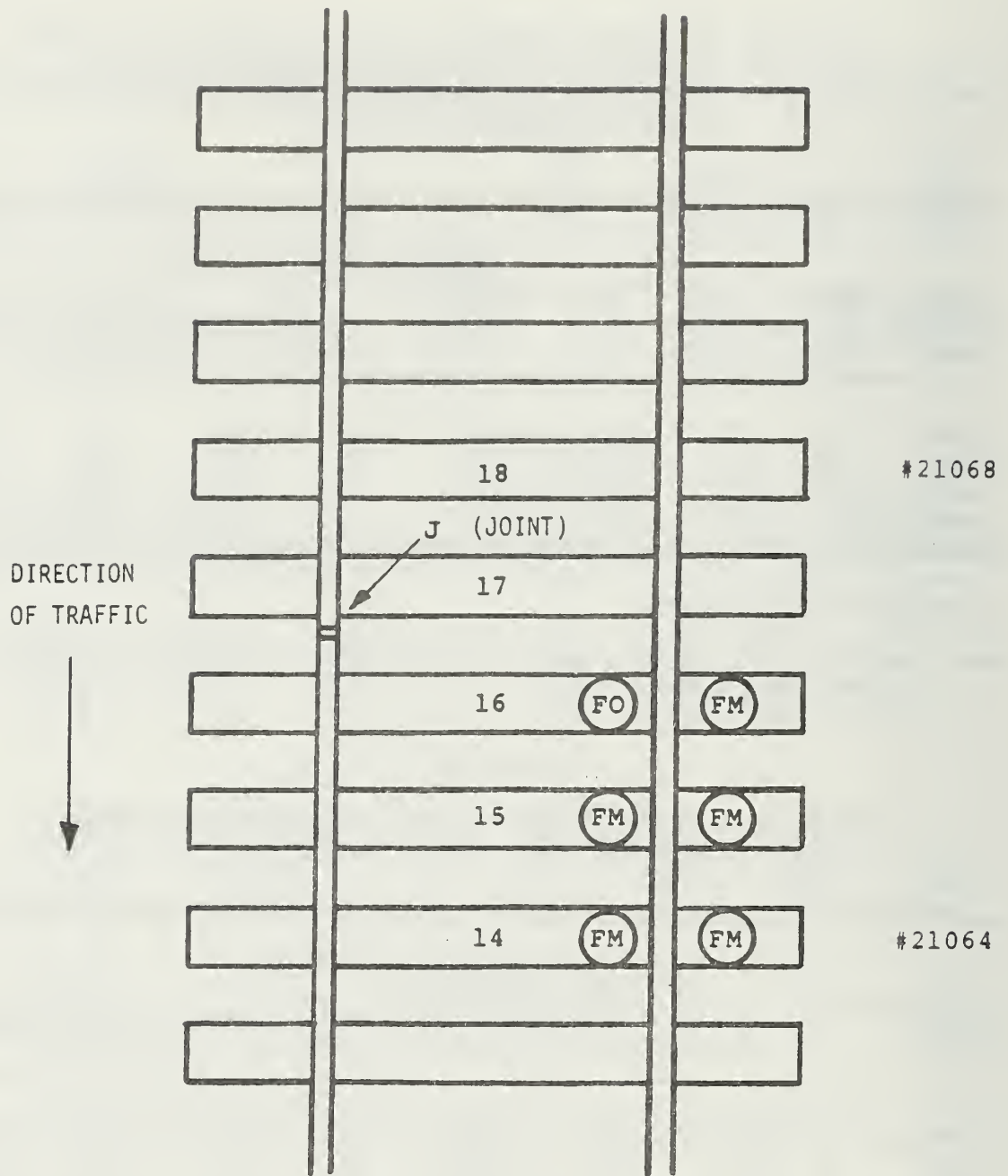
Note: Welds, joints at 400 ties, 410 unique values (only 10 occur opposite another at a given tie).

TABLE 3-8. OCCURRENCES OF FASTENER INCIDENTS* IN VICINITY
OF ENGINE BURN ANOMALIES--SITE 1

<u>Engine Burns</u>		Fasteners Moving or Out						
<u>Location</u> (Rail)	No.	<u>Location</u> (Rail)	Total No. Ties	Total No. Events	Number of Occurrences Within			
					<u>+0 Ties</u>	<u>± 1 Tie</u>	<u>± 3 Ties</u>	<u>± 5 Ties</u>
Right	22	Right	1717	2846	37	86	117	145
Right	22	Left	1917	3013	27	83	121	163
Left	33	Left	1917	3013	46	103	149	177
Left	33	Right	1717	2846	40	89	113	155

* Fasteners out or moving.

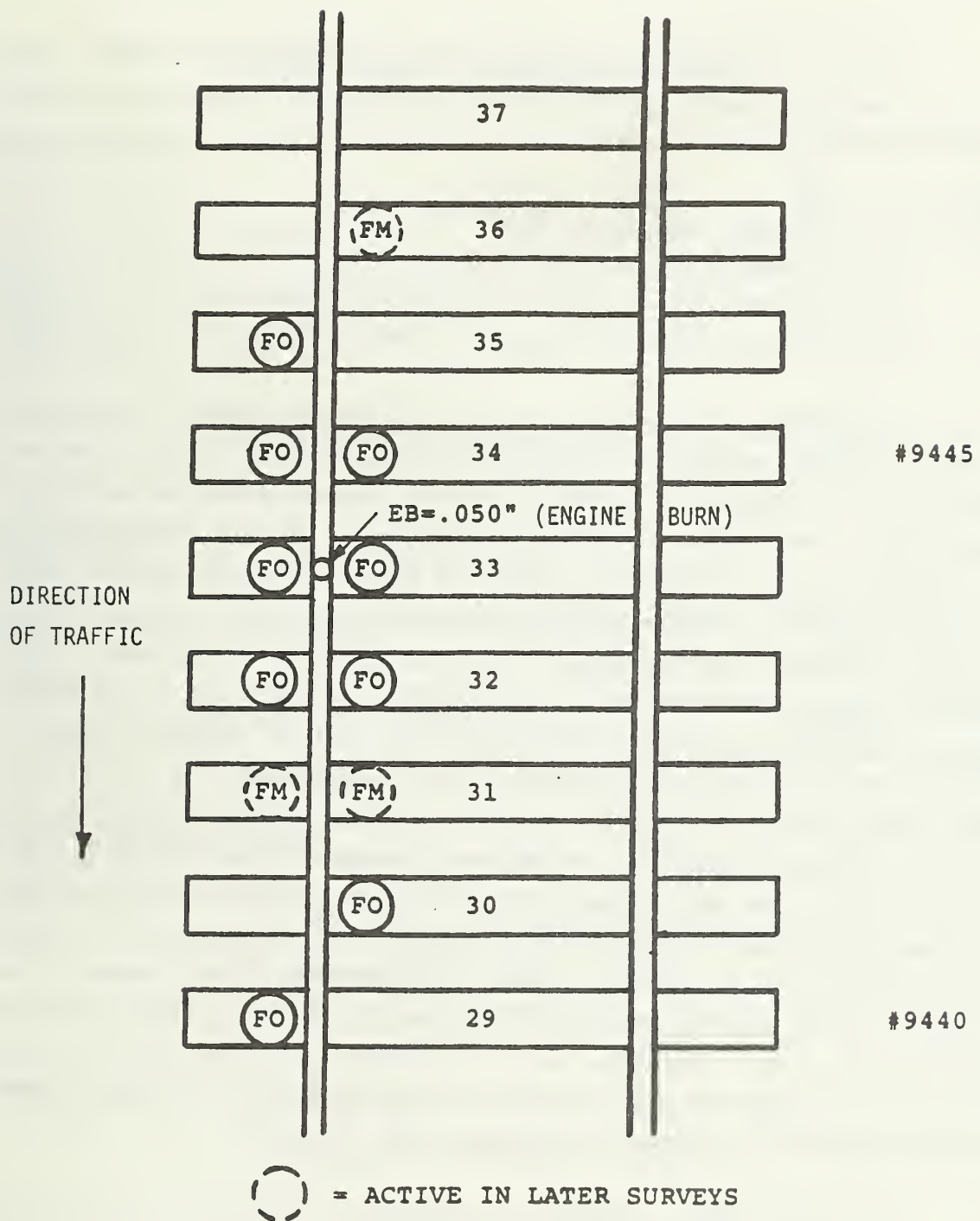
Note: Engine burns at 44 ties, 55 unique values (11 occur opposite another at a given tie).



SITE 2, SECTION 8, MP 47.62

SURVEY 4

FIGURE 3-5. EXAMPLE OF FASTENER FAULT CLUSTERING ON RAIL
OPPOSITE A RAIL JOINT OR BATTERED WELD



SITE 1, SECTION 11, MP 67.57

SURVEY 1

FIGURE 3-6. EXAMPLE OF FASTENER FAULT CLUSTERING ON SAME RAIL AS BATTERED ENGINE BURN

Several criteria for evaluating track strength from track walker survey data were examined in this study. Four different criteria can be used, based on fastener fault clustering:

- (1) Fasteners out, either side of the rail,
- (2) Fasteners out, one side of the rail only,
- (3) Fasteners moving or out, either side of the rail,
- (4) Fasteners moving or out, both sides of the rail.

The numbers of locations of clusters, and the number of consecutive ties for a cluster are shown in Table 3-9 for Site 1, Survey 1 data. The most conservative is Criterion 3, which shows the largest number of missing or moving clips. From track strength considerations, however, Criterion 4 is more realistic in its definition, based on a pair of clips missing or moving at a given location. Fastener event patterns by Criterion 2, fasteners out on one side of the rail, are tabulated for the four sites in Table 3-10. Site 1 showed the highest incidence of fault clustering, probably due to the greater number of engine burns on the older relay rail. Similar results are seen in Table 3-11 for Criterion 4, fasteners moving or out on both sides of the rail. Sites 2 and 3 exhibited little evidence of fastener events in clusters, and generally lower percentages per accumulated tonnage (MGT of traffic). Some rail grinding was done within these sites during the two-year period, however. Site 5 had more random fastener movement and fallout, possibly due to installation problems with the resilient pads. It has been noted, however, that rail within Site 5 was not properly straightened at welds, and these kinks may account for higher rail vibration levels. Fastener faults were evenly distributed on field and gauge sides of the rail except within Site 1, where roughly 35 percent more faults occurred on the gauge side of the rail.

Insulator events (broken or missing) are given in Table 3-12, showing clusters on one side of the rail. Insulator failures occurred in significantly greater numbers on the field side of the rail, possibly because lateral impact loads from passing wheelsets are carried primarily by the field-side insulator into the shoulder. However, installation is more difficult on the field side, particularly in curves in the summer, and

TABLE 3-9. COMPARISON OF FASTENER SAFETY EVALUATION CRITERIA
SITE 1, SURVEY 1 TRACKWALKER RESULTS

Evaluation Criteria		Total Number Ties	Total Number Fasteners	Number of Locations	Number Consecutive Ties
Fasteners out, either side of rail (FO)	- left rail	145	158	8 4 1	2 3 4
	- right rail	176	193	13 1	2 3
Fasteners out, one side of rail (FO)	- left rail, field side	86	86	6 1	2 4
	- gage side	72	72	4 3	2 3
	- right rail, field side	104	104	8	2
	- gage side	89	89	4	2
Fasteners moving or out, either side of rail (FM or FO)	- left rail	308	326	18 6 2	2 3 4
	- right rail	292	312	22 2 1	2 3 4
Fasteners moving or out, both sides of rail	- left rail	18	36	1	3
	- right rail	20	40	2	2

TABLE 3-10. FASTENER EVENT PATTERNS IN TEST SITES--
FASTENERS OUT ON ONE SIDE OF RAIL

Site	Survey	Side of Rail	Left Rail			Right Rail		
			Total Number Ties	Number of Locations	Number of Consecutive Ties	Total Number Ties	Number of Locations	Number of Consecutive Ties
1	1	Field	86	6 1	2 4	104	8	2
		Gage	72	4 3	2 3	89	4	2
2	1	Field	11	0	--	3	0	--
		Gage	1	0	--	11	1	2
2	4	Field	45	0	--	39	2	2
		Gage	45	2	2	23	0	--
3	1	Field	45	2	2	39	1	2
		Gage	40	1	2	33	2 1	2 3
3	3	Field	65	2 1	2 3	30	1	2
		Gage	29	1	2	23	1	2
5	2	Field	155	5 2	2 3	128	4	2
		Gage	126	1 1	2 3	126	1	2

TABLE 3-11. FASTENER EVENT PATTERNS WITHIN TEST SITES
--FASTENERS MOVING OR OUT ON BOTH SIDES OF RAIL

Site	Survey	Number of Ties		Left Rail		Right Rail	
		Left Rail	Right Rail	Locations	Consecutive Ties	Locations	Consecutive Ties
1	1	18	20	1	3	2	2
	2	32	16	1	2	0	--
	3	25	23	1	2	2	2
	4	45	41	2	2	4	2
2	1	1	1	0	--	0	--
	2	1	0	0	--	0	--
	3	5	2	0	--	0	--
	4	3	17	0	--	1	3
3	1	13	18	0	--	0	--
	2	2	5	0	--	0	--
	3	20	7	2	2	1	2
	4	16	14	0	--	0	--
5	1	26	5	1	2	0	--
	2	39	10	2	2	0	--
	3	40	12	0	--	0	--
	4	7	4	0	--	0	--

TABLE 3-12. INSULATOR EVENTS (BROKEN OR MISSING)
IN TEST SITES--ONE SIDE OF RAIL

Site	Survey	Side of Rail	Left Rail			Right Rail			Number of Consecutive Ties
			Total Number Ties	Number of Locations	Number of Consecutive Ties	Total Number Ties	Number of Locations		
1	1	Field	85	5 1	2 4	103	3		2
		Gage	22	2	2	31	1		2
2	1	Field	23	0	--	11	1		2
		Gage	1	0	--	5	0		--
2	4	Field	0	0	--	35	2		2
		Gage	3	0	--	8	0		--
3	1	Field	142	2 1	2 3	254	12 2		2 3
		Gage	99	1	2	167	4		2
3	3	Field	13	0	--	35	2		2
		Gage	3	0	--	8	0		--
5	2	Field	158	3	2	83	1		2
		Gage	29	0	--	16	0		--

failures may be installation-related. Field-side failures ranged from 1.7 to 3.5 times greater than gauge-side failures. Site 3 (with the highest accumulated tonnage) and Site 5 (with possible installation problems and improperly straightened rail) has the highest number of insulator failures at the time of Survey 1. These numbers dropped significantly in subsequent surveys as the result of maintenance. Few simultaneous occurrences of fastener and insulator faults were noted in the data base.

Shoulder/insert failures were found to occur two to three times more often on the field side in Sites 1 and 5, but were evenly distributed on field and gauge sides in Sites 2 and 3. There were relatively few shoulder/insert events, with the highest numbers and percent per MGT found within Site 1, with the older relay rail. Only one cluster of three field-side shoulder/insert failures in a row was found. These three clips were, of course, not effective; but the cluster did not coincide with a more extensive clip fallout cluster.

Site 5 (with the more resilient Trelleborg pads) has the highest incidence of pads moving, damaged or missing. Site 5 also had the highest number of skewed ties. One of the busier component fault arrays within Site 5 is shown in Figure 3-7 extending in either direction from a rail joint. The joint, 0.075 inch in depth, was the only apparent cause of all this activity; and the impact loads eventually loosened three of the four inserts in the immediate vicinity of the joint. Two of the skewed ties (47 and 48) were associated with missing clips on both field and gauge sides and broken field-side insulators, all on one rail. Two other ties (56 and 57) that were skewed by a later survey were associated with one clip out, three clips moving on one rail. It has been noted that ties will tend to skew toward the point of impact loading, as the ballast tends to loosen and migrate from under this location. However, no rail surface anomalies were noted at these two points.

Comparable (and small) numbers of cracked or damaged ties were noted in all four of the test sites. However, the surveys did not include the careful examination of ties within the cribs necessary to detect the hairline rail seat cracks noted in previous studies. If the rail seat crack extended to the insert, it was counted then as an insert failure.

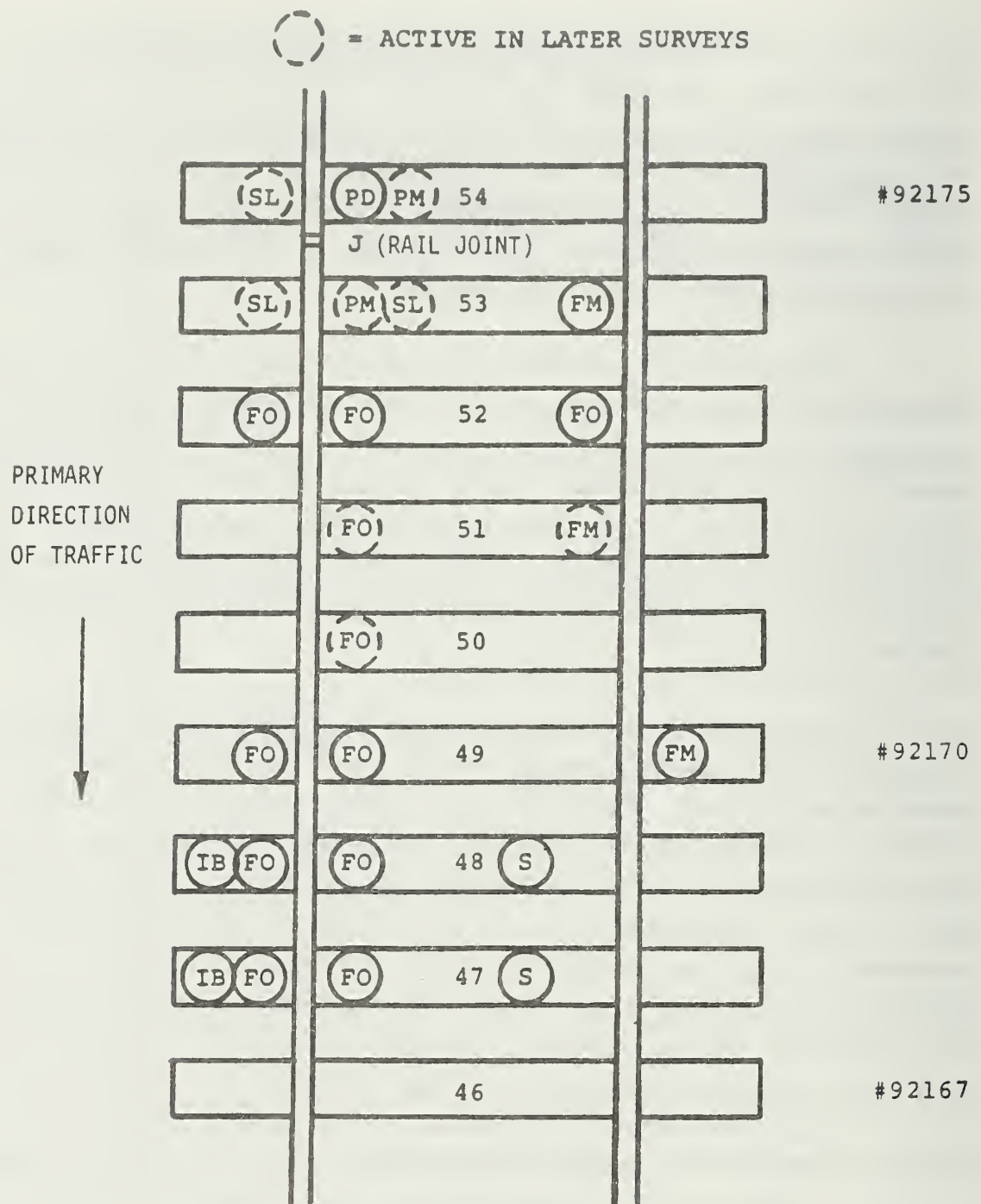


FIGURE 3-7. EXTENSIVE TRACK COMPONENT FAULT PATTERN NOTED IN SURVEY OF TEST SITE #5



= ACTIVE IN LATER SURVEYS

PRIMARY DIRECTION OF TRAFFIC			#92183
	63	(IB)	
	62	(PD)	
	61		
	60		
	59	(FM)	#92180
	58	(FO)	
	57	(FM) (S)	
	56	(FM) (S)	
	55	(FM)	
	54	(PD) (PM)	#92175
	J	(RAIL JOINT)	

SITE 5, SECTION 14, MP 63.74

SURVEY 2

FIGURE 3-7. (CONTINUED)

3.3 Summary of Track Condition Assessment

The results of the four track walker surveys of four representative test sites over an 18 to 23-month period showed the Northeast Corridor concrete tie track to be in generally excellent condition. Few specific problems were noted in the survey data. Less than one percent of the clips were out in any survey; and less than 3.6 percent of the clips were moving (clip end more than 1/4 inch inside the insert) in a survey. As many as 1.6 percent of the insulators (predominantly field-side) were broken or missing at the time of the first survey, but this number dropped to a very small percentage as the result of QC maintenance. Site 5 (with the resilient Trelleborg pads) had the highest number of pads displaced, broken or missing: up to two percent by the last survey. This may have reflected an installation problem with new pads. Very small numbers of broken or missing inserts were found in the four sites, and equally small numbers of cracked or damaged ties were observed. The greatest number of insert faults was associated with the older relay rail in Site 1, which contained a large number of engine burns and battered welds. Fewer engine burns were noted in the other sites with newer rail, possibly reflecting better wheel slip control on the more modern locomotives.

Correlation of clip movement and fallout with specific rail running surface anomalies was explored with the BASIS data management system. Within Site 1 with rougher rail, 32 percent of these fastener events occurred within ± 5 ties of a surface anomaly. In the other three sites, however, a more random pattern of fastener events was found, with less than 11 percent of the events occurring within ± 5 ties of a surface anomaly. Track vibrations from wheel roughness are therefore as important as specific rail anomalies in clip movement.

Clustering of clips moving or out was also investigated. In only one location within Site 1 were four clips in a row found missing on one side of the rail. This did not coincide with broken or missing insulators. The removal of 3 clip-pairs in a row, along with the field-side insulators, would reduce track lateral stiffness to that of good wood-tie track, since the rail base is restrained by the insert with this particular fastener design.

Increasing numbers of temporary mechanical joints were observed over the course of the study. This may induce greater numbers of insert failures and more clip movement. Rewelding the rail at these locations is recommended to reduce the number of running surface anomalies producing impact loads on the track.

4.0 REMEDIAL PROJECTS ASSESSMENT

Amtrak is conducting several remedial projects to improve tie and fastener performance. These projects include the use of resilient tie pads and a modified clip, removal of engine burns, and the use of an automated wheel impact load detector to identify wheel sets producing high impact loads. The effects of these remedial projects on the performance of the Northeast Corridor concrete-tie track are discussed in the following sections.

4.1 Wheel Impact Load Detector

A device for automatically measuring, analyzing and recording vertical dynamic wheel/rail loads was designed and fabricated by Battelle as a result of an investigation of concrete tie track performance [1, 5]. The primary use of the device is the detection of abnormal dynamic loads resulting from wheel tread irregularities, and the reporting of this information at a remote terminal. Using multiple microcomputers controlled by a 68000-based VME microcomputer system, the Wheel Impact Load Detector (WILD) reads vertical wheel loads from strain gage patterns installed on the rail web in successive tie cribs, sampling seven to ten percent of each wheel circumference per pattern (crib). Different data options are available at a remote terminal, including the matrix of all wheel loads (all wheels at all measurement sites) of the last train to pass, a short report of loads exceeding either of two adjustable load thresholds, or cumulative load statistics (axle counts in speed and load bands).

The first WILD was installed in mid-1983 on concrete-tie track, southbound Track 3 near Edgewood, MD. The detector is currently being used both as a means for monitoring wheel conditions for Amtrak's wheel maintenance program, and as a tool to develop statistical descriptions of the wheel/rail load environment under different types of traffic.

4.1.1 Dynamic Wheel Load Characterization

The initial problem which led to the development of the WILD was early signs of concrete tie rail seat cracking on Track 4 near Aberdeen, MD.

These cracks were first detected during a study to correlate the performance of concrete-tie track in revenue service with its performance at the Facility for Accelerated Service Testing (FAST) near Pueblo, CO [6]. Measurements taken near Aberdeen during that study included vertical and lateral wheel loads, tie center and rail seat bending moments, and rail and tie accelerations. An example of loads and tie bending moments under a typical wheel irregularity is given in Figure 4-1, showing the highly oscillatory "tone burst" response of the tie to impact loading. The data were originally analyzed with low-pass filters set at 300 Hz, a bandwidth that had proven adequate in previous studies on wood-tie track. The same data were then processed at a 2-kHz bandwidth, which showed substantially higher amplitudes of load and bending moment: one peak rail seat bending moment of 370 kip-in was measured in an 8-day block of recorded data [1].

The significance of dynamic loading can be seen in Figure 4-2, which compares the cumulative distribution of calculated nominal (static) wheel loads and measured dynamic wheel loads. Nominal loads were estimated from revenue freight and passenger train consist lists acquired over the time-period of measurement. About two percent of the wheels developed dynamic vertical loads significantly higher than the nominal wheel loads. Between 0.12 and 0.15 percent of the measured peak load samples (12 to 15 in 10,000) exceeded the 60-kip load level in this study. Roughly one measurement event in 10,000 exceeded the 85-kip level, as shown in Figure 4-2.

4.1.2 Description of Detector

The detector system utilizes strain gage patterns attached directly to the rail web and calibrated to read vertical load under each passing wheel. Four circuits on one rail were used in the original Edgewood installation. Each circuit has a trapezoidal "influence zone" roughly 16 inches in length, and 8 inches of this zone is at full calibrated sensitivity. For a 36-inch diameter Amcoach wheel, the four circuits monitor loads under at least 28 percent of the wheel tread during one roll-by. By increasing the number of consecutive circuits to 8 and adjusting the circuit spacing, about 70 percent inspection per pass can be achieved. Only one rail was instrumented on the premise that tread roughness would occur on both wheels of a given wheelset.

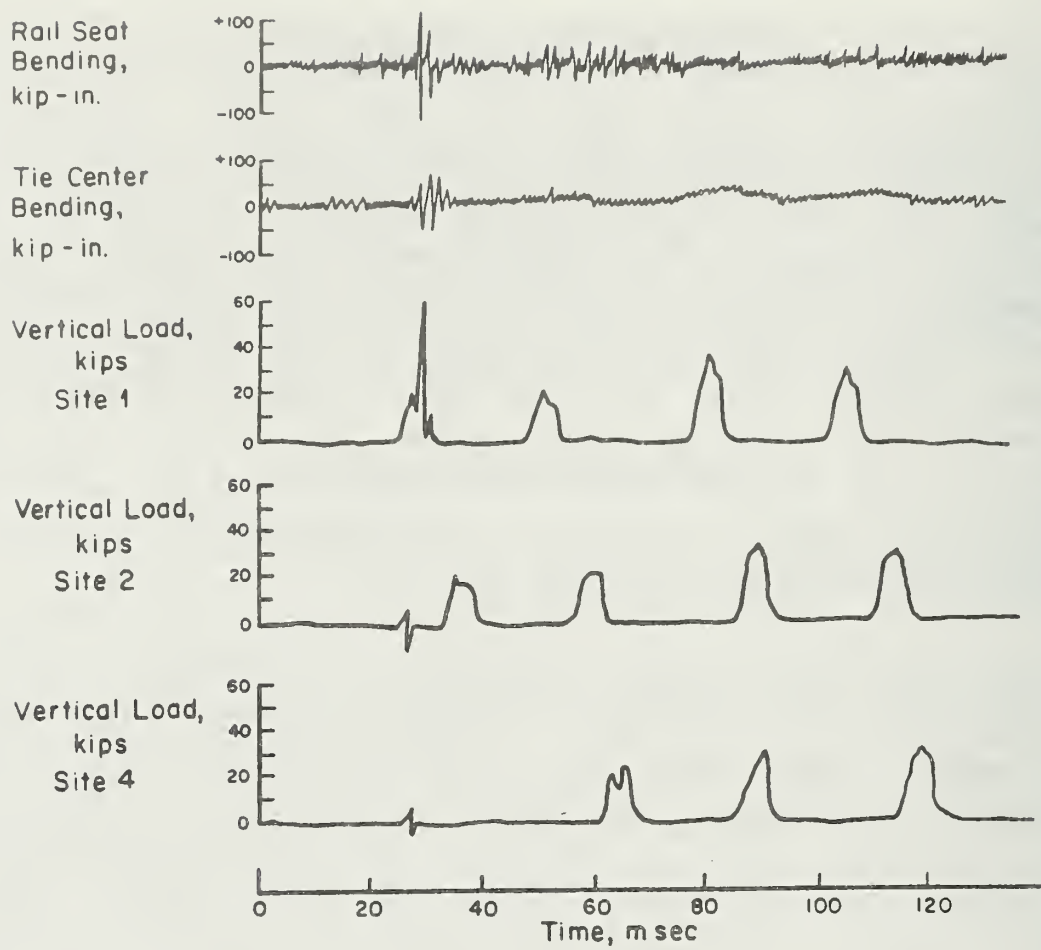


FIGURE 4-1. EXAMPLE TIME HISTORIES OF TIE BENDING MOMENTS AND VERTICAL WHEEL LOADS UNDER ADJACENT TRUCKS OF FREIGHT CARS ON CONCRETE TIE TRACK

STATIC VS. DYNAMIC EXCEEDANCE CURVES

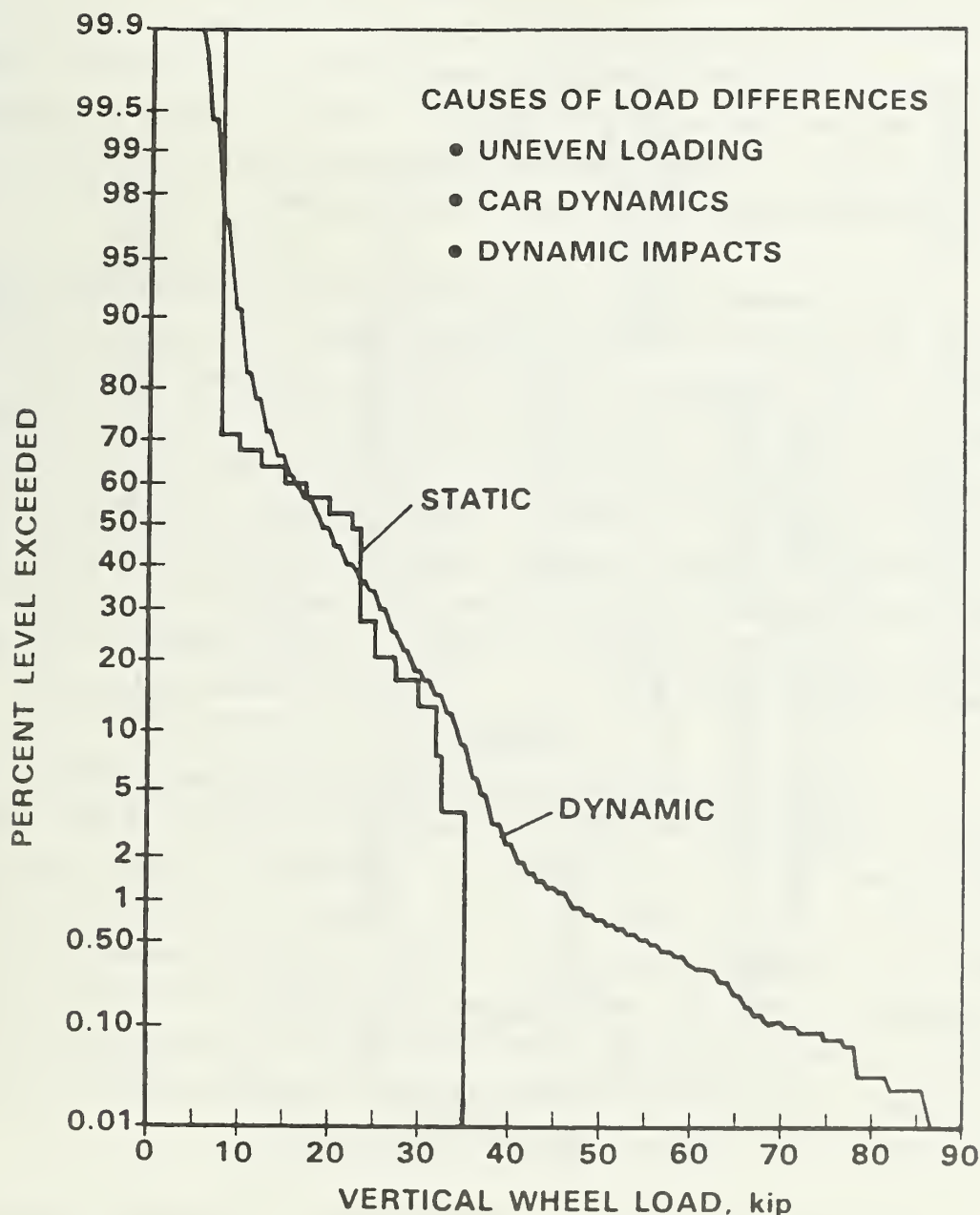


FIGURE 4-2. CUMULATIVE PROBABILITY CURVES OF STATIC AND DYNAMIC VERTICAL WHEEL LOADS ON NORTHEAST CORRIDOR CONCRETE TIE TRACK (ALL TRAFFIC)

A typical circuit output time-history is shown in Figure 4-3, showing the response to a "nominal" wheel, a rough wheel, and an impact outside the zone of influence. The impact load itself is typically a half-sine pulse of 1 to 2 milliseconds in duration. To measure and capture this peak within a 5 percent accuracy, a sampling rate of 30 kHz was chosen. At the other extreme, the system must be able to monitor a 600-axle freight train moving at 25 mph, which requires continuous sampling for 6 to 8 minutes, about 100 million data samples for an eight-circuit system.

To accommodate these high sample rates and storage requirements, a multiple microcomputer configuration was chosen as the most cost-effective approach. Each measurement circuit utilizes a dedicated "front-end" microcomputer to sample the analog signal from the circuit and to determine the peak wheel load for each passing wheel, transmitting only this single value to the "master" computer for temporary storage and post-train analysis. After train passage, the master computer verifies the quality of the data and circuit calibrations, and selects the largest overall load for each passing wheel from the four (or eight) circuits. A block diagram of the detector system is given in Figure 4-4.

A report is then prepared noting all wheelset numbers exceeding either of two preset load limits. These data, along with time, date, train speed, ground and box temperatures are transmitted to one or more remote terminals on a dial-up telephone line. Examples of three wheel exception reports, two passenger trains and a freight train, are shown in Figure 4-5. The detector system will also respond to incoming calls, and a menu of commands can produce listings of all wheel loads for the last train to pass the detector, front-end calibration checks, or detailed wheel load statistics in the form of wheel counts in speed and load bands.

The Amtrak detector is currently housed in a sealed steel enclosure 2 ft x 2 ft x 1 ft in size, about 15 ft from the instrumented track. Track circuits are protected by rugged rail web shields, and wiring is protected by armored hydraulic hose. System power is provided by standard 100 Hz, 110 volt wayside C&S power. A standard two-wire communications line is connected from

CIRCUIT OUTPUT TIME HISTORY

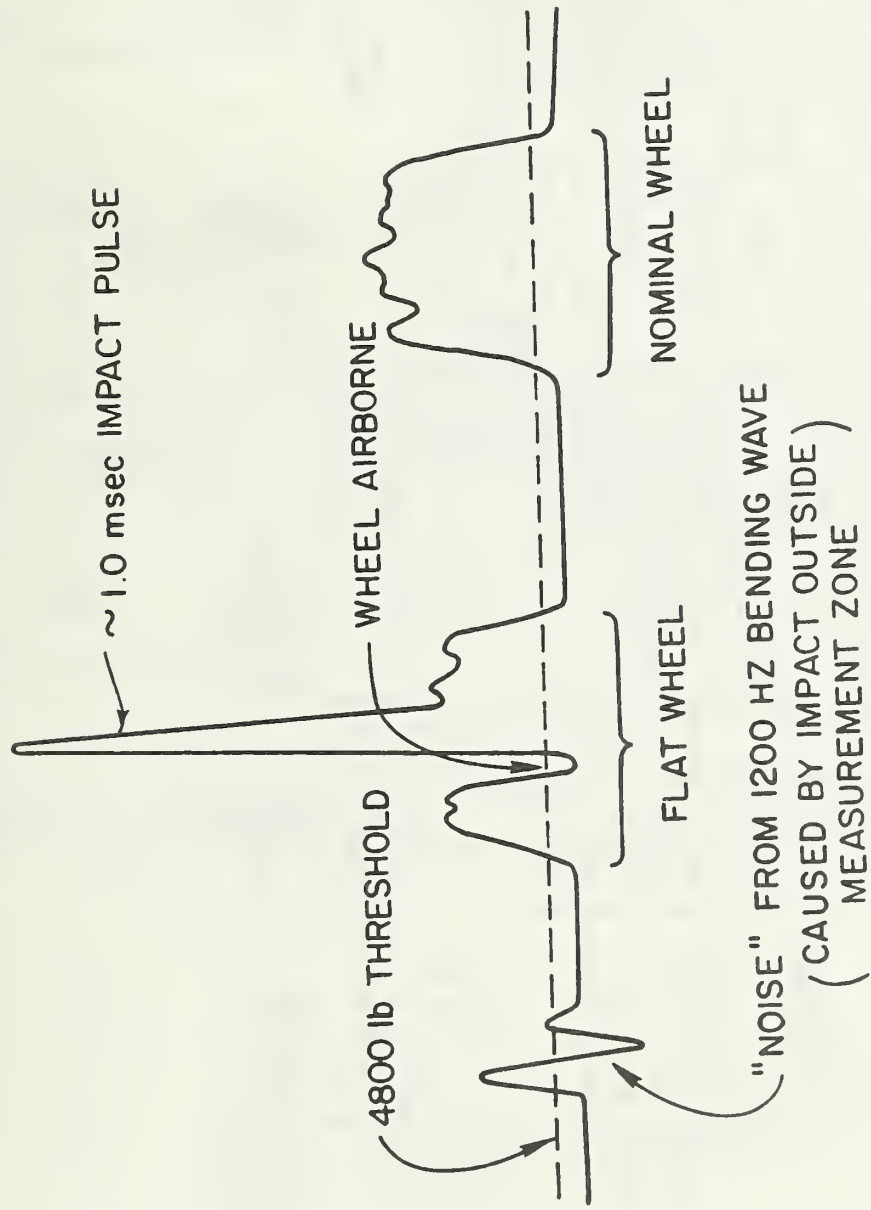


FIGURE 4-3. EXAMPLES OF TYPICAL IMPACT LOAD DETECTOR CIRCUIT OUTPUTS

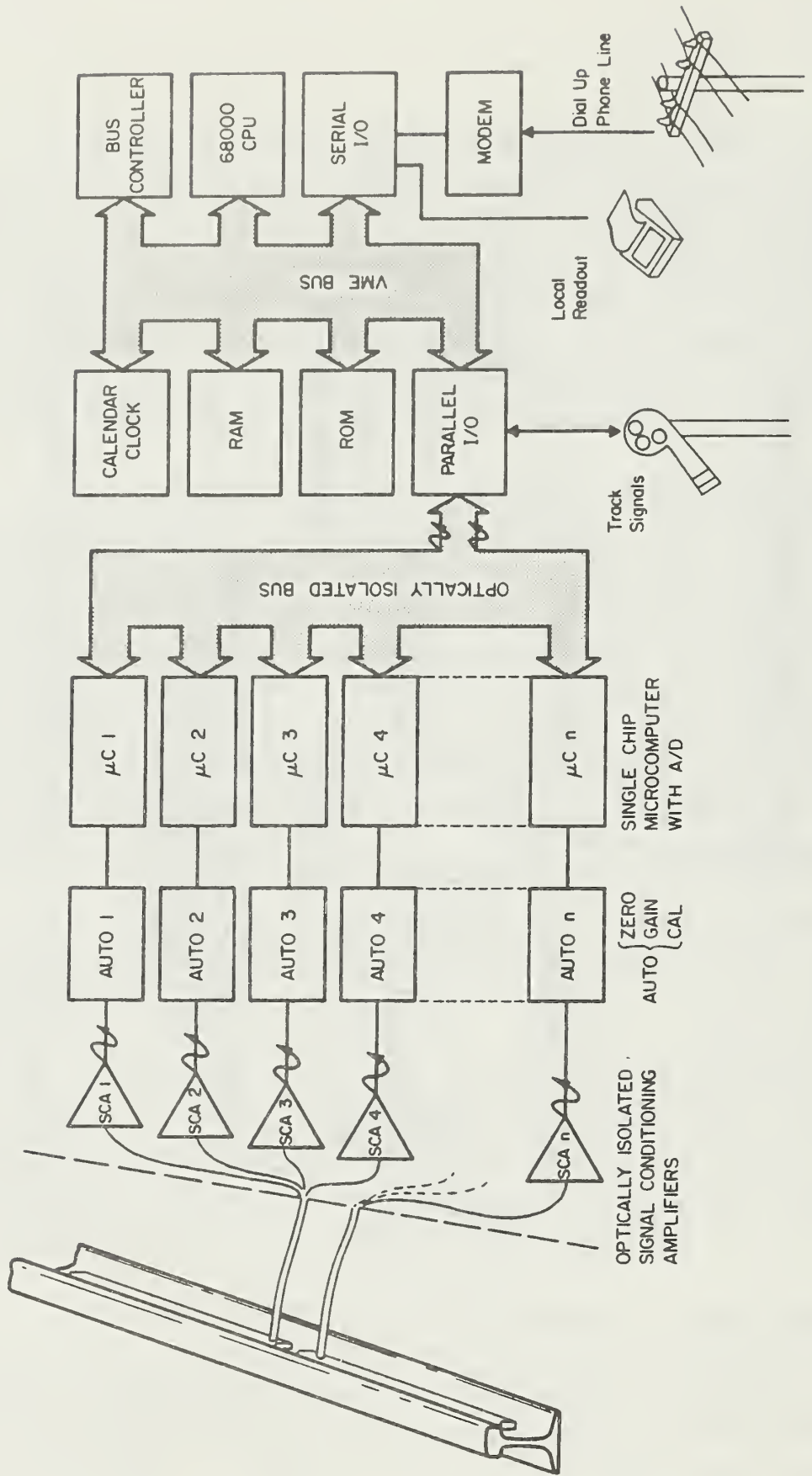


FIGURE 4-4. WHEEL IMPACT LOAD DETECTOR BLOCK DIAGRAM

WHEEL EXCEPTION REPORT

Train Passed at 14:42:16 84/06/02
Speed = 121. Axle Count = 28
Ground Temperature = 83. Box Temperature = 122.

Levels = 40. 55. kips

Axle Number	Car Number	Level 1 Exceeded	Level 2 Exceeded
9	3		Yes 62.

Train Passed at 14:47:09 84/06/02
Speed = 61. Axle Count = 12
Ground Temperature = 83. Box Temperature = 126.

Levels = 40. 55. kips

Axle Number	Car Number	Level 1 Exceeded	Level 2 Exceeded
-------------	------------	------------------	------------------

No Loads Above Limits

Train Passed at 15:01:27 84/06/02
Speed = 48. Axle Count = 272
Ground Temperature = 87. Box Temperature = 126.

Levels = 40. 55. kips

Axle Number	Car Number	Level 1 Exceeded	Level 2 Exceeded
4	1	Yes 43.	
10	3	Yes 40.	
90	23	Yes 41.	
96	24	Yes 42.	
167	42		Yes 58.
168	42	Yes 52.	
190	48	Yes 47.	
193	49	Yes 40.	
194	49	Yes 43.	

FIGURE 4-5. THREE EXAMPLES OF WHEEL EXCEPTION REPORTS

the system's integral modem to a commercial telephone junction box located in the Edgewood interlocking tower, about one mile away. Connections to the Amtrak signal system are made at a nearby signal cabinet.

4.1.3 Detector System Development

The WILD was installed and calibrated in late Spring of 1983. During the initial verification phase, analog signals were processed both by the detector microcomputer and by manual processing of oscillographic recordings. This allowed the correction of several minor problems. For example, a program modification was made to the front-end processors to prevent false wheel triggering due to the 1200-Hz rail "ringing" caused by nearby wheel impacts. An example of this is shown in Figure 4-3. The current front-end algorithm can eliminate "false wheels" and can accommodate wheels "airborne" part way through the influence zone. Only an exceptionally bad wheel on a long freight train will occasionally confuse the axle count.

Several other improvements were made to the system during this development phase. Modifications were made to the chronograph power supply to enable the chronograph to function during low voltage conditions. Some problems were noted when the line voltage dropped below 100 volts. The corrected system should function with line voltage as low as 85 volts. Internal heat exchanger fins were added to the enclosure after a late-June heat wave sent ambient air temperatures up to 100 F, and internal circuit board temperatures rose to 160 F. These internal heat fins reduced the board temperatures 10-15 F to within applicable limits. The wiring and connectors in the tie-mounted junction box were modified to provide better strain relief in this severe shock and vibration environment. This was necessary due to early fatigue failures in solder connections at the connector.

Programming changes were made to the system to improve output formats. During August-September 1983, modifications were made to enable the detector to collect and store cumulative load statistics. Each peak load from each circuit for each wheel is treated as a separate event to be indexed and summed according to load and train speed ranges. Load statistics were addi-

tionally separated by temperature bands in this first phase: 20 F and under, 21 to 35 F, and over 35 F.

Shortly after these changes were made, the system suffered electrical damage during a severe thunderstorm. The detector was removed and shipped to Battelle for repairs, and the following items were found damaged:

- (1) Three of four front-end microprocessors were damaged and required replacement. An additional level of protection was added to the A/D converter precision voltage reference for each microprocessor on the advice of the manufacturer.
- (2) The electronic buffer between the trackside relay circuit and the main microprocessor was shorted, probably from a voltage transient on the ground reference side of the relay sensing circuit. Additional current limiting protection was built into this circuit.
- (3) The modem surge protection circuitry had failed, indicating a major voltage transient on the communications line. Additional overvoltage protection was placed on the communications line.

Other "growing pains" associated particularly with the modem and the communications line have been overcome, and the detector system has functioned with minimal problems for the past 6 to 8 months.

4.1.4 Applications of the Detector

Amtrak Wheel Truing Program

The main objective in developing the WILD was to detect, identify and facilitate the removal of wheel sets from Amtrak equipment causing track-damaging impact loads. Beginning in January 1984, wheels causing loads above 60,000 lb were identified from the wheel exception reports. Tower operators identified the specific train passing the detector, and car inspectors examined the particular wheels at the nearest terminal. Many of these load-producing wheels had no visual profile exceptions by current interchange rules.

Shortly after identification had begun, a program to turn tagged wheels was initiated, and a new wheel truing machine was installed at the Ivy City Yard (Washington, D.C.) Wheelshop. An immediate drop was noted in the probability of occurrence and worst-case magnitude of impact loads above the 60-kip maintenance threshold, as shown in Figure 4-6. In this figure, the results of a running four-week average of the statistics for both freight and passenger equipment are shown. A steady decline in the percent of total measurement events exceeding the 60-kip limit under passenger wheels was noted, bottoming at a level near 0.04 percent. A later rise in the curve can be attributed to a few cars with rougher wheels put into service for the Memorial Day weekend rush.

It is evident from Figure 4-6 that the impact load statistics for freight traffic has remained about constant, since there is yet no impetus to improve this population of wheels. The relative importance of damage caused by freight traffic is now greater than before. An estimated two percent of all freight wheelsets cause impact loads greater than 60,000 lb, and 0.5 percent cause loads greater than 75,000 lb, the approximate crack-inducing load on a concrete tie. This is equivalent to 100 wheelsets per week through the detector site capable of producing rail seat cracks. Each week, several freight wheel loads are measured which exceed the 102-kip digital saturation limit of the WILD.

The program for reducing wheel impact loads under passenger equipment has been an extraordinary success because of the accurate identification of these loads by the detector, and the diligence of Amtrak personnel involved in the maintenance program. Extreme loads (over 80,000 lb) under passenger equipment were virtually eliminated in about two months, and the exception limit has since been lowered from 60 to 55 kips, thus progressively improving the fleet wheel conditions.

Wheel Load Statistics

Programming modifications to the detector system allowed the accumulation of wheel load statistics as axle counts in speed and load ranges. In

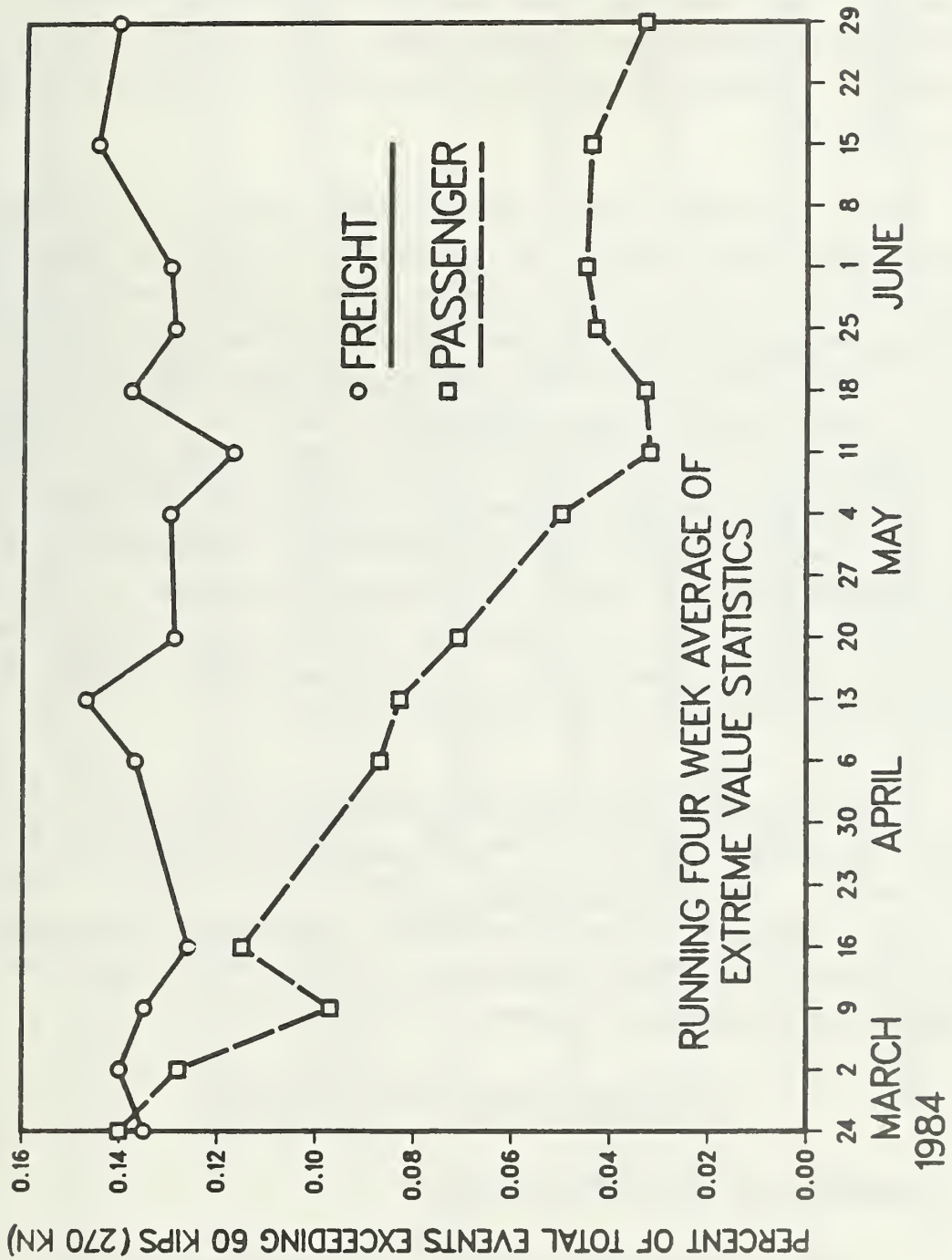


FIGURE 4-6. EFFECT OF WHEEL TRUING PROGRAM ON PASSENGER WHEEL EXTREME LOAD STATISTICS

addition, the load statistics could be stored separately according to the prevailing ballast temperature in three ranges: less than 20 F, 21 to 35 F, and over 35 F. Examples of load statistics printed at a remote terminal are shown in Figure 4-7.

Cold temperatures during January 1984 provided an opportunity to evaluate whether frozen ballast had a significant effect on impact loads. Problems with the mix of traffic during warmer daytime hours and colder nighttime hours were noted. Daytime traffic could have been "salted" with recently reconditioned, dual-brake coaches in Metroliner service. In addition, initial work on older Heritage car wheels on the truing machine began to affect the load statistics as warmer weather approached. Evaluation of the freight traffic for mid-January (mostly freezing temperatures) and traffic for mid-February (above-freezing temperatures) showed nearly identical cumulative distributions of loads. The subsequent conclusion was that frozen ballast has only a small, and probably insignificant, influence on the magnitude of vertical wheel loads on the already-stiff (10,500 lb/in/in modulus) concrete tie track on the Northeast Corridor.

Some investigations have been conducted by the NECIP staff to correlate the impact load data from the detector with specific types of freight traffic. Preliminary results of this work are shown in Table 4-1. These results indicate that wheel conditions on unit coal trains produce a greater share of impact load exceedances on a percent per population basis than other types of equipment in general freight traffic.

4.2 Passenger Wheel Profile Conditions

4.2.1 Experiments on the Northeast Corridor

A series of tests was conducted on the Northeast Corridor in late November of 1983 using a special Amtrak test train. In these tests the train was run over a wide range of speeds through a wayside test zone, the Edgewood impact detector site. The objectives of these tests were twofold: (1) to determine the influence of speed on wheel/rail vertical loads produced by worn

DO YOU WANT CURRENT OR ARCHIVAL STATISTICS ?
ENTER "1" FOR CURRENT, "2" FOR ARCHIVAL

¹WHEEL IMPACT STATISTICS COMPILED AT 15:01:14 84/01/30

RAW STATISTICS FOR TEMPERATURE RANGE 1 20 F or less

LOAD,KIPS	SPEED RANGE ,MPH						ALL
	0-50	50-65	66-80	81-95	96-110	>110	
0-10	8099	2063	0	4	9	36	10211
11-15	7714	2088	42	215	385	1116	11560
16-20	3241	660	50	604	720	2058	7333
21-25	2660	471	15	197	284	938	4565
26-30	2293	428	16	115	197	629	3678
31-35	2966	469	6	97	107	284	3929
36-40	970	154	1	29	52	100	1306
41-45	178	24	1	27	19	69	318
46-50	57	10	0	10	15	27	119
51-55	33	4	0	2	11	16	66
56-60	16	5	0	3	5	11	40
61-65	8	2	0	0	2	9	21
66-70	6	0	0	1	0	4	11
71-75	5	0	0	1	0	1	7
76-80	3	0	1	1	0	0	5
>80	5	0	U	2	0	0	7
ALL	28254	6378	132	1308	1806	5298	43176

RAW STATISTICS FOR TEMPERATURE RANGE 2 21 to 35 F

LOAD,KIPS	SPEED RANGE ,MPH						ALL
	0-50	50-65	66-80	81-95	96-110	>110	
0-10	29420	8394	0	11	46	279	34150
11-15	19101	8474	54	946	2148	6934	37657
16-20	6852	3288	202	2386	3548	8465	24741
21-25	7930	2977	84	759	1358	3234	16342
26-30	12473	2123	79	452	1039	2426	18592
31-35	21212	3301	117	428	482	933	26473
36-40	5921	1002	45	139	197	423	7727
41-45	971	179	9	67	96	246	1568
46-50	318	64	1	24	52	109	568
51-55	153	24	U	15	31	68	291
56-60	83	17	0	4	14	24	142
61-65	68	8	1	4	9	19	109
66-70	33	9	2	2	4	9	59
71-75	24	3	0	0	2	4	33
76-80	12	2	0	0	1	3	18
>80	37	5	0	1	1	8	52
ALL	100608	29870	594	5238	9028	23184	168522

RAW STATISTICS FOR TEMPERATURE RANGE 3 Greater than 35 F

LOAD,KIPS	SPEED RANGE ,MPH						ALL
	0-50	50-65	66-80	81-95	96-110	>110	
0-10	5371	2434	0	0	1	49	7855
11-15	3676	1349	0	309	561	1679	7574
16-20	1037	135	0	741	827	1815	4555
21-25	1351	265	0	227	323	738	2904
26-30	2625	256	0	163	233	538	3815
31-35	4139	330	0	101	75	229	4874
36-40	1216	111	0	30	37	142	1536
41-45	181	11	0	19	14	59	284
46-50	36	8	0	14	9	21	88
51-55	23	3	0	2	4	11	43
56-60	12	3	0	0	2	5	22
61-65	11	0	0	0	2	5	18
66-70	4	2	0	0	0	0	6
71-75	8	0	0	2	0	1	11
76-80	3	0	0	0	0	0	3
>80	7	1	0	0	0	0	8
ALL	19700	4908	0	1608	2088	5292	33596

FIGURE 4-7. EXAMPLES OF WHEEL VERTICAL LOAD STATISTICS:
EVENT COUNTS IN DIFFERENT SPEED AND LOAD BANDS
IN THREE DIFFERENT BALLAST TEMPERATURE RANGES

TABLE 4-1. CORRELATION OF WHEEL IMPACT LOADS AT EDGEWOOD DETECTOR SITE WITH SPECIFIC TYPES OF FREIGHT TRAFFIC -- DATA FROM 4-2-84 to 4-30-84, 6-29-84 to 7-6-84

CODE	TRAFFIC	AXLE COUNT	SUMMARY OF EVENTS IN BAND				100+
			50-59	60-69	70-79	80-89	
1 COAL - UNIT		8,222	60	39	18	17	5
2 GENERAL MERCHANDISE		18,604	53	25	14	4	3
3 TRAILER VAN		4,848	18	4	2	0	0
4 GRAIN - UNIT		1,008	15	5	3	1	1
5 MISC - WORK TRAINS, ETC.		236	0	0	0	0	0
6 UNKNOWN		1,806	10	9	5	1	2
TOTALS		34,724	156	82	42	23	7

CODE	TRAFFIC	AXLE COUNT	SUMMARY OF PERCENT IN BAND				100+
			50-59	60-69	70-79	80-89	
1 COAL - UNIT		24	38	48	43	74	56
2 GENERAL MERCHANDISE		54	34	30	33	17	11
3 TRAILER VAN		14	12	5	5	0	0
4 GRAIN - UNIT		3	10	6	7	4	11
5 MISC - WORK TRAINS, ETC.		5	6	11	12	4	22
6 UNKNOWN							0
TOTALS		100	100	100	100	100	100

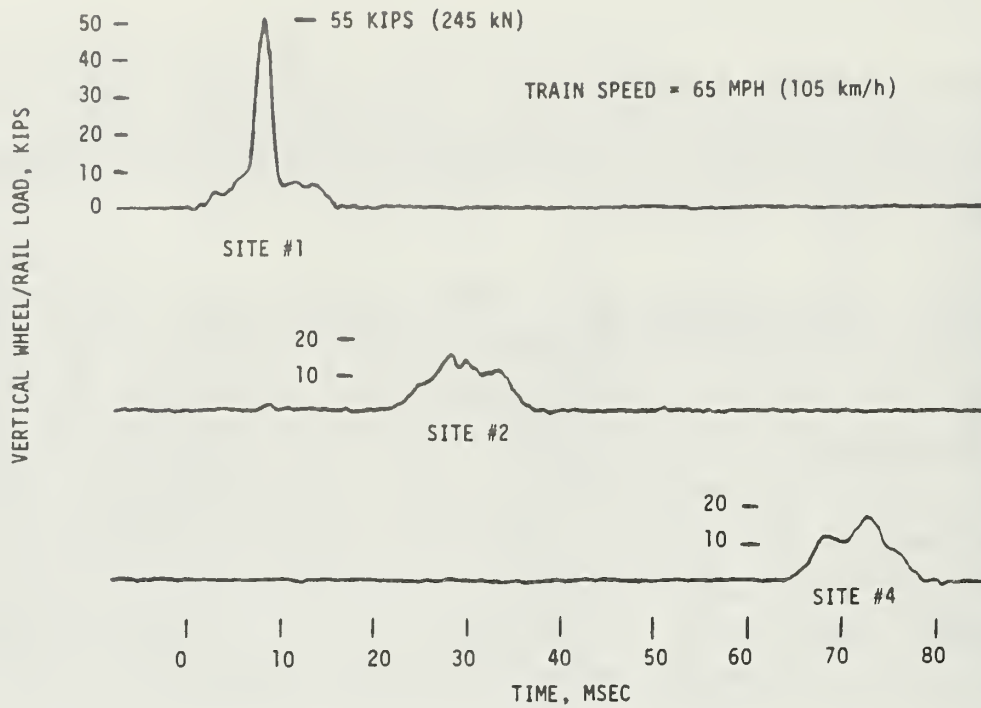
wheel profiles on passenger equipment, and (2) to correlate wheel tread conditions with the resulting impact loads. Other experiments were also conducted during this time period to characterize the track dynamic response to impact loads.

The test train consisted of an AEM-7 electric locomotive, three Amcoach cars, and two "Heritage" cars (older passenger equipment from pre-Amtrak service). The cars were selected from revenue trains based on high impact loads developed by one or more wheelsets when passing the impact detector site. Several wheelsets newly cut to the standard AAR 1:20 taper were also included in the consist. These cars represent fundamentally different truck designs: The Amcoach with the Budd Pioneer III truck with its elastomeric primary suspension, and the Heritage car with its equalizer beam, coil spring primary suspension and swing-hanger supported secondary suspension.

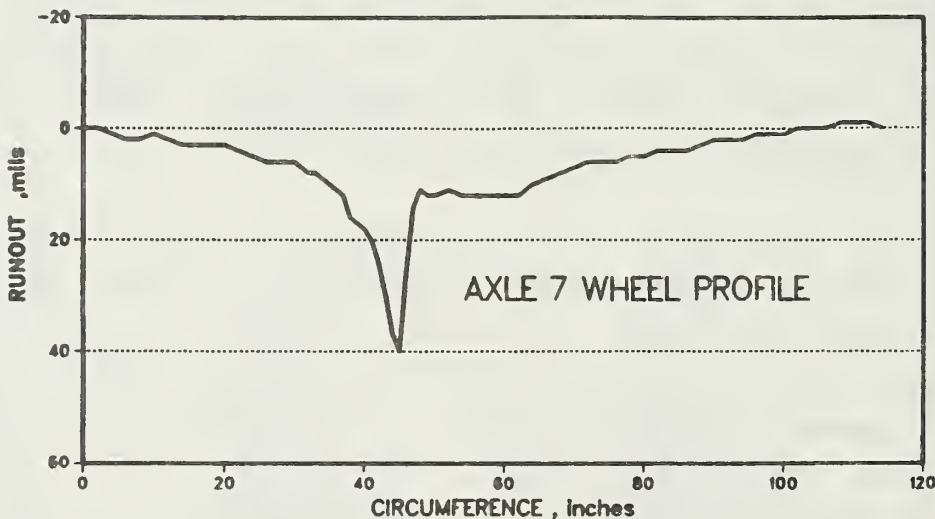
The track structure through the impact detector site is the current standard Northeast Corridor track: concrete ties on 24-inch centers, 140 lb/yd CWR with stiff EVA pads and Pandrol 601A clips. The track has a measured vertical stiffness under a nominal wheel load of 650,000 lb/in (tangent), or a track modulus of 10,500 lb/in/in per rail.

During the tests, wheel load measurements were recorded from the impact detector circuits in both analog and peak-load (tabulated) formats. The standard rail web strain gage patterns used as vertical load transducers in four successive cribs at the detector site provided trapezoidal load influence zones, approximately 8 inches long at full amplitude. Therefore, the impact detector in this configuration provides four successive "snapshots" of passing wheel load, and a 25 to 30 percent probability of capturing a particular impact load from a passing wheel. Repeated runs were therefore required at each test speed to increase the probability of measuring the true maximum under each wheel of the train.

An example of vertical wheel loads under a given wheel passing the impact detector site is shown in Figure 4-8a. This wheel had a single



a. VERTICAL LOADS UNDER AMCOACH AXLE #7



b. CIRCUMFERENTIAL PROFILE OF AMCOACH AXLE #7, RIGHT WHEEL

FIGURE 4-8. EXAMPLE OF WHEEL VERTICAL LOADS THROUGH IMPACT DETECTOR SITE UNDER AMTRAK TEST TRAIN

distinct profile anomaly, as shown in Figure 4-8b, that impacted directly over Site #1 in this particular run. Loads within the influence zones of the other two sites show relatively little dynamic variation about the nominal 16,000-lb vertical wheel load.

Vertical Wheel Load Versus Speed

Vertical load statistics for the Amtrak test train are compared in Figure 4-9 with the load statistics for one week of revenue traffic, passenger and freight. The higher concentration of impact loads from the collection of rough wheels is evident in the resulting cumulative probability curves. For example, slightly more than two percent of the measured wheel/rail vertical loads exceeded 50 kips for the test train, while only 0.4 and 0.6 percent exceeded 50 kips for freight and passenger traffic, respectively. (Note that these statistics were gathered prior to the start of Amtrak's wheel truing program.) Although the test train had a higher than normal population of rough wheels, the impact detector measurement site was capable of detecting about 19 to 23 percent* of a particular wheel's circumference as it passed, or roughly a one-in-four chance of measuring the highest load under the worst spot on a wheel. The random nature of the peak measured loads for repeated runs in different speed bands is seen in the load-versus-speed plots of Figures 4-10 and 4-11.

Load-versus-speed plots for the most severely worn wheel on the test train's Amcoach and Heritage cars are given in Figures 4-10 and 4-11, respectively. A sufficient number of repeated runs were made in each speed band to assure that representative load maxima were measured. In each figure two curves have been drawn, one a linear envelope of the largest loads measured at each speed, and the other a linear least-squares fit of the largest loads at each speed. The curves indicate that there is a measurable

* Site 3 was "Inoperative" as explained in Section 4.3, Rail Running Surface Profiles.

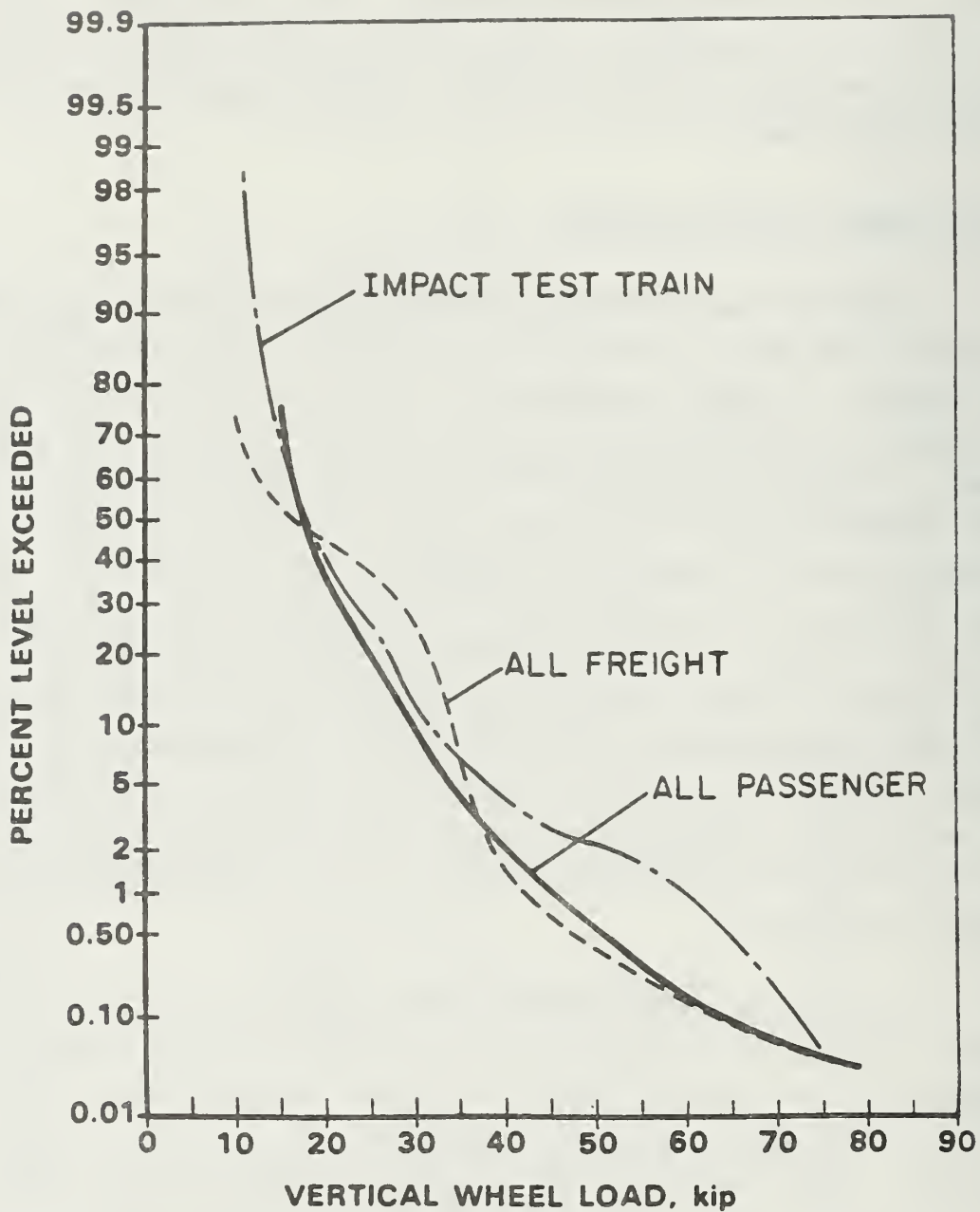


FIGURE 4-9. COMPARISON OF TEST TRAIN WHEEL LOAD STATISTICS WITH REVENUE FREIGHT AND PASSENGER TRAFFIC

PEAK LOADS FOR THREE WORST AMFLEET WHEELS

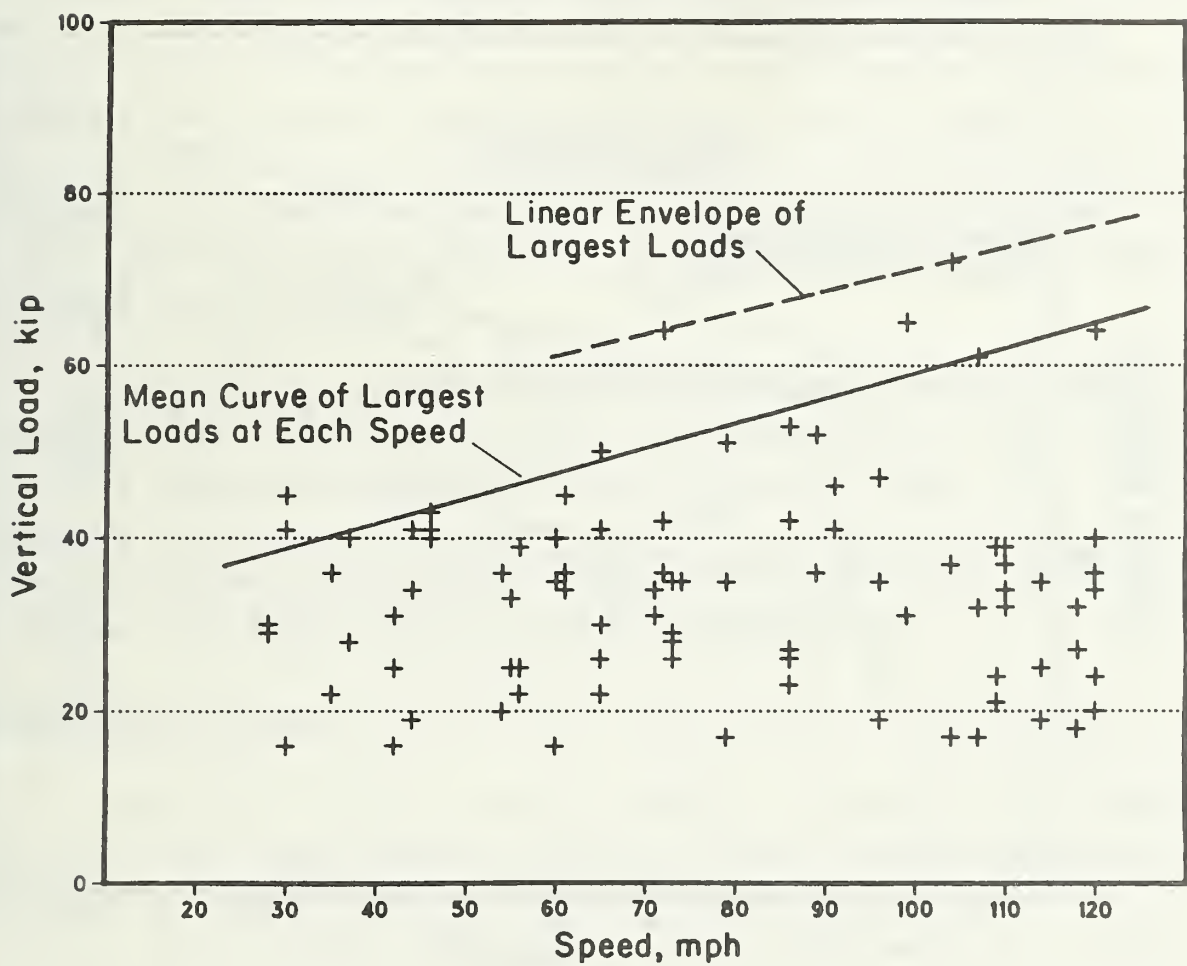


FIGURE 4-10. PEAK VERTICAL WHEEL LOAD MEASUREMENTS VERSUS SPEED FOR AMCOACH WHEELS ON IMPACT TEST TRAIN

PEAK LOADS FOR FOUR WORST HERITAGE WHEELS

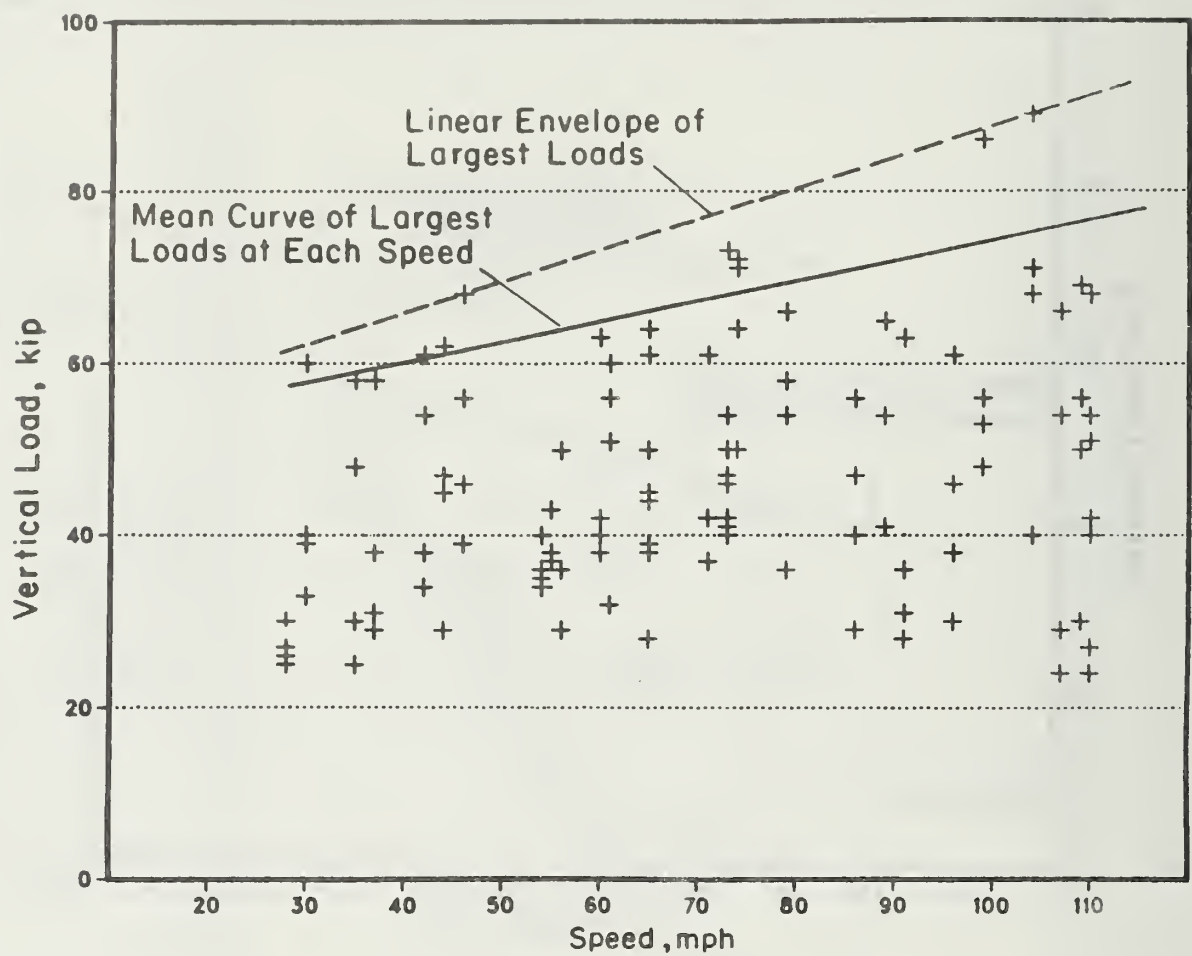


FIGURE 4-11. PEAK VERTICAL WHEEL LOAD MEASUREMENTS VERSUS SPEED FOR HERITAGE WHEELSETS ON IMPACT TEST TRAIN

increase in load with increasing speed. Based on the least-squares curves, the increase in load for a factor of four speed increase (25 to 100 mph) is about 33 percent for Heritage wheelsets and about 60 percent for Amfleet wheelsets. These relatively modest increases in peak load suggest that it would probably be neither effective nor economical to place slow orders on trains with "bad" wheelsets as an alternative to removing the wheelsets from service, since those wheelsets may cause damaging loads even at lower speeds, as shown in these two figures.

The differences between loads measured from the Heritage and Amfleet equipment are attributed mainly to the larger population of out-of-round wheels and longer-wavelength profile errors on the Heritage cars. These differences in wheel profile characteristics in turn may be caused by different mileages accumulated by the equipment, and possibly by differences in response due to truck suspension or brake characteristics.

Measured Wheel Profiles

Immediately following the tests, some of the wheelsets were removed from the cars for measurement of profiles at the Ivy City (Washington, D.C.) wheel shop. A special profilometer was designed to measure the changes in effective radius of wheel rotation around the circumference of the wheel. This profilometer consisted of a piece of rail head guided in the plane of rotation of the wheel, on the desired cant angle. The rail head was spring-loaded on a plunger to move in or out on the wheel radial line. The wheel was then rotated while cradled in its own bearings, and changes in the radial position of the rail head as it followed the contact patch were measured at the plunger with a dial indicator. These measurements provided a direct indication of tread vertical roughness or runout as "seen" by the contact patch. Examples from six of the test train wheels, two Amcoach (Axles 9 and 10) and four Heritage car (Axles 19-22), are shown in Figure 4-12. Vertical loads from several of these wheel sets were evaluated to correlate wheel profile condition with impact load level. Example cases are discussed below:

- ① Axle 9. The major anomaly on this Amcoach wheelset was a 1 x 1 inch spall indicated in Figure 4-12 by the 0.050 inch dip near

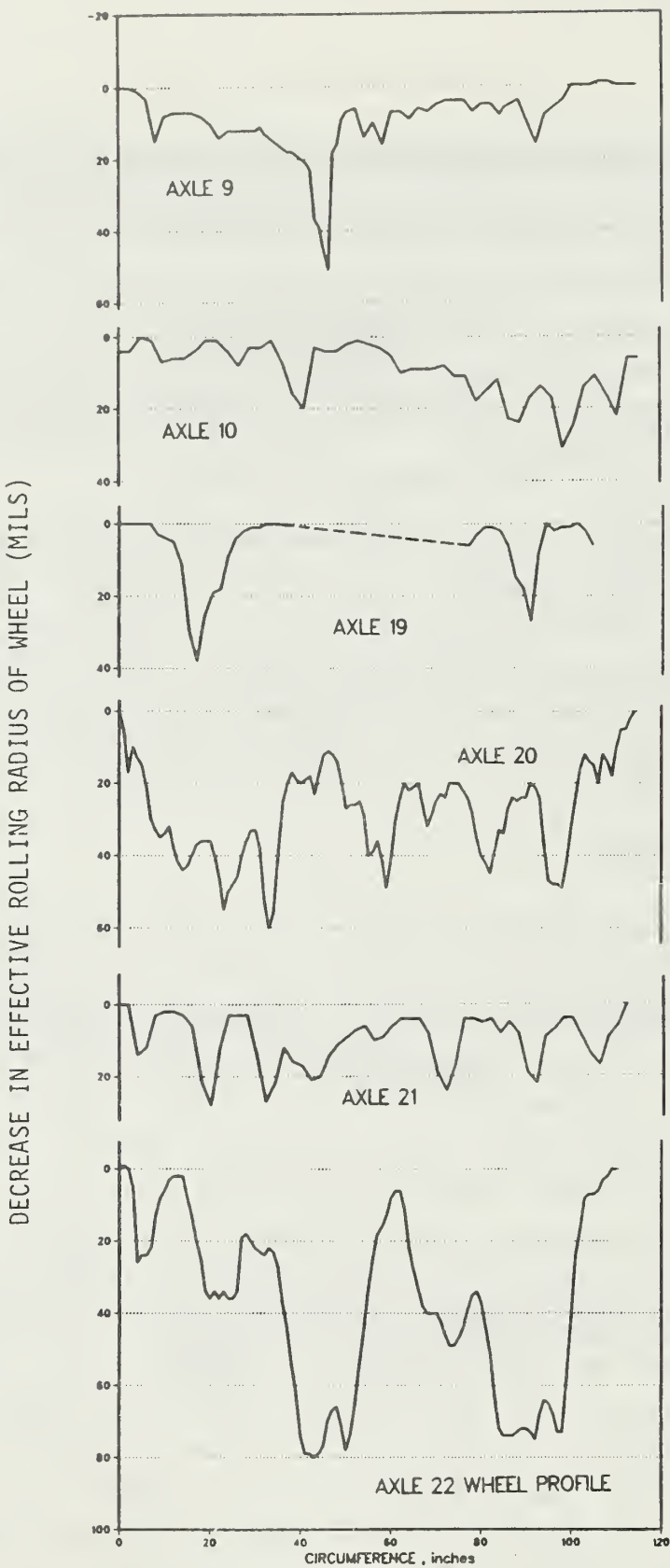


FIGURE 4-12. MEASURED CIRCUMFERENTIAL WHEEL PROFILES (RUNOUT) OF AMTRAK TEST TRAIN WHEELS

the 45-inch circumference location. The measured loads from this wheel showed peaks in the 65 to 75-kip range at speeds above 70 mph.

- ⑥ Axle 10. A significant characteristic of this Amcoach wheelset was that it was not condemnable by current AAR standards*. The principal anomaly on the wheel set was long, narrow chain of spalls which is shown in Figure 4-12 by the 0.035 inch runout near the 35 inch circumference location. The highest impact loads were measured under this wheel were 45 kips at 30 mph, 61 kips at 108 mph.
- ⑦ Axle 19. This Heritage wheelset was characterized in Figure 4-12 by two distinct irregularities with runouts of 0.038 and 0.027 inch. (Profiles were not measured outside these two areas.) The load data for this wheelset showed a small speed effect, with peak impact loads of 60 to 75 kips over a wide speed range.
- ⑧ Axle 21. This Heritage car wheelset was another example of a non-condemnable profile which would pass the AAR criteria. As shown in Figure 4-12, small spalls (less than 0.030 inch runout) were present around the circumference. These irregularities were sufficient to cause peak impact loads of up to 70 kips.
- ⑨ Axle 22. This heritage car wheelset was the roughest on the test train. As seen in Figure 4-12, the wheel was visibly out-of-round, with a spread rim and spalls everywhere on the tread except at locations of maximum runout, where spalls were cold-rolled out. The load data plotted in Figure 4-13 for this wheelset indicate a possibly strong speed effect. Peak measured loads ranged from less than 40 kips at 30 mph to nearly 90 kips at over 100 mph. This case might be considered academic, since the wheelset was condemnable, even though not necessarily for the right reasons. Evidence of bearing grease loss and incipient bearing failure had made Amtrak mechanical personnel reluctant to use the wheelset, even on a test train. This case emphasizes the need to detect and remove such a wheelset quickly from the fleet to avoid potentially severe track and equipment damage.

* AAR Interchange Rule 41A1m which states that a wheel is "condemnable at any time" if the following conditions exist: "Out of round: in excess of 1/32 inch within an arc of 12 inches or less with use of gage as shown", or Rule 41A1 on Slid Flats: "A. Two inches or over in length, b. Two adjoining spots each $1\frac{1}{2}$ inch or over in length. (Rule 41A1m has been dropped in recent editions of the AAR manual.)

PEAK LOADS FOR WORST WHEEL IN CONSIST

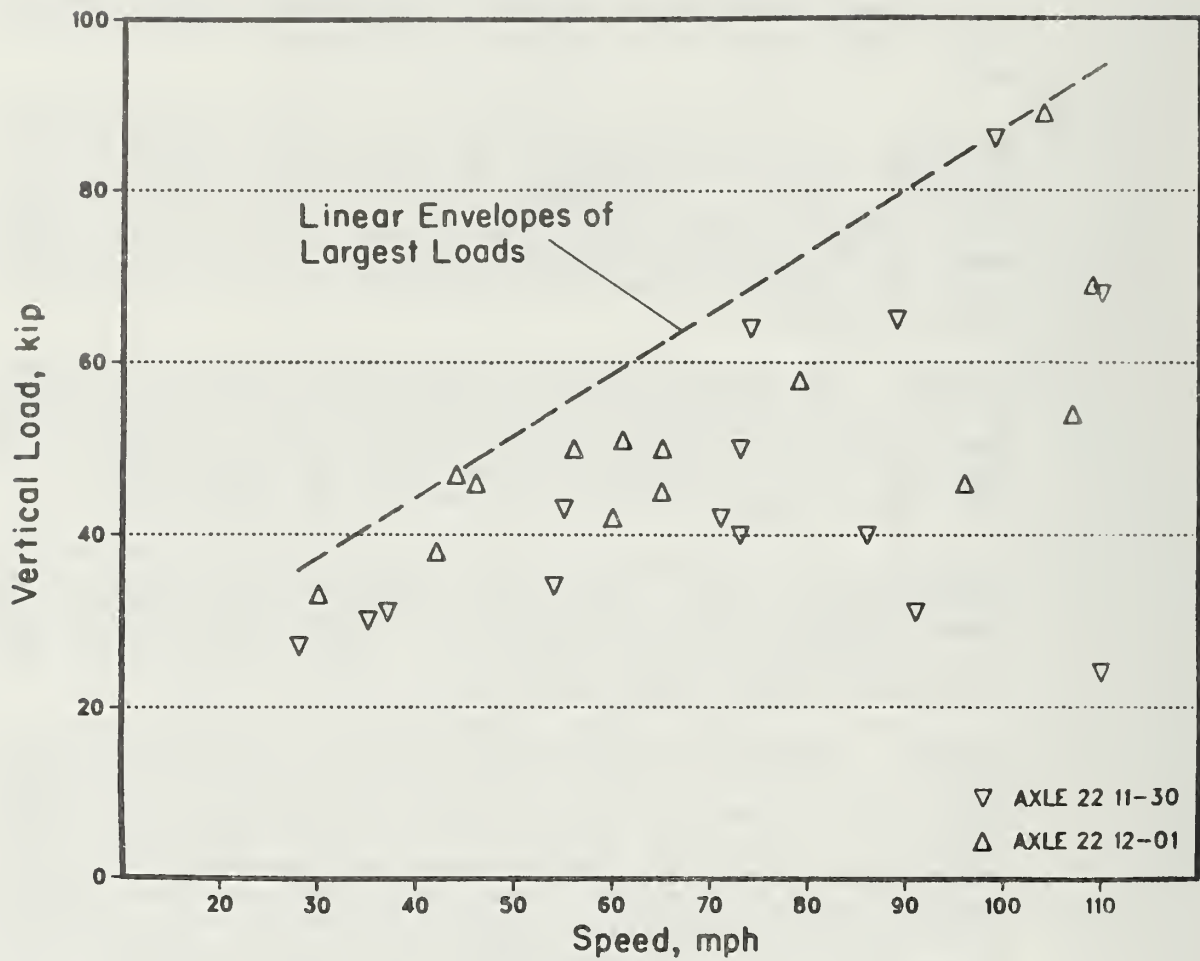


FIGURE 4-13. PEAK VERTICAL WHEEL LOAD MEASUREMENTS VERSUS SPEED FOR HERITAGE CAR WHEELSET, AXLE 22, OF IMPACT TEST TRAIN

Two of the Heritage car wheelsets, Axles 17 and 18, were freshly turned just prior to the tests to provide a "control" case. As expected, the loads from these wheels were extremely consistent. Peak loads versus speed for these wheels are plotted in Figure 4-14. The loads are essentially constant with speed over the range of test speeds from 25 to 110 mph. A histogram, expanded in scale, is also shown in Figure 4-14. The mean load for these axles was 16.5 kips with a standard deviation of 0.9 kips, or 5 percent. When compared with the variation in loads under the worn wheels, the 5 percent variation is indeed small.

4.2.2 Computer Simulation Development

The widespread interest in wheel/rail impact loads has led to the development and use of a wide variety of analytical models. These range in complexity from simple two-mass models to complex finite-element models of the track. Sato and Kosuge [7] have recently employed a simple lumped-parameter model consisting of the wheelset (unsprung) and rail effective masses to study rail head surface roughness on the high-speed Shinkansen line of the Japanese National Railways. Newton and Clark of British Railways, on the other hand, have used a much more complex hybrid model [8], which consists of a Discrete Support Model with a simple Euler beam to calculate the wheel/rail contact force, and then a Timoshenko beam model on elastic (Winkler) foundation to calculate rail strains in response to this force. In this discrete support model, a modal analysis is used to calculate the forced motion of the track, using the normal modes associated with the undamped track natural frequencies. A similar approach was employed by Mair [9,10] in his study of rail corrugation.

Battelle's vertical wheel/rail impact load model was originally developed to explore the effects of rail joint and flat wheel geometries on wood-tie track structures [11]. This simplified lumped-parameter model consisted of two track masses (the effective rail and tie/ballast masses) and two vehicle masses (an unsprung wheelset and a sprung half-car body). The nonlinear contact stiffness at the wheel/rail interface described by Jenkins, et al [12] was used, and track mass, stiffness and damping parameters were

PEAK LOADS FOR FRESHLY TURNED WHEELS

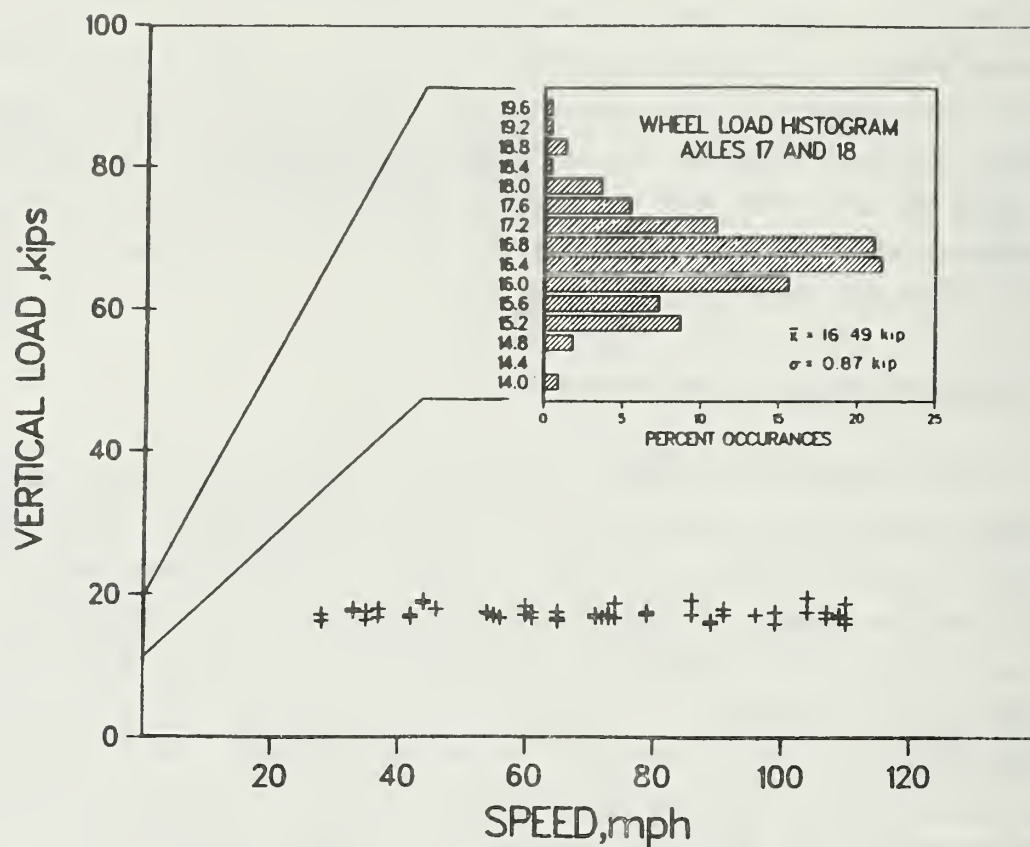


FIGURE 4-14. PEAK VERTICAL WHEEL LOAD MEASUREMENTS VERSUS SPEED UNDER FRESHLY-TURNED HERITAGE CAR WHEELS

calculated from the traditional beam-on-elastic-foundation (BOEF) relationships. Model-predicted loads compared well with wheel loads measured with an instrumented wheelset on a 100-ton hopper car [13]. In this same study, impact loads were measured by rail strain-gage circuits under passing revenue trains. Although the actual wheel profile geometries were not known, the load magnitudes and time durations compared well with predictions from the model using assumed wheel flat shapes.

Efforts to use this simple model to predict impact loads on concrete-tie track, however, were not successful. As predicted by Newton and Clark [8], the simple BOEF model tended to overestimate the peak impact loads. Additional degrees of freedom were added to the model, including the side frame/equalizer beam mass and mass-moment of inertia. Tie and ballast masses were separated and a nonlinear rail/tie (pad) stiffness was added, based on laboratory test results. This seven degree-of-freedom (DOF) model predicted impact loads that compared well with measured loads under a known wheel profile [4].

A more controlled synthesis and validation of the model was possible after the experiments with the Amtrak test train were completed. From these tests, measured wheel load time-histories under measured wheel profiles on a well-defined track structure were at last available to us.

A specialized version of the computer program, called IMPWHL, was created to use the measured profile data. The measurements are introduced in tabular form, up to 120 points, on given increments. The program currently uses a simple linear interpolation between points to generate the wheel/rail vertical error position and velocity. Other mathematical methods for providing a smoother input function, such as the cubic spline, have been considered; but the results to date do not justify the use of these more complex algorithms.

Initial computer runs with the measured profiles were compared with time-history traces of impact loads "captured" within the influence zones of the impact detector circuits. This provided a short time-history "snapshot"

of the passing wheel load -- roughly 8 milliseconds at full amplitude at 60 mph, only 4 milliseconds at 120 mph. If the initial impact occurred at the leading "skirt" of the circuit, the secondary load peaks could be observed. By repeated runs, a fairly complete picture of load response could be reconstructed.

These first computer runs showed a strong oscillatory load response at 330 Hz which was not observed in the measured loads. This frequency is prominent in the track response to a drop-hammer impact load with no preload, as shown in Figure 4-15: it is associated with the second (asymmetrical) transverse bending mode of the concrete tie. Tests showed that this response peak is suppressed as the preloading wheelset is moved closer to the point of impact. Upon reflection, it occurred to us that this tie bending mode could be acting as a tuned absorber, and we decided to include the first four tie transverse bending modes in the model.

Concrete tie bending modes were defined in laboratory tests on a similar tie, supported by pads under the rail seats. A modal analysis was performed on this tie using a Hewlett-Packard Model 5423A dual-channel analyzer by attaching an accelerometer to one corner and striking locations along the tie with an instrumented hammer. Results for the first three transverse bending modes are shown in Figure 4-16. (Two torsional bending modes at 365 and 406 Hz were also observed.) Based on an average bending rigidity from the first three measured modes, the fourth (asymmetrical) bending mode frequency was calculated to be 1033 Hz. Only the first bending mode of the tie appears to shift significantly in the track from the laboratory-measured value, increasing from 108 Hz to 154 Hz, as seen in Figure 4-15. Measured damping of these modes was small, roughly 0.5 percent of critical: as expected, the concrete tie literally "rings like a bell".

A comparison of model-predicted forces for a portion of one of the measured wheel profiles of Figure 4-12, with and without the tie beam-bending modes, is shown in Figure 4-17. A rather dramatic difference in the force time-histories can be seen. An example comparing the measured load from a "direct hit" on a rail load circuit with the predicted load for the same wheel

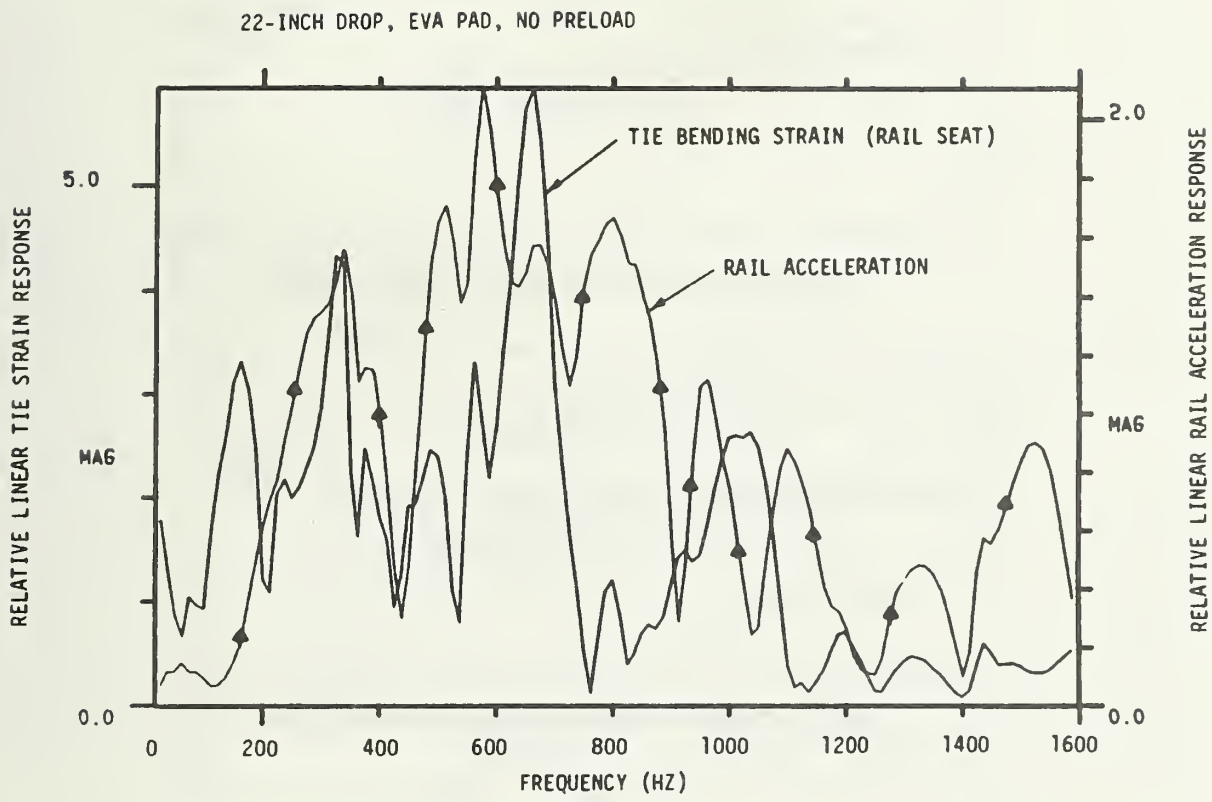
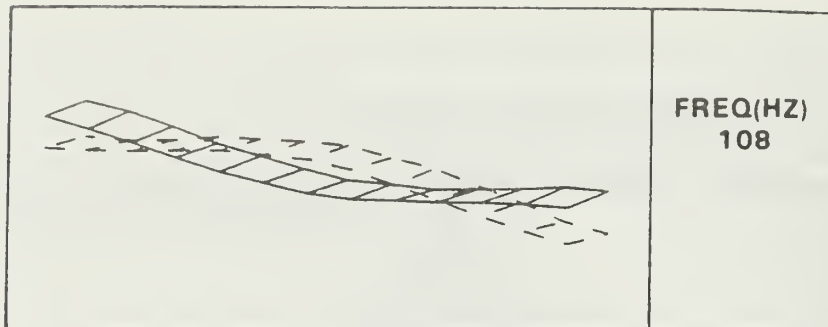
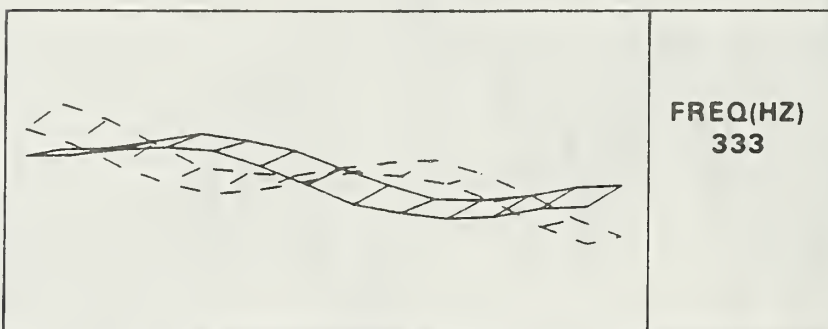


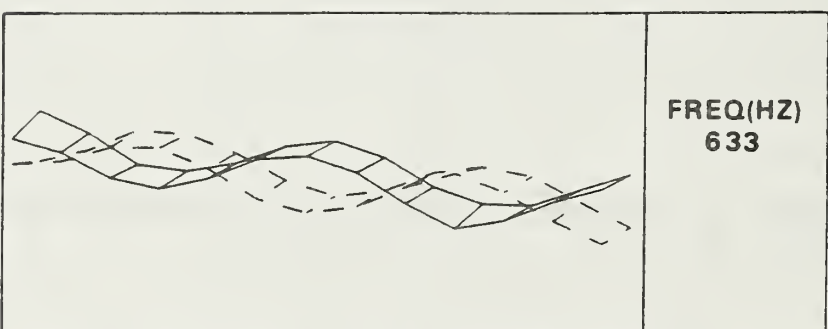
FIGURE 4-15. CONCRETE TIE TRACK RESPONSE TO DROP-HAMMER IMPACT LOAD



(A) FIRST BENDING MODE RESPONSE



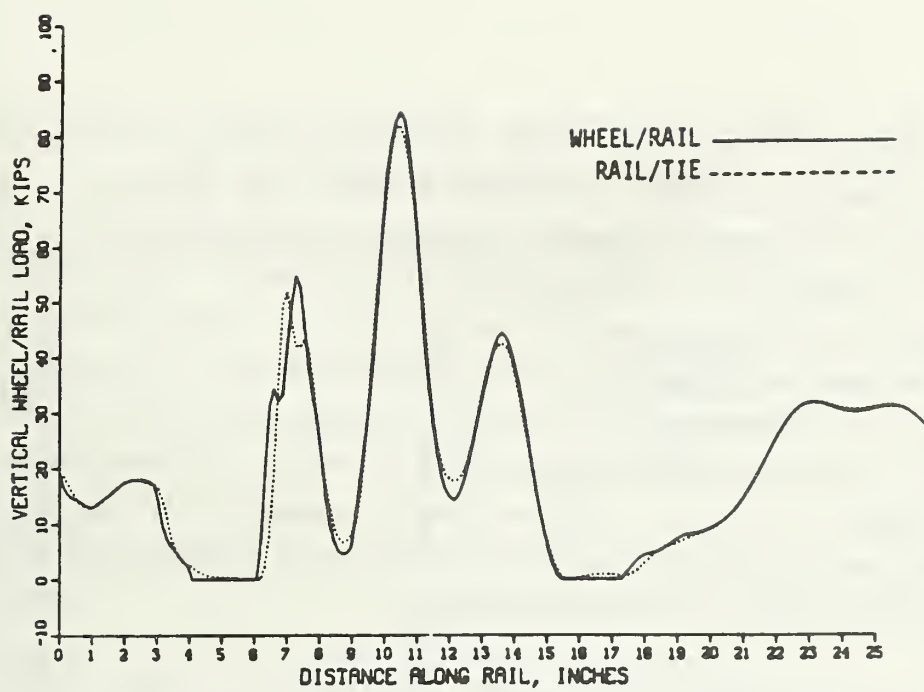
(B) SECOND BENDING MODE RESPONSE



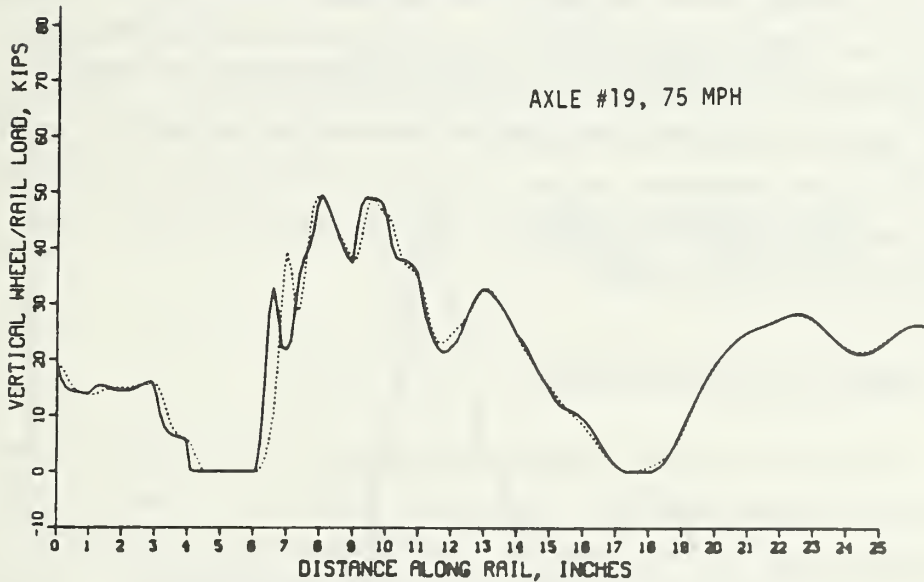
(C) THIRD BENDING MODE RESPONSE

**SAMPLES OF FIRST THREE BENDING MODES
FOR CC-244-C CONCRETE TIE**

FIGURE 4-16. SHAPES OF CONCRETE TIE TRANSVERSE BENDING MODES



a. 7 DEGREE-OF-FREEDOM MODEL (WITHOUT TIE BENDING MODES)



b. 11 DEGREE-OF-FREEDOM MODEL (WITH TIE BENDING MODES)

FIGURE 4-17. COMPARISON OF WHEEL IMPACT LOAD SIMULATION
WITH AND WITHOUT CONCRETE TIE BENDING MODES

profile anomaly is shown in Figure 4-18. The predicted load shows an oscillatory load response beyond the peak load, which in the measured time-history is beyond the influence zone of the circuit. The predicted response also shows minor oscillations in the 800-1000 Hz frequency range. This may be due to the one-inch piecewise linear representation of the wheel profile. On the other hand, the rail itself exhibits a transverse bending mode near 800 Hz that is not specifically considered in the model. This mode is influenced by static wheel load and by adjacent wheels. However, it may act as a tuned absorber itself at these frequencies, effectively suppressing any oscillations in the 800 Hz region in the measurements.

The predicted load versus speed curve for Axle 19 is plotted in Figure 4-19 along with the measured maximum loads for this wheel profile. Predicted peak loads were based on the larger of two profile anomalies, shown near the 20-inch circumference position in Figure 4-12. Correlation is quite good at speeds below 80 mph. Above 80 mph the predicted values are much higher than the measured values, which indicates that the peak values of impact load were not captured for Axle 19 within the rail circuit influence zones at these higher speeds.

4.2.3 Energy Loss Considerations

One of the more interesting aspects of the study was the calculation of the energy dissipated by worn wheel profiles. Since a time-integration solution was used in the computer simulation program, it was a simple matter to calculate the damping forces and relative displacements for each time-step and sum these for the vehicle and the track, separately, over the total solution time. This typically ran 20 milliseconds, or 20 to 30 inches of the wheel circumference. Typical values are given in Table 4-2 for three of the wheel profiles of the test train. Just the larger of the two measured divots on Axle #19 is considered in this table. For a wheel rough around its whole circumference (such as Axle #20, and probably Axle #19), the energy consumed by wheel roughness can easily exceed 20 hp (15 kW) per wheel. In terms of the Davis equation for calculating drawbar resistance, Axle 19 would apply roughly 150 lb of drag at 74 mph, or 2 lb/ton per wheelset. This assumes that the

VERTICAL LOADS UNDER HERITAGE CAR AXLE #19 OF TEST TRAIN (74 MPH)

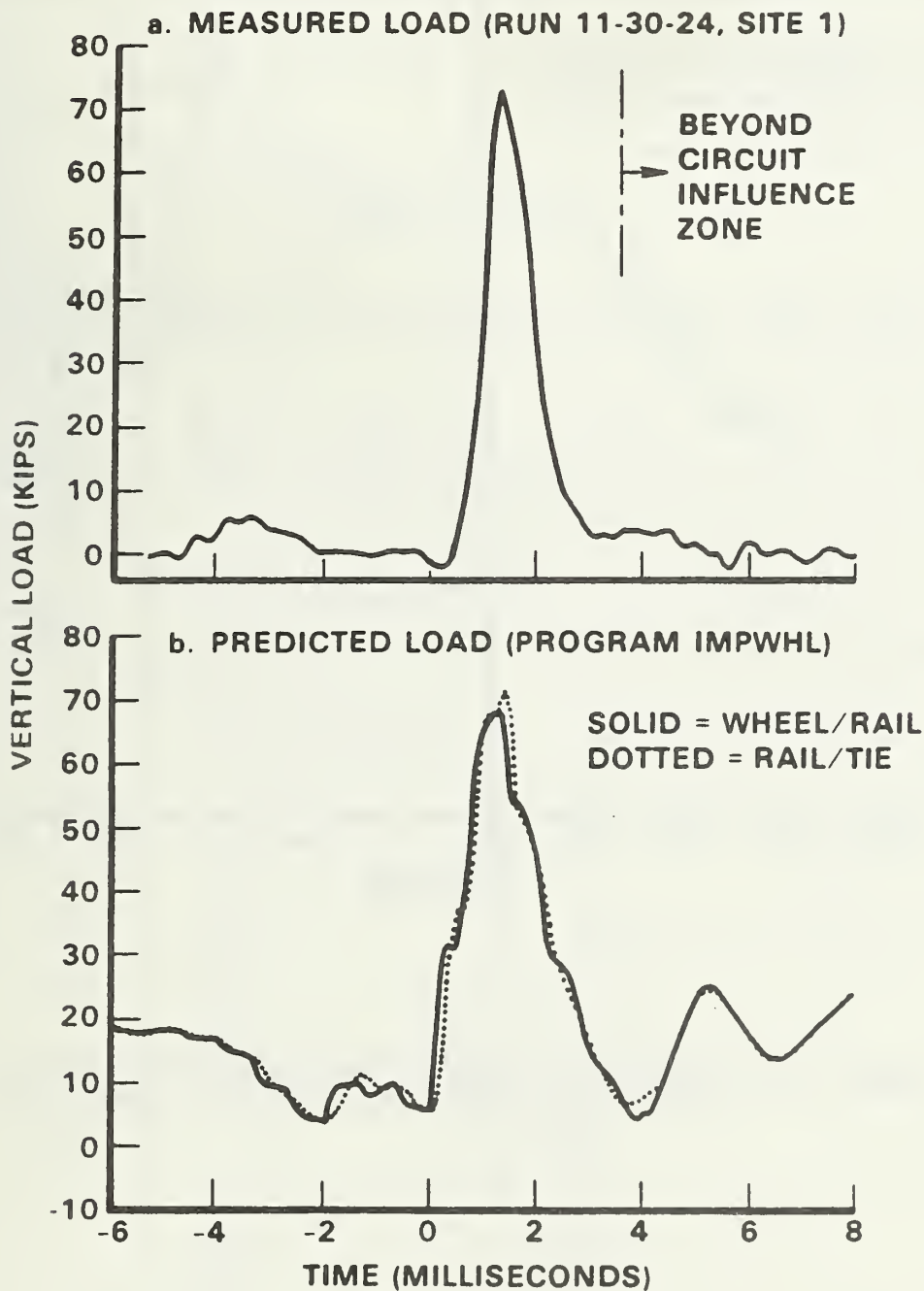


FIGURE 4-18. COMPARISON OF PREDICTED AND MEASURED LOAD TIME-HISTORIES FOR HERITAGE CAR WHEEL TREAD ANOMALY

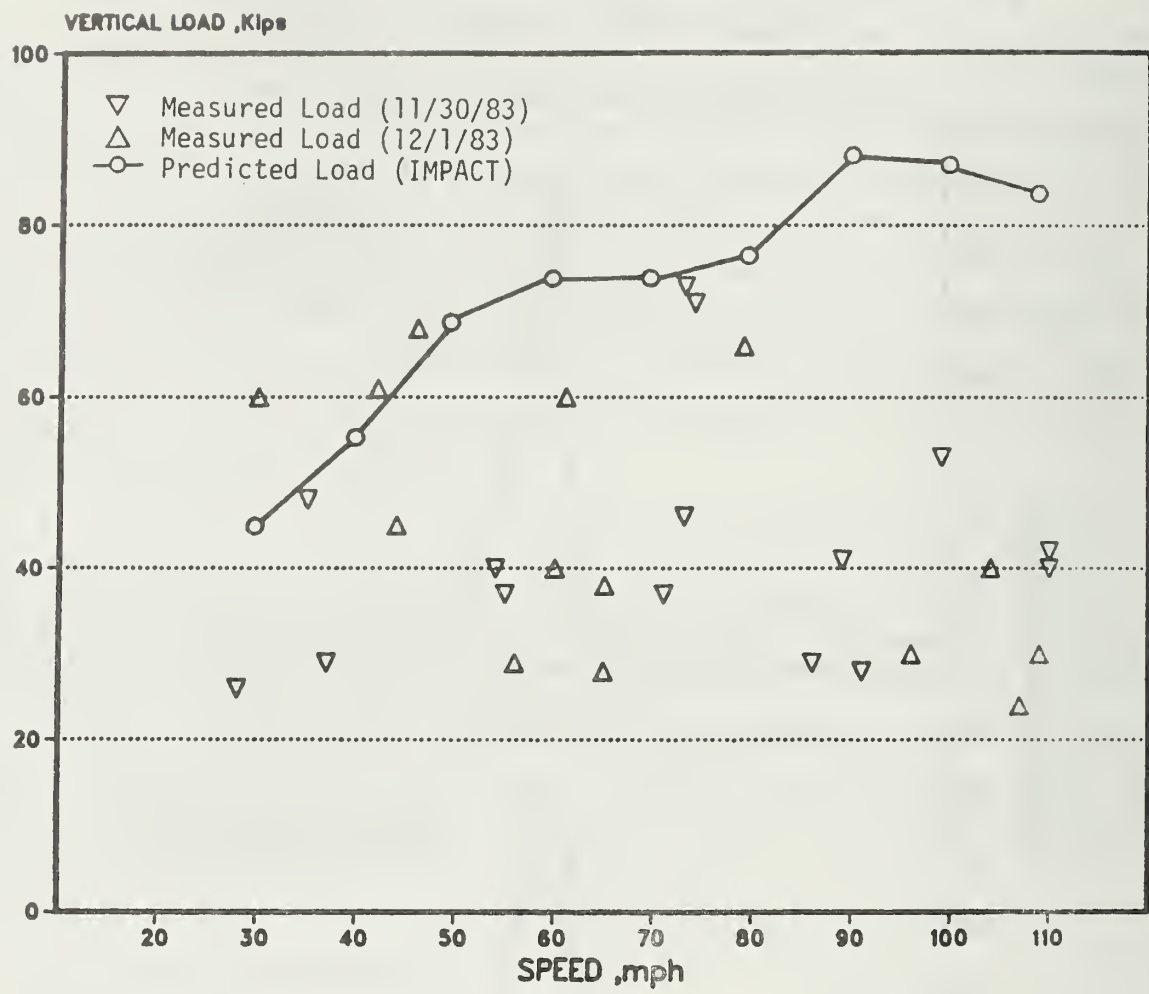


FIGURE 4-19. COMPARISON OF PREDICTED AND MEASURED PEAK LOADS FOR AXLE 19 OF IMPACT TEST TRAIN OVER SPEED RANGE

TABLE 4-2. ENERGY DISSIPATED BY TYPICAL ROUGH WHEEL PROFILES

Axle*	Speed (mph) (km/h)	Vehicle (ft-lb) (Joules)	Track (ft-lb) (Joules)	Over Divot (hp) (kW)	Average Power Over Wheel# (hp) (kW)					
7	65	105	25	34	214	290	22	16	4.4	3.3
9	71	114	33	45	270	366	28	21	6.1	4.6
19**	74	119	38	52	356	483	36	27	8.3	6.2

* See Figures 4-8 and 4-12.

** Larger profile error only

Remainder of wheel circumference assumed smooth

second divot dissipates about two-thirds the energy that the larger divot dissipates, and that both wheel profiles are the same. It is of interest to note that only about ten percent of the energy is dissipated in the vehicle suspension, the rest in the track structure.

4.3 Rail Running Surface Profiles

An additional opportunity to validate the model was gained when by chance an "engine burn" or rail surface anomaly occurred during October 1983 almost centered on one of the rail strain-gage circuits of the Edgewood impact detector. This defect was initially described as 1.75 inch in length, 0.017 inch in depth, from the rail centerline outward, and rusty on its bottom surface. Load time-histories were recorded during runs of the Amtrak test train, and comparative runs with the impact load model were made with "best-guess" profile shapes with some success. In April 1984, a newly-designed rail running-surface profilometer was used to measure rail anomalies (engine burns, welds) on the Northeast Corridor track. This provided an accurate definition of the "engine burn" at Site #3 of the impact detector, as well as a description of rail surface anomalies within the Track Condition Assessment Test Sites.

4.3.1 Rail Profile Measurements

The rail longitudinal surface profilometer shown in Figure 4-20 was designed and fabricated, and checked for sensitivity and accuracy in the laboratory. This profilometer consists of a one-radian (36-inch) segment of wheel to represent a 36-inch Amcoach wheel. The precision-ground wheel segment center of rotation is guided vertically on pairs of bearings in a A-frame and an intermediate link assembly, all of which in turn are guided longitudinally on linear bearings and two parallel, hardened and ground rods. This assembly is fastened to a horizontal frame that rests on two points on the rail being measured (roughly 50 inches apart) and one point on the opposite rail, establishing the plane of the track. Pivoted shims on this third point allow the effective wheel taper of the precision wheel segment to

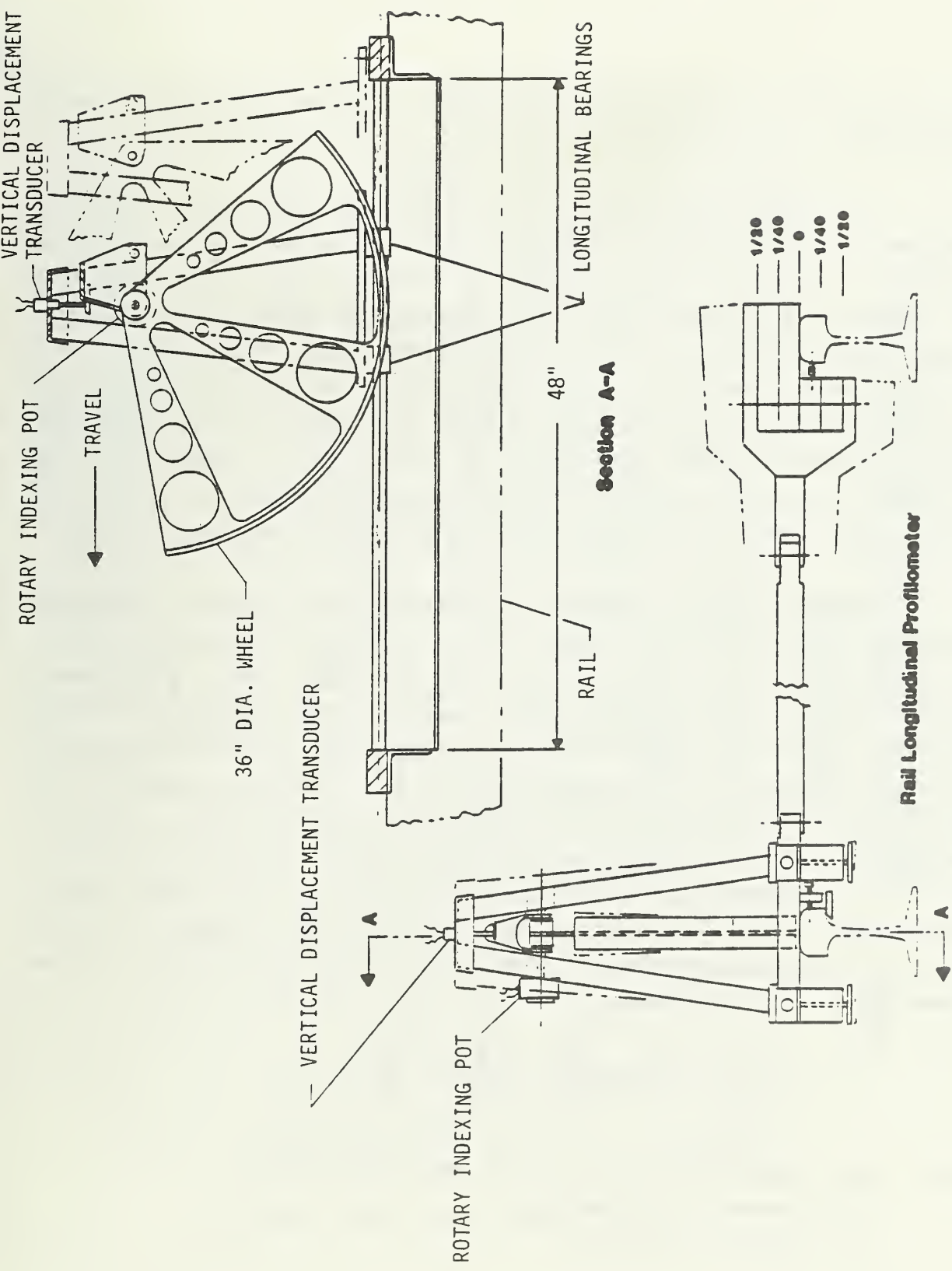


FIGURE 4-20. RAIL LONGITUDINAL RUNNING-SURFACE PROFILOMETER

be varied from +1:20 (the standard AAR taper) to a minus 1:20 (a hollow-work wheel tread).

The actual measurement of the rail surface anomaly, which is centered in the wheel travel, is done by slowly moving the wheel segment from one end to the other. Vertical motions of the pivot point within its guides are translated by the DCDT into Y-axis displacement of the plotter pen with distance along the X-axis. This represents the forced displacement of the wheelset center of rotation by the geometry error, and is a direct input into the dynamic model without the need for geometric translation. The model then provides vertical dynamic deflections of the track in response to load variations. Some minor distortion of the wheel/rail geometry will occur, of course, due to changes in contact patch stresses under the high impact loads.

Tests of the profilometer were conducted in the Aberdeen, MD area on April 19, 1984. Profiles of several of the more prominent engine burns within the Track Survey Site 1 test sections were measured. These engine burns generally occur in pairs (one each rail), sometimes under two wheelsets at the same time. Profiles at four different wheel tapers at a typical engine burn are shown in Figure 4-21. The engine burn itself is seen in the center of the profile plot as a sharp dip 0.005 to 0.010 inch in depth. What is striking, however, is the long wavelength depression of the rail on the order of 40 to 60 inches, apparently due to service-bending of the rail under dynamic loading. The engine burn begins to look very much like a dipped rail joint after some time under traffic. In Figure 4-21, the long wavelength profile assumes approximately the shape:

$$e_z = D_e [1 - \sin (\frac{\pi x}{L_s})], \quad \frac{-L_s}{2} < x < \frac{L_s}{2}$$

where... D_e = geometry error depth (under long straight-edge)

L_s = geometry error total span

x = distance along rail.

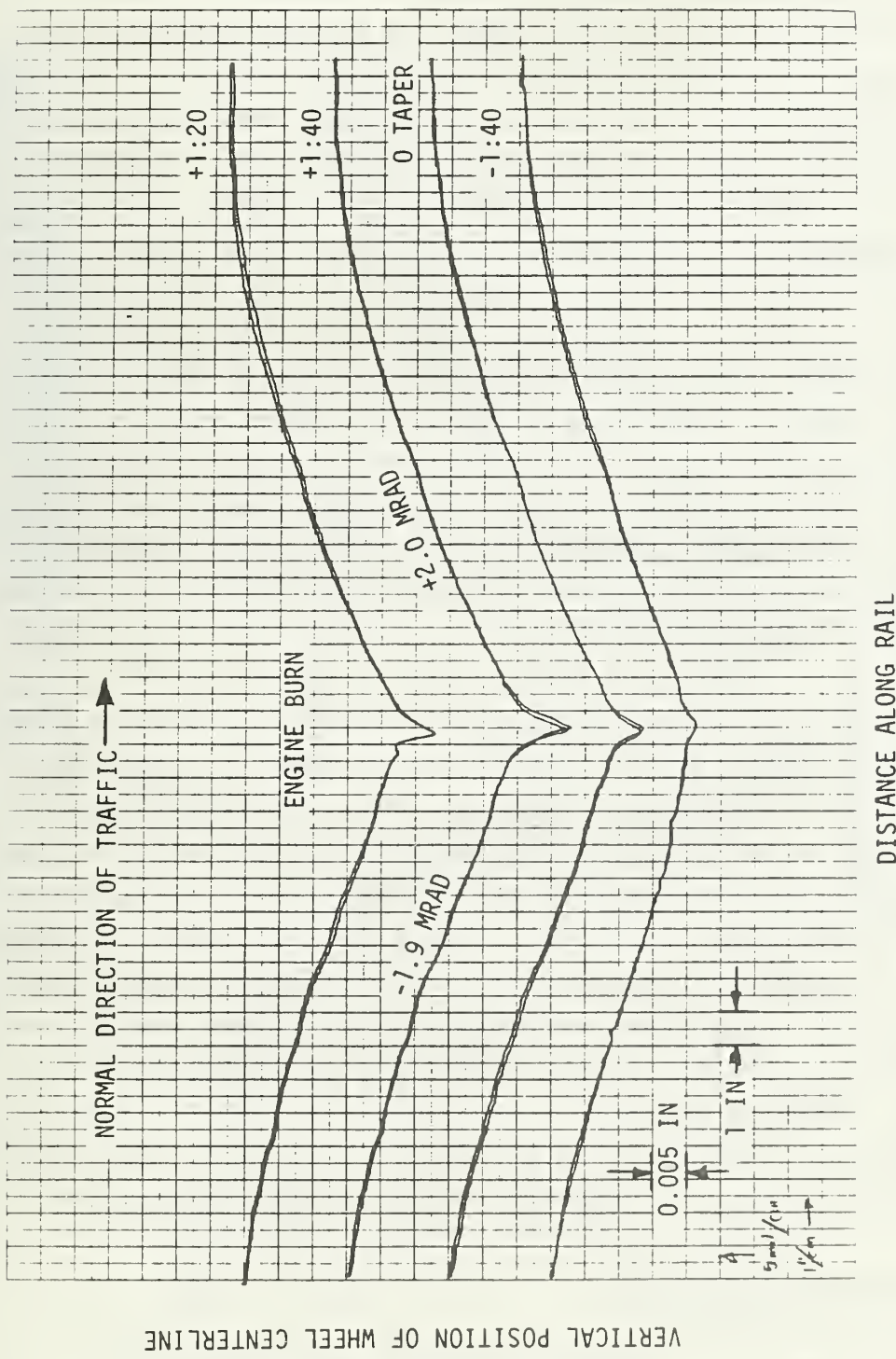


FIGURE 4-21. MEASURED RAIL RUNNING-SURFACE PROFILE NEAR ENGINE BURN, M.P. 67.00, SITE 1, SECTION 1, TIE 72, E. RAIL

The long wavelength geometry assumes a ramp angle of roughly 2 milliradians within the ten-inch span before and after the anomaly itself, which in itself is within established maintenance limits. For example, Australian National [14] uses a weld misalignment ramp angle limit of 7 milliradians to avoid rail seat pad damage; and British Rail considers a ramp angle of 10 milliradians as a maintenance exception level. Both field and gauge-side fasteners at the location in Figure 4-21 had fallen out, been replaced, and were again moving out of the inserts.

An example of a more severely battered engine burn is shown in Figure 4-22. Here the ramp angle entering the damaged area (in the normal direction of traffic) is roughly 2 mrad, but the angle out of the engine burn is at least 7 mrad. At this location, track damage (other than the engine burn itself) included the gauge-side clip out, both inserts loosening with a visible field-side insert crack, and extensive spalling of the rail on the gauge side of the running surface.

The most severe engine burn profile measured is shown in Figure 4-23, with a total depth (to the bottom of the burn) of 0.090 inch. The wavelength of this disturbance was longer than the 50-inch span of the profilometer and was estimated to be 60 inches. In the direction of traffic, a 4 mrad ramp angle steepens to 11 mrad in the last few inches before the engine burn, with an included angle of about 24 mrad over a 5-inch span. Track damage included field and gauge-side clips missing, a broken insulator, and a loose insert. To estimate the dynamic vertical forces generated at this site, the profile of Figure 4-23 was used (in place of a wheel profile) in the impact model. Predicted load response is shown in Figure 4-24 for a simulated Amcoach wheelset at 120 mph. A peak load of 66,300 lb was predicted, dissipating 417 ft-lb into the track, 80 ft-lb into the vehicle suspension.

4.3.2 Impact Detector Site Tests

Measurements were made of the Edgewood impact detector site "engine burn" (Circuit #3). This anomaly was first noticed (as an impact load-producing site) during October 1983. The profile shape was estimated at the

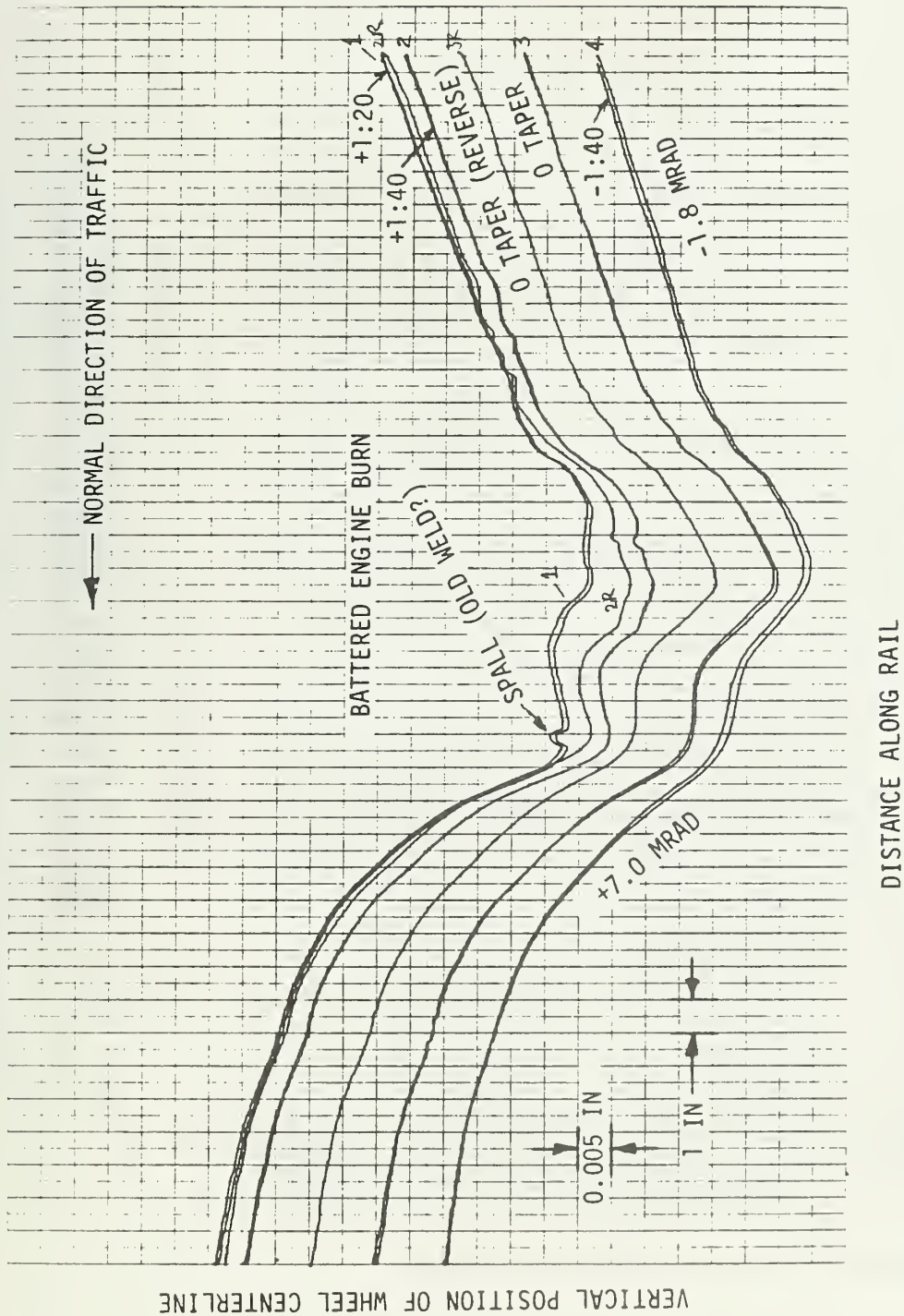


FIGURE 4-22. MEASURED RAIL RUNNING-SURFACE PROFILE NEAR ENGINE BURN, M.P. 67, SITE 1, SECTION 4, TIE 8, W. RAIL

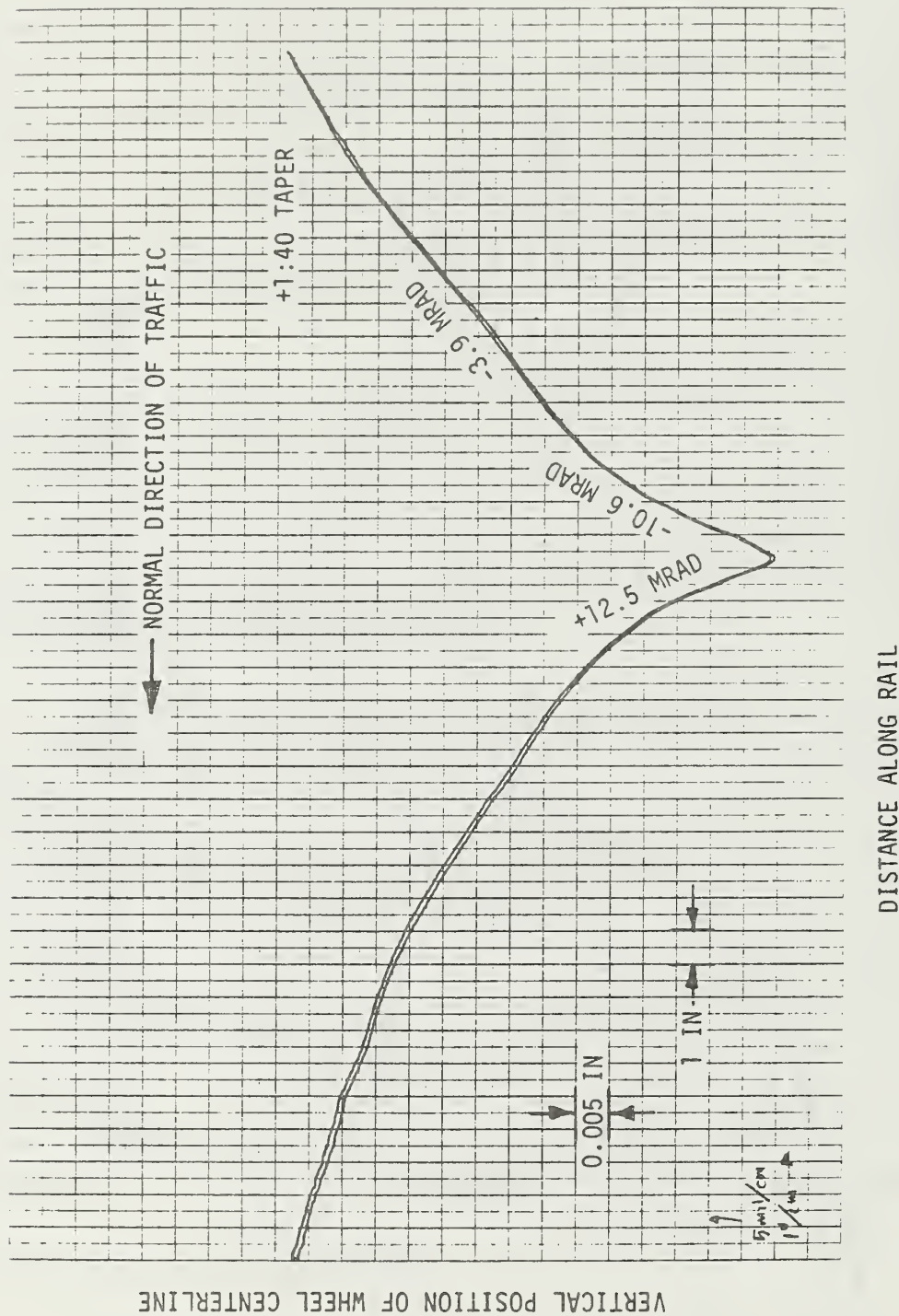


FIGURE 4-23. MEASURED RAIL RUNNING-SURFACE PROFILE NEAR ENGINE BURN, M.P. 66, SITE 1, SECTION 1, TIES 121/122, W. RAIL

AMCOACH ON NEC CONCRETE TIE TRACK, BATTERED ENGINE BURN

SITE #1, SECTION #1, TIE #121, WEST RAIL, MEASURED PROFILE

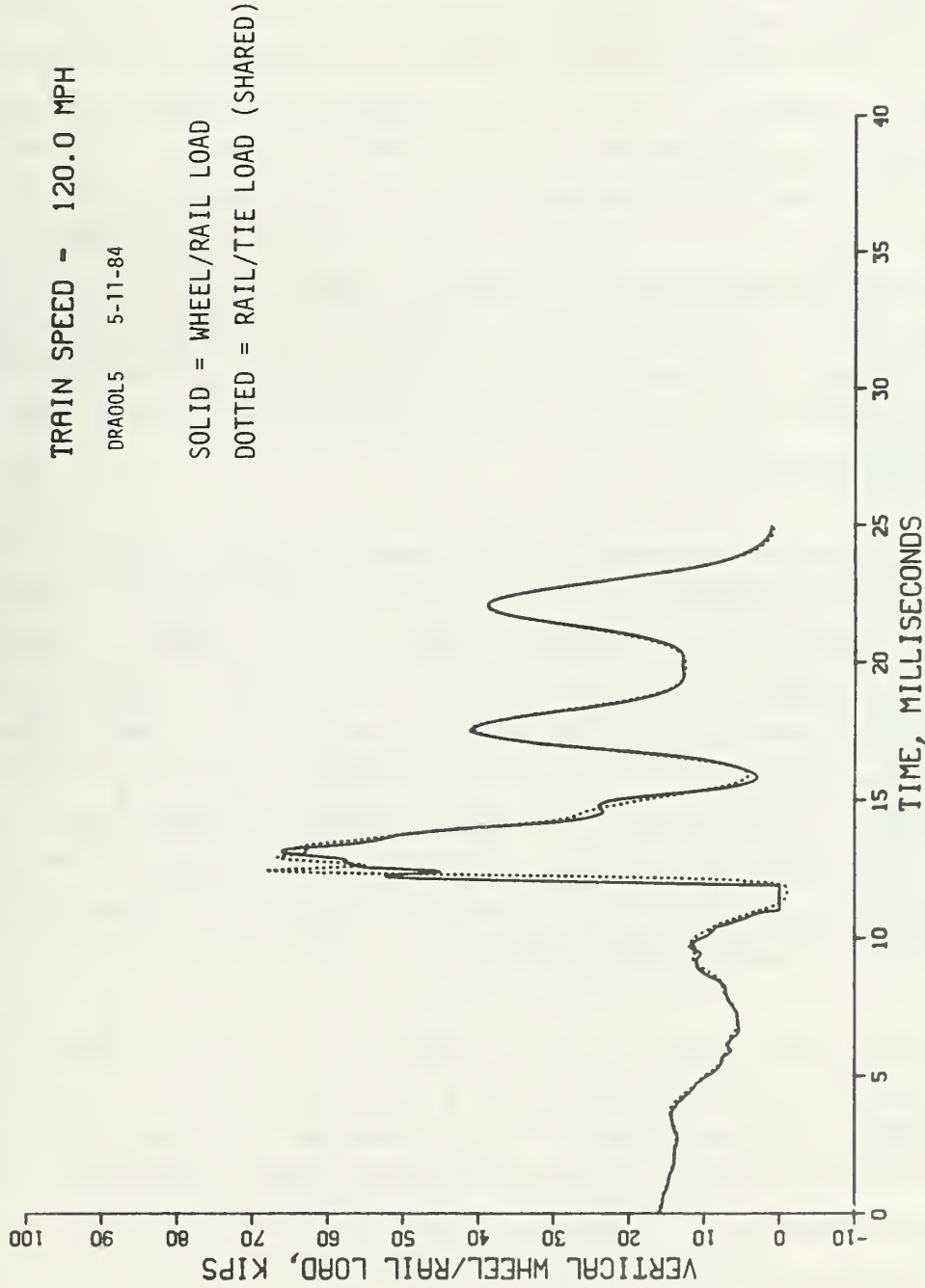


FIGURE 4-24. PREDICTED DYNAMIC VERTICAL WHEEL LOAD AT BATTERED ENGINE BURN UNDER HIGH-SPEED PASSENGER CAR

time of the impact test train runs using a straight edge and feeler gage. Time histories of vertical loads from Circuit #3 were recorded during the test train runs. The running-surface profile at the Edgewood location measured in April 1984 is shown in Figure 4-25. The ramp angle of the long wavelength dip into the site was quite modest at this time: less than 1 milliradian. The "burn" itself (there is no evidence of distress on the opposite rail) caused the wheel to drop .015 to .018 inch in a span of 6 to 7 inches. A gradual increase in the impact factor under Amcoach wheels -- from 1.71 to 1.83 -- was noted over the first eight months, indicating that the dip was increasing slowly in size as it battered out. Recent checks on passing high-speed passenger trains have shown the impact factor under Amfleet cars to have stabilized at about 1.84.

An example print-out from the impact detector is shown in Figure 4-26 for an AEM-7 locomotive and six Amfleet cars at 118 mph. The increased peak loads under the rail anomaly are seen in the Processor 3 column. Note that a wheel anomaly on Axle 24 impacted at Site 4 with a 38.8-kip peak wheel load. Typical time histories of vertical load under the newly-turned wheels of the impact test train -- Axle #11 on an Amcoach, Axle #17 on a Heritage car -- are shown in Figures 4-27 and 4-28. Modestly higher impact loads were recorded under the Heritage car wheelset, possibly due to the different effective wheel taper (and depth of anomaly) for the outside-bearing wheelset, versus the inside-bearing Amfleet wheelset.

Predicted loads from the impact model using the measured profile from Figure 4-25 are plotted in Figure 4-29 for the three train speeds of Figure 4-28. Predicted response for the measured 1:20 taper profile matches more closely the response of the Heritage car wheel, as shown in Table 4-3. It must be remembered in comparing Figures 4-28 and 4-29 that the measured load is captured only within the 8-inch influence zone of the rail circuit. Secondary load response oscillations of the "continuous" predicted load are therefore only present in the 20-mph run, where the measured load stays within the circuit influence zone for two complete oscillations. The rail surface anomaly is seen in Figure 4-25 to be battered smoother in the normal direction of traffic, with a sharper dropoff, but easier rise in this direction.

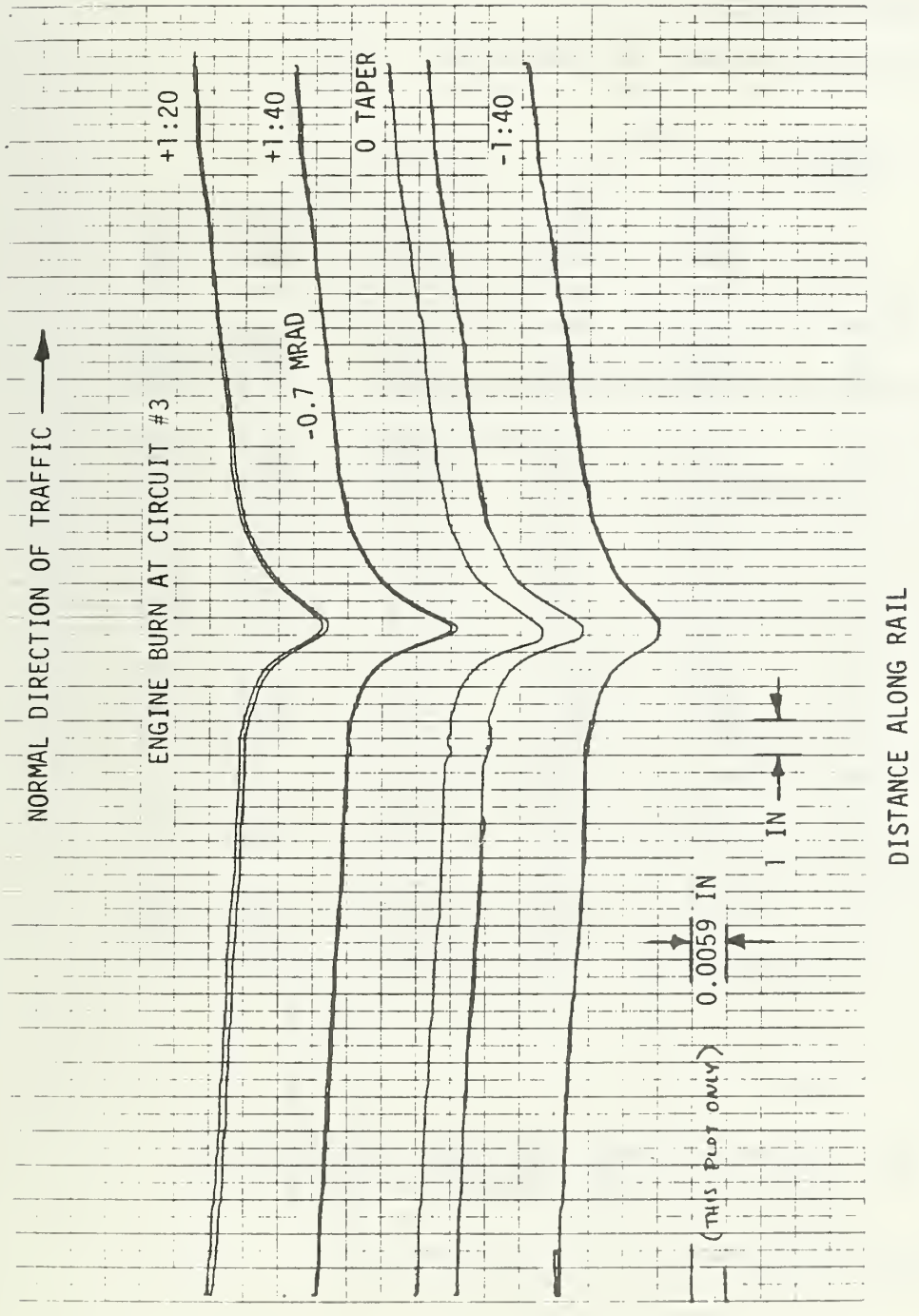


FIGURE 4-25. MEASURED RAIL RUNNING-SURFACE PROFILE AT ENGINE BURN, EDGEWOOD IMPACT DETECTOR CIRCUIT #3

ENTER OPTION
VTRAIN PASSED AT 09:33:26 84/03/09
SPEED = 118. AXLE COUNT = 28

GROUND TEMPERATURE = 32. BOX TEMPERATURE = 87.

AXLE NUMBER	CAR NUMBER	PROCESSOR			4
		1	2	3	
1	1	30.4	31.2	40.8	22.8 KIPS
2	1	27.6	24.0	37.2	24.8 KIPS
3	1	31.2	26.0	44.0	24.4 KIPS
4	1	27.2	29.6	57.2	24.0 KIPS
5	2	14.0	16.0	27.2	14.4 KIPS
6	2	13.2	14.0	31.6	16.8 KIPS
7	2	14.4	16.8	32.8	16.4 KIPS
8	2	14.4	14.8	34.4	18.8 KIPS
9	3	15.2	14.4	37.2	18.8 KIPS
10	3	24.4	23.6	35.6	24.0 KIPS
11	3	15.2	14.0	27.2	20.4 KIPS
12	3	19.2	16.4	32.4	19.2 KIPS
13	4	16.0	13.6	28.8	16.0 KIPS
14	4	15.2	16.8	29.6	14.8 KIPS
15	4	13.6	14.4	29.2	16.0 KIPS
16	4	14.0	16.4	29.6	18.0 KIPS
17	5	12.8	13.2	28.0	14.4 KIPS
18	5	13.2	14.8	30.0	19.6 KIPS
19	5	12.8	14.4	32.8	17.2 KIPS
20	5	24.0	14.0	31.2	17.6 KIPS
21	6	24.0	15.6	30.0	17.2 KIPS
22	6	13.2	15.2	31.6	18.0 KIPS
23	6	14.8	18.8	30.8	16.8 KIPS
24	6	14.4	14.8	31.2	38.8 KIPS
25	7	16.0	28.4	27.2	14.0 KIPS
26	7	16.4	13.2	30.8	30.4 KIPS
27	7	14.8	14.4	29.6	16.0 KIPS
28	7	13.6	15.6	26.4	16.4 KIPS

FIGURE 4-26. EXAMPLE OF LOADS FROM IMPACT DETECTOR SITE UNDER HIGH-SPEED PASSENGER TRAIN

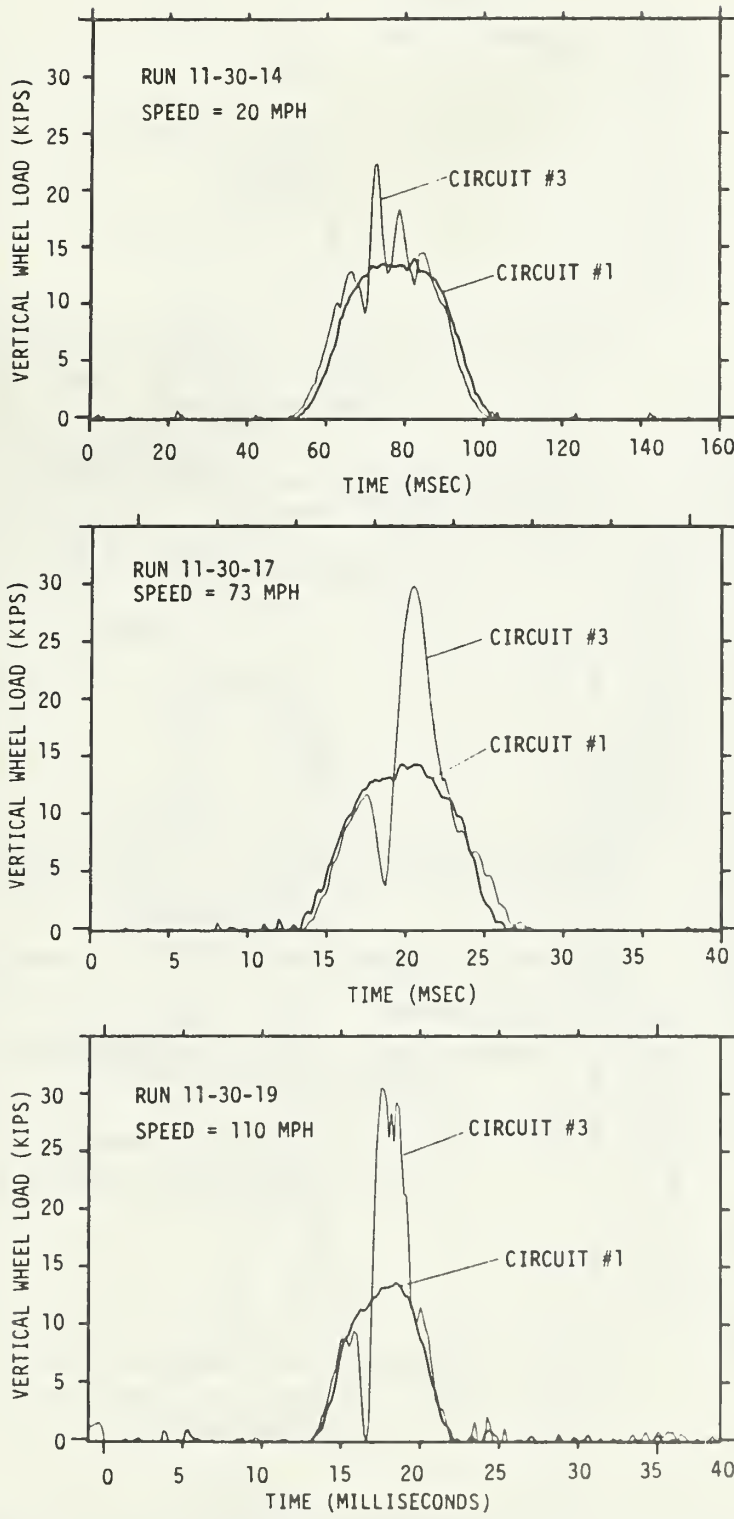


FIGURE 4-27. COMPARISON OF VERTICAL LOADS OVER SMOOTH TRACK (CIRCUIT #1) AND ENGINE BURN (CIRCUIT #3) -- AMCOACH AXLE #11, NEWLY-TURNED WHEEL PROFILES

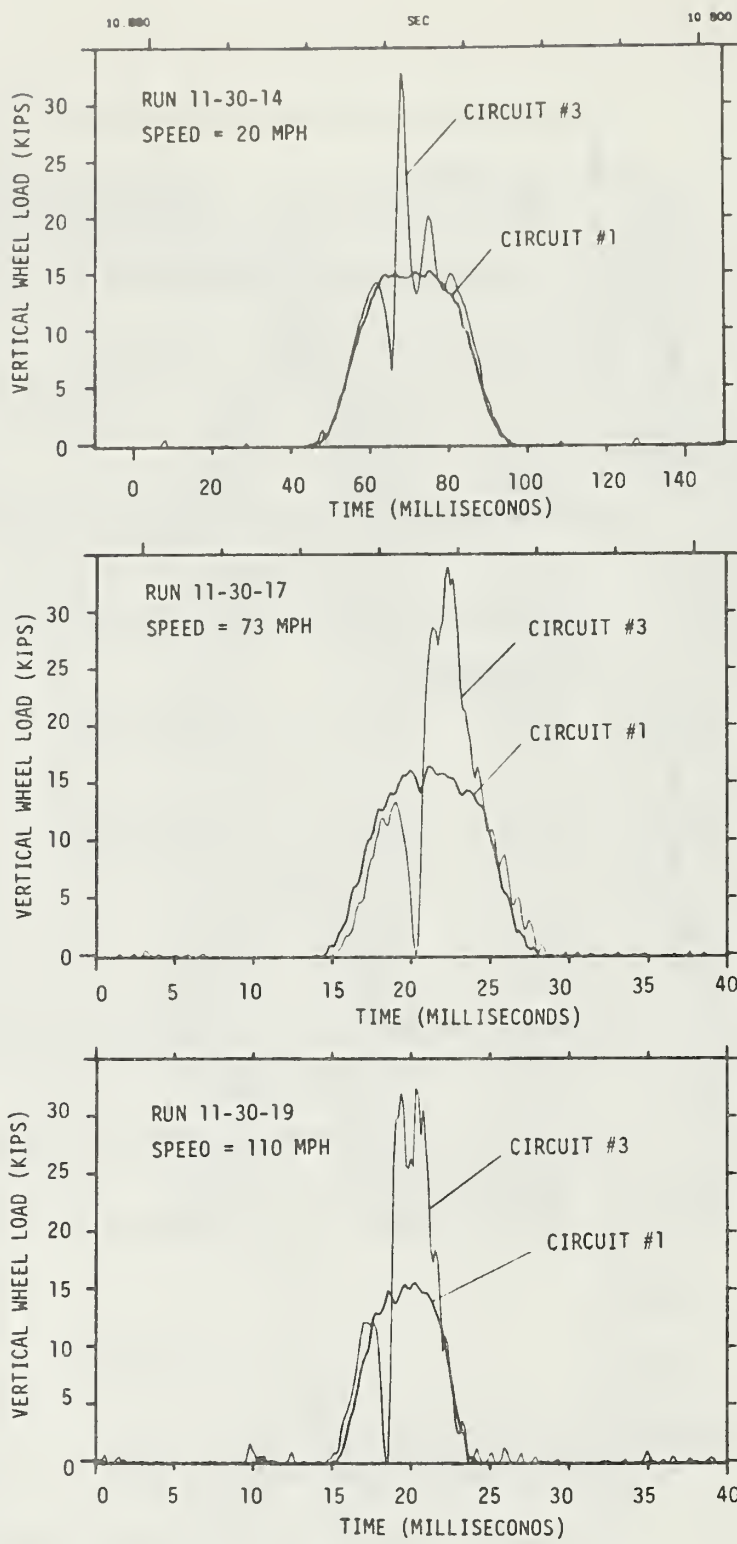


FIGURE 4-28. COMPARISON OF VERTICAL LOADS OVER SMOOTH TRACK (CIRCUIT #1) AND ENGINE BURN (CIRCUIT #3) -- HERITAGE CAR AXLE #17, NEWLY-TURNED WHEELS

SOLID = WHEEL/RAIL LOAD
DOTTED = RAIL/TIE LOAD (SHARED)

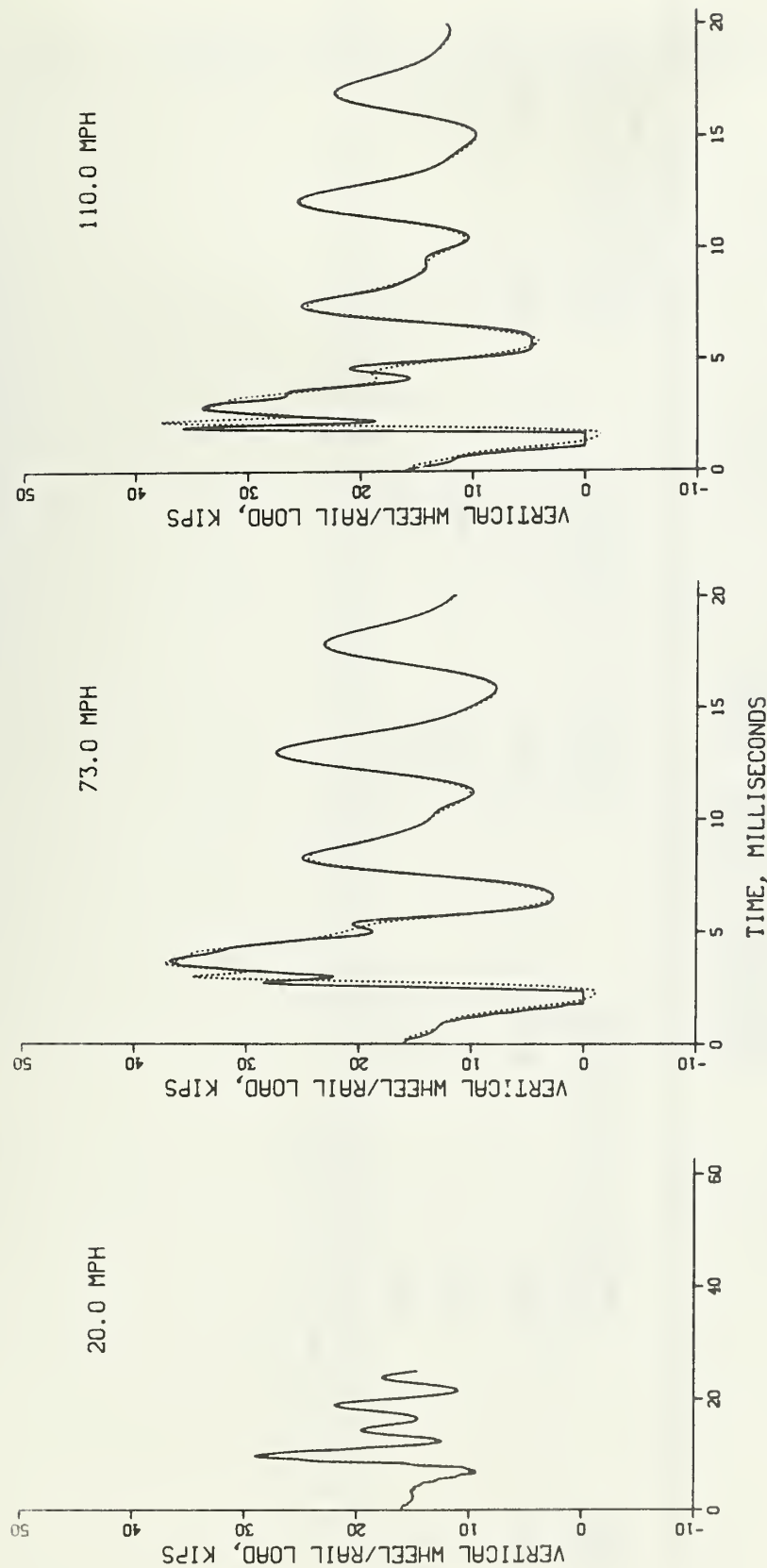


FIGURE 4-29. PREDICTED VERTICAL WHEEL LOADS FOR SIMULATED HIGH-SPEED PASSENGER CAR OVER MEASURED RAIL SURFACE ANOMALY AT EDGEWOOD IMPACT DETECTOR CIRCUIT #3

TABLE 4-3. COMPARISON OF MEASURED AND PREDICTED PEAK VERTICAL LOADS OVER
EDGEWOOD RAIL SURFACE ANOMALY

Speed (mph)	Measured Load (Kips) Amcoach	Predicted Load (Kips) Normal	Predicted Load (Kips) Reverse	Predicted Energy* Loss Per Wheel (ft-lb) Car	Predicted Energy* Loss Per Wheel (ft-lb) Track
20	22.0	32.8	29.0	29.3	6.5
73	29.9	34.1	36.9	38.9	7.3
110	30.7	32.5	35.8	48.4	4.3

* In normal direction of traffic.

Similar effects have been noted in the wheel profiles where cars are normally run in a preferred direction.

5.0 TRACK COMPONENT DYNAMIC PERFORMANCE

Wheel/rail impact loads occur over a brief time interval, typically less than three milliseconds, and contain energy over a wide frequency range. Thus the impacts will excite those structural components in the track which have natural frequencies of oscillation within that frequency range. The structural integrity of a track component can be influenced strongly by this response to wheel/rail impacts. Consequently, a static evaluation of a component is incomplete, and in many cases misleading. For example, the dynamic response of a concrete tie to impact loading can induce negative bending at the rail seat opposite the point of impact. This reaction is not obvious from static analysis or tests. Further, the fatigue life of a component may be much less than that predicted by considering only static or quasi-static loading conditions, depending on its natural frequencies and modal damping.

Recent track research has focused on the processes of track component deterioration due to wheel/rail impact load. The simplified flow chart shown in Figure 5-1 describes the dynamic nature of these processes. Control of component deterioration relies to a large extent upon detection, inspection, and repair of component damage, and on effective maintenance procedures. Without these controls, impact-induced component deterioration is an unstable feedback process. Of course, the amount of control which is required depends ultimately on cost-benefit trade-offs. This is established in the "feedback" portion of the two maintenance paths shown in Figure 5-1.

Extensive dynamic measurements were made in Battelle's mechanical engineering laboratory and on the Northeast Corridor under a wide range of loading conditions and for several combinations of track components. The results of these tests, in conjunction with the analytical models, were used to evaluate the relationships between track component dynamic behavior and tie cracking, rail clip movement and shoulder insert loosening. These experiments and analyses are described in the following sections.

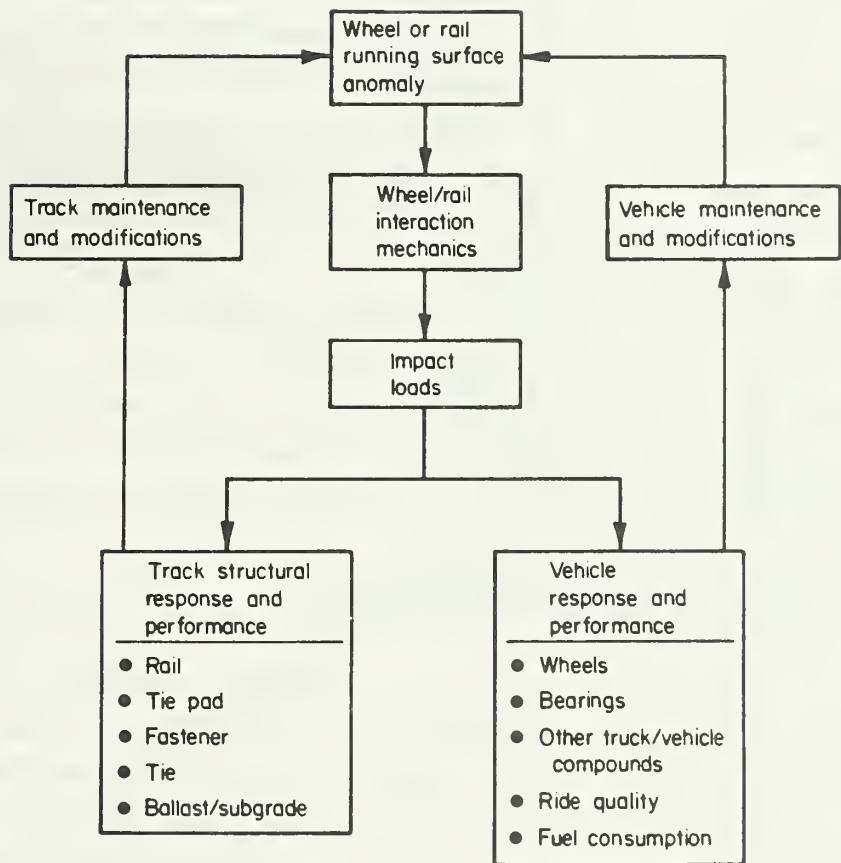


FIGURE 5-1. RELATIONSHIPS OF IMPACT LOADS WITHIN THE VEHICLE AND TRACK STRUCTURES

5.1 Track Structure Performance Experiments

Field tests were performed in November 1983 near Aberdeen and Edgewood, MD on the Northeast Corridor track. These tests involved instrumenting the tie, rail fastener, rail, and ballast. Strain gages were used to measure tie bending moment and wheel/rail vertical load, while non-contacting displacement transducers were used to measure fastener motions. Accelerometers were used on rail, tie, and a "ground rod" driven deep into the ballast to determine component accelerations and "transfer functions". The track response was measured under revenue traffic loading and under impacts from an automated drop hammer, which was designed to simulate moderate wheel/rail vertical impacts. Parameter variations included impact energy, fastener type, tie pad type, and different tie locations. Similar tests were performed in the laboratory on a 5-tie NEC track replica. The taped analog data were evaluated using Fast Fourier Transform (FFT) analyzers which computed transfer functions and frequency spectra for selected signals.

5.1.1 Impact Simulation With Drop Hammer

To provide a controlled, repeatable simulation of the impact force generated at the wheel/rail interface, a drop hammer was developed for laboratory testing [3]. For this study, the device was modified for use in the field, and for automatically impacting the track at rates of about 4 seconds per drop. This is shown in Figure 5-2. The pulse shape generated by the drop hammer is controlled by the mass of the hammer, the stiffness of the shim pad mounted behind the striking face, and the drop weight. In-track tests were performed to find a shim pad that would provide a representative input spectrum at a peak force level typical of a passenger-car wheel impact. For the 115-lb hammer, a 55-durometer neoprene pad of 0.38-inch (10 mm) thickness was found satisfactory. The performance of the drop hammer with this shim is shown in Figure 5-3 in comparison with a representative wheel impact load pulse. The hammer has been demonstrated to simulate with reasonable accuracy moderate wheel/rail impacts, i.e., those in the 40 to 60 kip range.

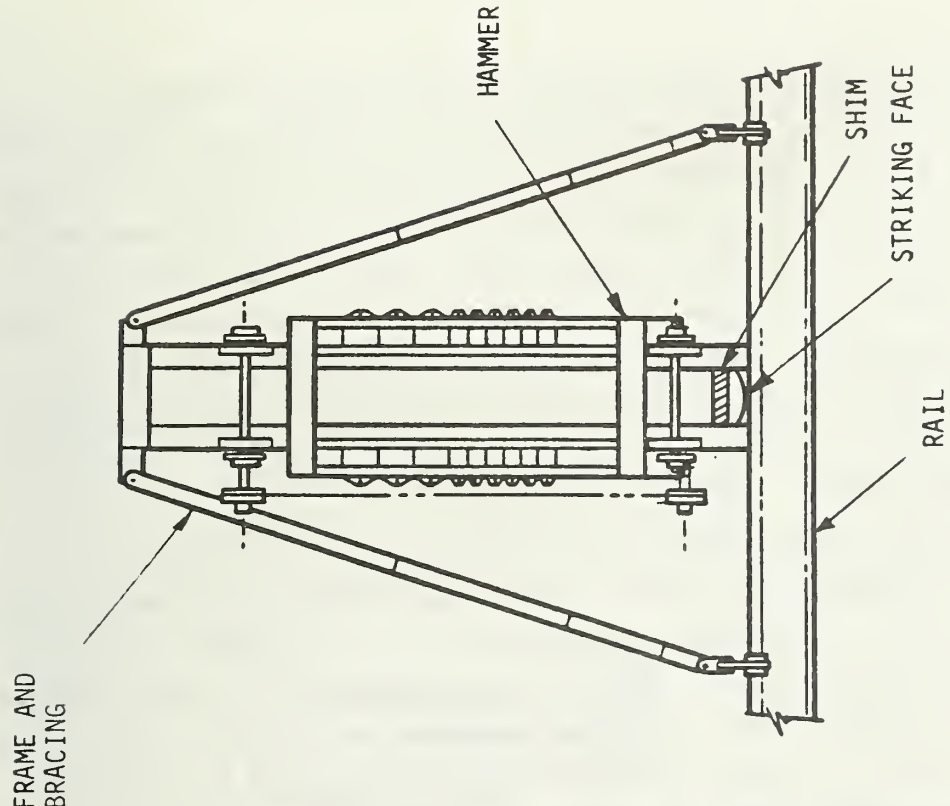


FIGURE 5-2. SKETCH OF AUTOMATED DROP HAMMER

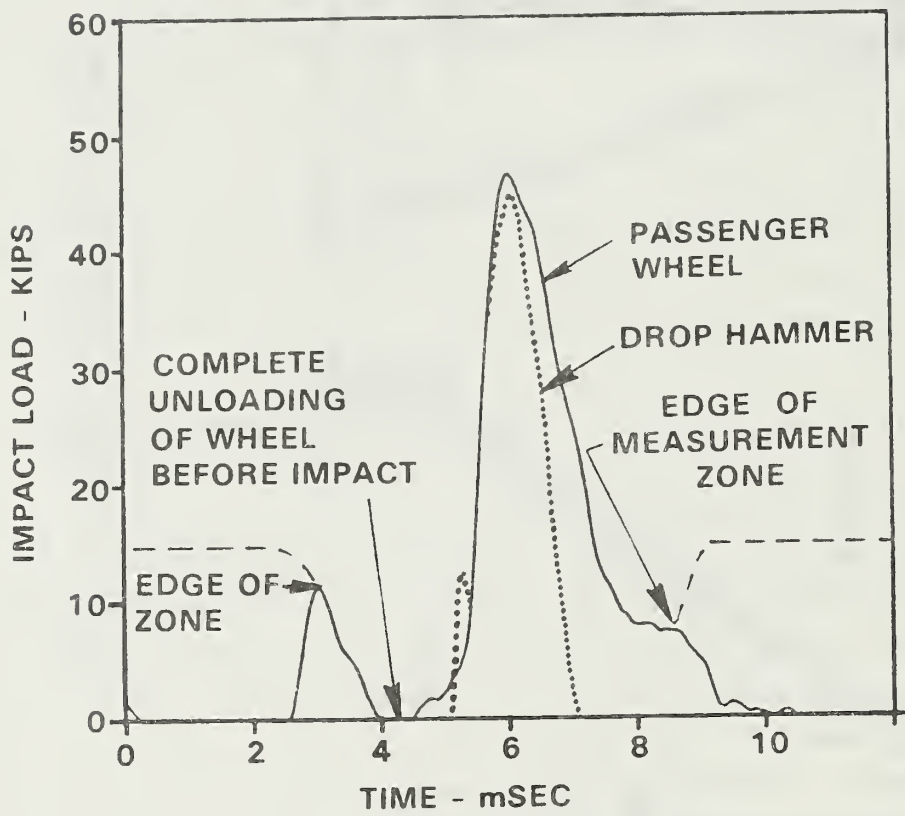


FIGURE 5-3. COMPARISON OF IMPACT LOAD TIME-HISTORIES FOR PASSENGER CAR WHEEL AND DROP HAMMER

Spectral energy from this drop hammer configuration is concentrated below 1500 Hz and falls to that point monotonically from a maximum in the 100-200 Hz range. This produces dynamic responses in track components which are representative of those measured under actual wheel impact loads. The adequate simulation of more severe impacts, particularly those sufficient to crack ties, would require a different shim pad design. The drop weight with the nominal shim pad could not cause tie cracking at the nominal drop heights of 18-22 inches, and the shim deteriorated rapidly for drops from above 22 inches.

Some of the field tests with the drop hammer on the NEC track were done adjacent to a loaded hopper car. The nearest wheelset of this car could be moved to within two ties of the hammer impact point. Thus, the preload on the track panel was varied by changing the location of the car. Peak impact loads for preloaded track were consistently higher than for unloaded track. For example, an 18-inch drop produced peak loads 3 to 5 kips higher for the maximum preload configuration. In contrast, the effect of preload on tie bending strain was to decrease the tie response, particularly in the first three tie bending modes, as shown in Figure 5-4.

Successive drops with the hammer produced decreasing peak impact loads under field conditions. After 12 drops, peak load decreased by roughly 10 percent. This may have been exaggerated by the cold ambient temperatures and the change in pad characteristics with absorbed energy from a sequence of drops.

5.1.2 Laboratory Simulation of Track Impact Dynamics

Since the drop hammer simulated wheel/rail impacts adequately, it was possible to perform controlled tests in the laboratory. Laboratory tests were performed on both single-tie and 5-tie mock-ups of NEC concrete tie track. The primary purpose of the single-tie tests [3] was to evaluate the dynamic behavior of various track components, such as tie pads, rail clips and ties. The 5-tie laboratory track was developed to investigate the sources and

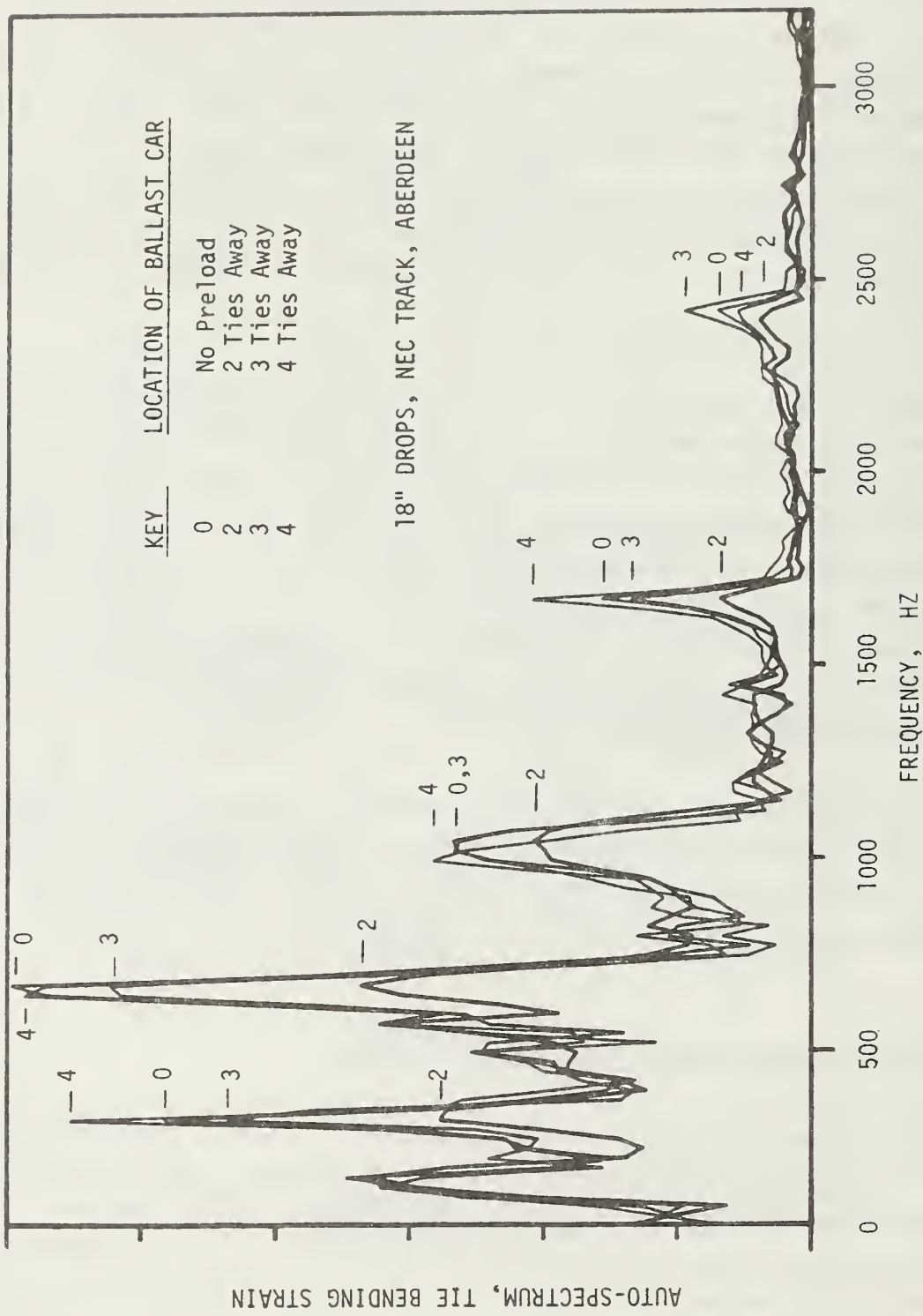


FIGURE 5-4. INFLUENCE OF WHEEL VERTICAL PRELOAD
ON RAIL-SEAT TIE BENDING STRAIN

mechanisms for track damage such as tie cracking, insert loosening and clip fallouts, where a finite span of rail was necessary for proper simulation.

The value of the laboratory track as a research tool depends on how well the laboratory results match the field results for similar test conditions. Consequently, tests were performed both in the field on NEC track and in the laboratory on the track panel to determine the range of validity and limitations of the simulation. Time histories of tie bending moment under the rail seat are shown in Figure 5-5 for similar impact tests with the drop hammer on NEC track (a) and on the 5-tie track panel (b). The frequency content of the impacted tie response was evaluated for several test conditions and was found to be similar. The largest differences between the field and laboratory data were found at the second tie bending natural frequency (about 330 Hz), where the spectral amplitude of response in laboratory tests was about twice that from field tests. These differences may be caused by the tie support conditions, which in the laboratory consisted of neoprene strips between the ties and the building floor, rather than a ballast section.

Comparisons of peak amplitudes of tie bending response from the field tests and laboratory tests over a range of drop heights are shown in Figure 5-6. Results from the NEC and 5-tie track tests show close agreement for heights from 10 to 22 inches, using a 3/8-inch neoprene drop hammer shim pad. Results from the 5-tie track panel are also compared with single-tie tests from previous experiments [3], using a 6.5 mm shim pad. Both laboratory simulations appear to be suitable for evaluating certain types of track component performance. The differences in frequency content of tie bending response, particularly at the second tie bending mode, may be reduced by adjusting the support conditions of the ties as appropriate.

5.2 Results of Experiments

The results of the experimental work conducted during this program are discussed below for three track component categories. These are (1) tie/tie pad, (2) shoulder insert, and (3) rail fastener (clip/insulator). The structural performance issues experienced in the NEC track related to each

COMPARISON OF TIE DYNAMIC RESPONSE UNDER RAIL SEAT

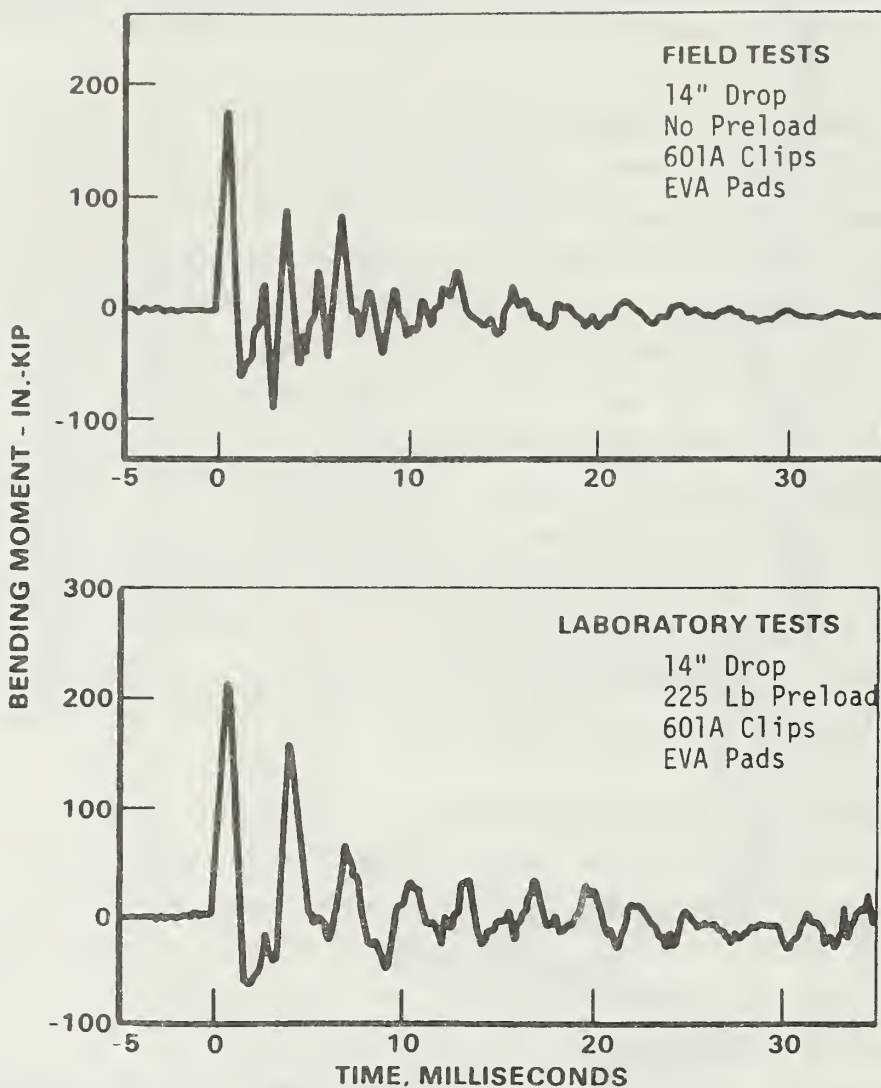


FIGURE 5-5. COMPARISON OF TIE DYNAMIC BENDING RESPONSE
BENEATH RAIL SEAT, NEC VERSUS 5-TIE TRACK

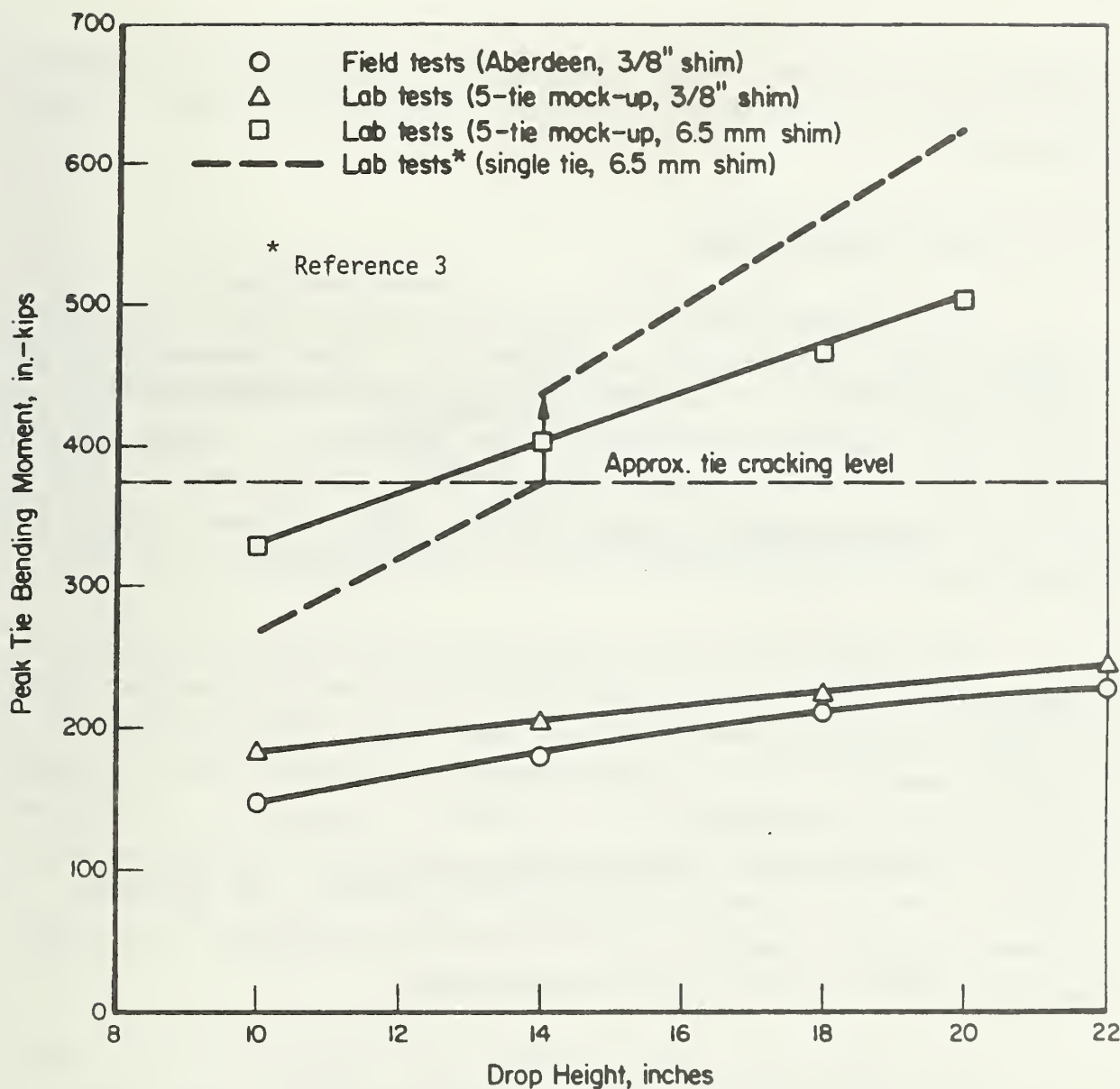


FIGURE 5-6. INFLUENCE OF HAMMER DROP HEIGHT ON PEAK TIE BENDING MOMENT UNDER RAIL SEAT FOR DIFFERENT TEST CONDITIONS

component are described. Examples of dynamic measurements of the component impact response are presented and evaluated in the context of track structural performance.

5.2.1 Tie/Tie Pad Performance

As discussed previously, wheel/rail vertical impact loads have a pronounced effect on concrete tie performance and life. Cracks in the rail seat and insert areas, and loss of insert-to-tie bond have been attributed to impact loads. Typical tie failures are shown in Figure 5-7. Dynamic analyses of the concrete tie have defined the important transverse bending modes of vibration that are strongly excited by impacts. These are shown in Figure 5-8 along with typical frequency spectra for stiff and resilient rail seat pads.

The second and third bending modes, at about 333 and 633 Hz, respectively, for the test tie are particularly important because strain amplitudes are near-maximum in the rail seat region. Phase relationship of frequency components of the transient response is critical, since the second vibration mode is asymmetrical, and the third is symmetrical: if response peaks to an impact fall in-phase, high, crack-initiating strains can be produced in the outer fibers of the tie at the bottom or the top surface. A rail-seat crack may consequently occur on the tie end opposite a single impact load, for example at a rail joint or battered weld.

The primary load path into the tie for wheel/rail vertical impact loads is through the rail-seat tie pads. Consequently, the dynamic characteristics of the tie pad are critical to tie performance. The first tie pad used on the NEC was an ethylene vinyl acetate (EVA) pad of high stiffness: about 5,000 kip/in secant stiffness over a typical range of wheel loads. The selection of this pad was made on the assumption that an effectively rigid pad would reduce clip deflections. This assumption did not prove correct.

It was evident from the earlier investigation [3,4] that a reduction in tie pad stiffness can reduce significantly the levels of tie strain due to impact loads by reducing the peak force transmitted to the tie. This is not

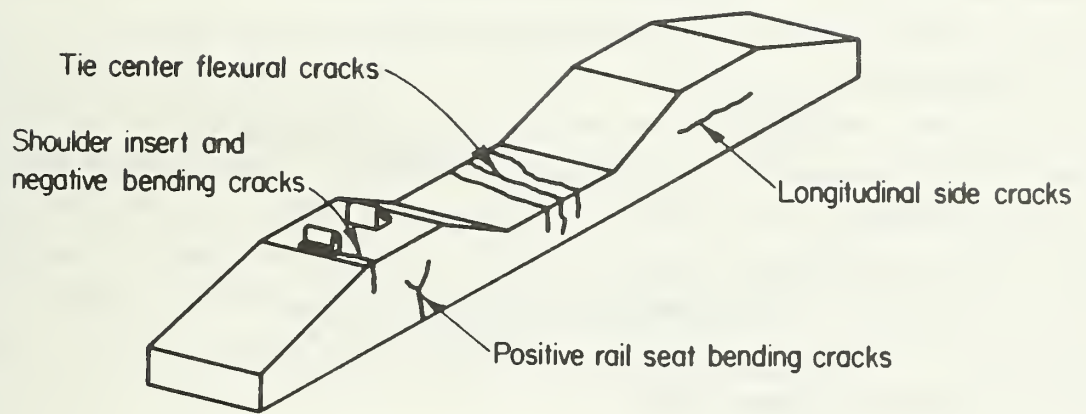


FIGURE 5-7. TYPICAL FLEXURAL CRACKS FOUND IN CONCRETE TIES

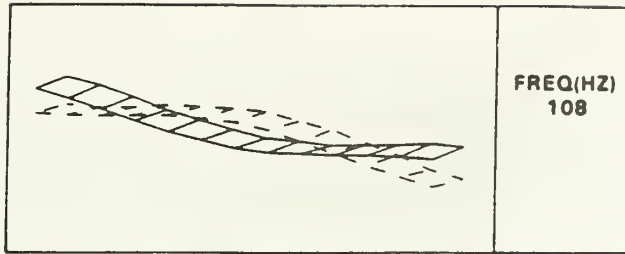
obvious from a static analysis because over the range of existing tie pad stiffness there is no significant effect on the load distribution to adjacent ties. However, the pad acts dynamically as a low-pass filter, and the filter characteristics of the pad are the key to tie performance. A desirable filter characteristic is a "break frequency" low enough to attenuate most of the energy at the second and third tie bending modes. An example of this filtering characteristic is evident in Figure 5-8, where the tie bending response with the more resilient 6.5 mm pads (with a secant stiffness typically below 1000 kip/in) is compared with the stiff EVA pad. These results are from the recent experiments on the NEC. Bending-moment time histories for these two pads from in-track drop tests are shown in Figure 5-9, where a marked reduction in the peak bending moment is seen with the resilient pad. A similar reduction in ground rod (ballast vertical) acceleration for the same drop tests is shown in Figure 5-10.

Therefore, the use of a properly-designed resilient tie pad will reduce the probability of tie cracking, and will reduce the impact load energy transferred to other track components, such as fasteners and ballast.

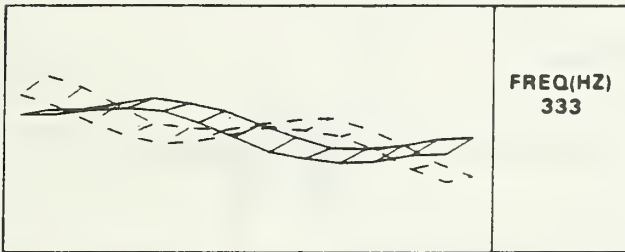
5.2.2 Rail Fastener Performance

The rail fastening system used on the NEC concrete tie track consists of a steel spring clip driven into a shoulder/insert, which is cast into the concrete tie. Plastic insulators center the rail base within the fastener inserts. The spring clip, when new, preloads the rail base to 2000-3000 lb per clip. This "toe load" provides a longitudinal restraint of about 2500 lb per rail, per tie, depending on pad characteristics and friction coefficient.

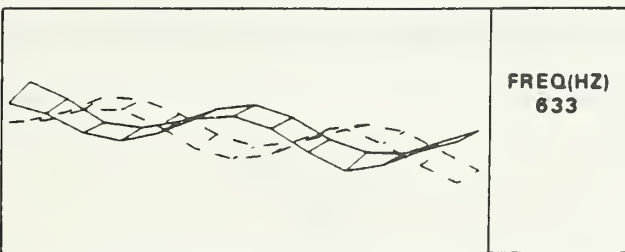
For the current design (the Pandrol 601A clip), progressive clip movement out of the insert is resisted only by the frictional forces at the clip/rail and clip/insert interfaces. Clip relative movement will occur when the net static and dynamic forces on the clip exceed the friction "breakout" levels. Fluctuations in vertical preload occur in response to wheel/rail loads. For wheel/rail impact loading, the dynamic motions of the clip and tie may be sufficient to cause large momentary reductions in preload, which in



(A) FIRST BENDING MODE RESPONSE

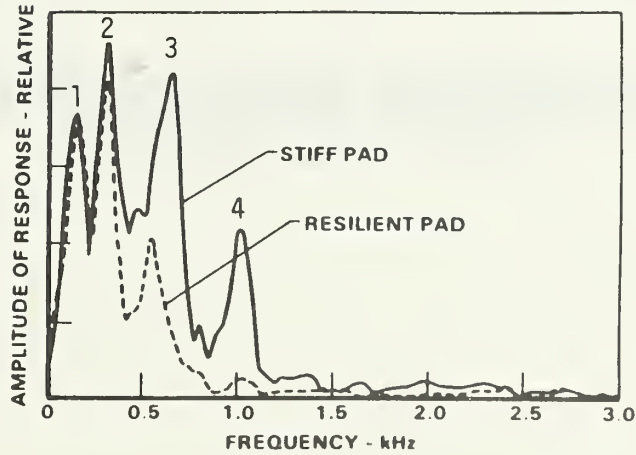


(B) SECOND BENDING MODE RESPONSE



(C) THIRD BENDING MODE RESPONSE

(A) SAMPLES OF FIRST THREE BENDING MODES
FOR CC-244-C CONCRETE TIE



(B) TIE BENDING RESPONSE AT RAIL SEAT

FIGURE 5-8. ATTENUATION OF TIE BENDING RESPONSE TO IMPACT LOADING
WITH RESILIENT RAIL-SEAT TIE PAD

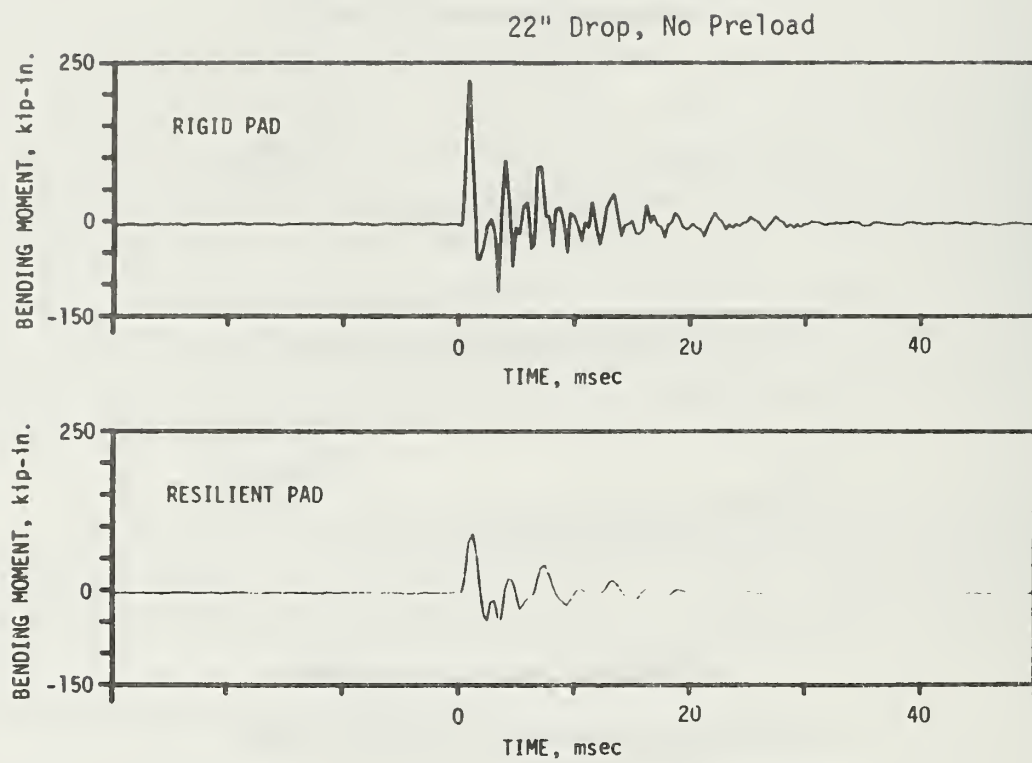


FIGURE 5-9. TIE BENDING RESPONSE TO IN-TRACK DROP TESTS WITH STIFF EVA PADS AND RESILIENT (DAYCO) TIE PADS

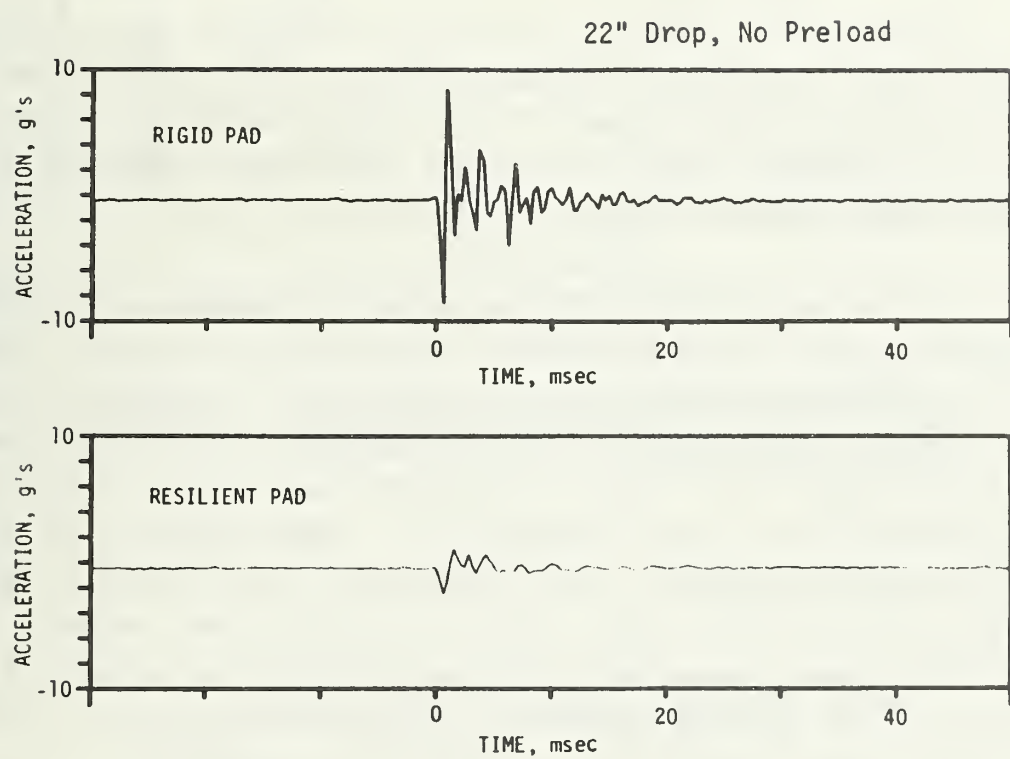


FIGURE 5-10. GROUND ROD VERTICAL ACCELERATION RESPONSE TO IN-TRACK DROP TESTS WITH STIFF EVA TIE PADS AND RESILIENT (DAYCO) TIE PADS

turn may cause incremental movement of the clip out of the shoulder. Clip fallout therefore could result from repeated impact loads or from the high vibration levels of rail and tie under traffic.

A series of laboratory and field experiments was performed to investigate the clip fallout phenomenon. The laboratory tests included modal vibration testing on free clips and repeated impact tests on the 5-tie track section. Field tests on the NEC included hammer impact tests as well as measurements under revenue traffic.

The tie pad influences the clip deflection response by its effect on the relative vertical and rocking motions between the rail and tie. Measurements of clip deflection response under revenue traffic loading have indicated that rail rocking displacements are smaller with the resilient pads than with the very stiff pads [3]. Similar measurements made under simulated impact loading conditions are shown in Figure 5-11. These results show that the clips are loaded more severely with the effectively rigid EVA pad. Although the initial "peak-to-peak" clip vertical deflections are comparable (about 0.030 to 0.035 inch), the maximum clip spreading deflection due to rail uplift relative to the tie is about 40 percent less with the resilient pad than with the stiff EVA pad. The reduction in preload corresponding to the maximum initial depression of the pad is, however, about 50 percent greater with the resilient pad.

From the standpoint of clip performance, the differences in clip spreading deflections (which correspond to the highest clip stresses) for stiff and resilient pads may be more important than the differences in preload reduction. On both the stiff and resilient pads, the maximum measured pad depressions represent a preload reduction of less than 5 percent of the nominal toe load. Thus, the tendency for clip movement longitudinally due to momentary reductions in preload may be similar for both pads. It should be noted, however, that tests on NEC track with 5 mm thick resilient pads (versus the recommended 6.5 mm pad) did produce excessive tie skewing, confirming some loss in toe load. Previous tests on the Type "A" clips have measured static strains of up to 10,000 microstrain in tension after installation.

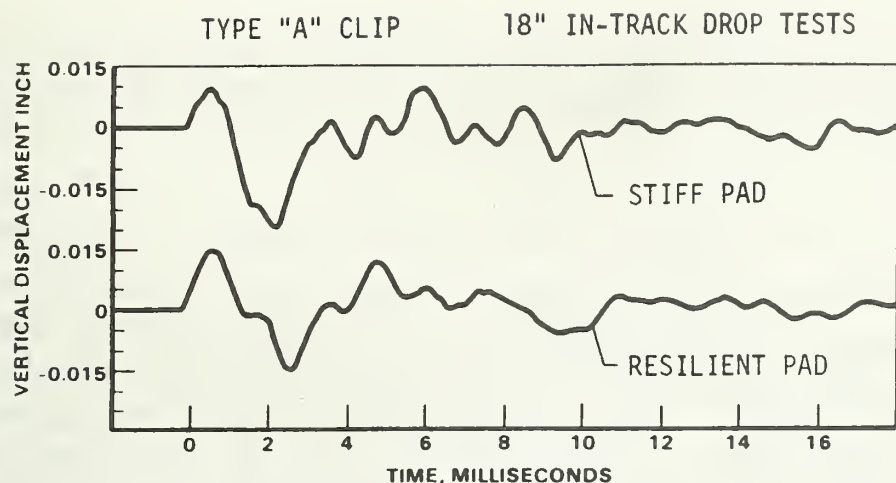


FIGURE 5-11. COMPARISON OF CLIP (TOE) VERTICAL DISPLACEMENTS WITH STIFF EVA AND RESILIENT TIE PADS

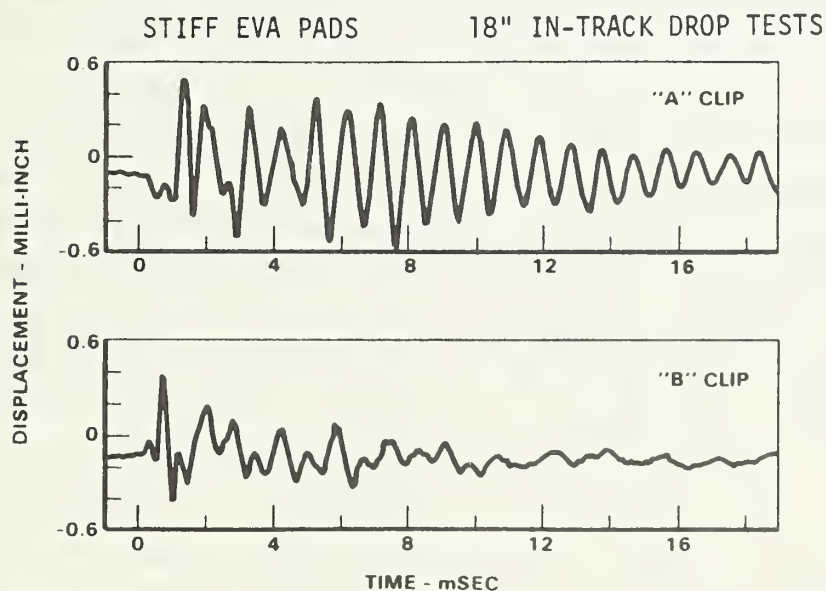


FIGURE 5-12. COMPARISON OF CLIP LONGITUDINAL DISPLACEMENT AT CENTER LEG FOR TWO CLIP DESIGNS

Consequently, the larger clip spreading deflections experienced with the stiff pads may result in plastic deformation, loss of toe load and reduced fatigue life.

The vertical motions of the Type "B" (Pandrol E) clip were similar to those of the Type "A" clip shown in Figure 5-11. For example, with a resilient pad and an 18-inch hammer drop, the Type "A" clip toe motions were ± 0.015 inch, while the Type "B" clip toe motions were +0.013 (unloading), -0.008 inch (loading). These results reflect the relatively low clip stiffness, either type, when compared to the high pad stiffness. Clip stiffness has a small effect on initial pad compression, but controls rail uplift when the pad is unloaded.

Comparison of the laboratory and field tests show that under impact loading, the clips respond strongly to the tie dynamics, particularly at the frequencies near the third and fourth tie bending modes (630 and 1000 Hz, respectively). Further, clip resonant conditions in the 800-2000 Hz range are also excited and influence response in the longitudinal axis of clip fallout movement. Typical time histories of clip longitudinal displacements are shown in Figure 5-12 for two clip designs. Type "A" (the Pandrol 601A) is used predominantly in the current NEC concrete tie track (see Section 3) and has experienced some fallouts and fracture occurrences. Type "B" (the Pandrol E clip) is a somewhat stiffer design, providing about 14 percent more preload. A number of these clips have been installed on the NEC, and no failures have been reported to date. As shown in Figure 5-12, the dynamic behavior of these two clips is strikingly different in the longitudinal (fallout) direction. The longitudinal displacements of Type "A" at the clip-shoulder interface (parallel to the rail) consist of a strong "ringing" oscillation at about 1050 Hz, which is near the fourth tie bending mode and in the range of clip resonant frequencies measured in the laboratory. In contrast, the impact response of Type "B" involves a more highly-damped, broad-band characteristic, with no evidence of the "ringing" measured with Type "A".

Modal vibration tests on several Type "A" clips showed that clip installed position (i.e., over-driven versus under-driven) has a strong

influence on the clip natural frequencies. Modest variations in the installed position may tune or detune the clip natural frequencies from those of the tie, and consequently increase or decrease the probability of clip fallout motion. From these tests, clip natural frequency was observed to increase by roughly 20 percent as it was driven further into the insert.

Test results indicate that the dynamic characteristics of the rail clip may influence its tendency to move out of the insert. Therefore, clip dynamics should be an important consideration in track design, along with the fastener response to nominal wheel loads (particularly on curved track). From the standpoint of clip fallout, the Type "B" clip dynamics are more desirable than the Type "A", since its natural frequencies are more highly damped and not strongly coupled to tie natural frequencies. It should be noted that in none of the field or laboratory tests was clip migration actually measured or observed. Thus, the precise mechanism of clip fallout has not been determined for a repeatable set of conditions. However, it seems reasonable to project that clip fallout results from a combination of several factors, including (1) clip and insert manufacturing tolerances, (2) high track vibration levels from rail surface or passing wheel roughness, and (3) the dynamic response of the clip to tie or rail vibrations at closely-coupled natural frequencies.

5.2.3 Shoulder/Insert Performance

A series of tests was performed to explore the cause of bond loss between the cast-in fastener insert and the tie shoulder. Although the tests have not fully identified the failure mechanisms, observations and test results indicate that insert loosening can be caused by vertical impact loads of a magnitude less than that necessary to crack the tie. Observations of field damage and laboratory impact load tests imply that perhaps 100,000 impacts of moderate amplitude are necessary to cause gross insert looseness.

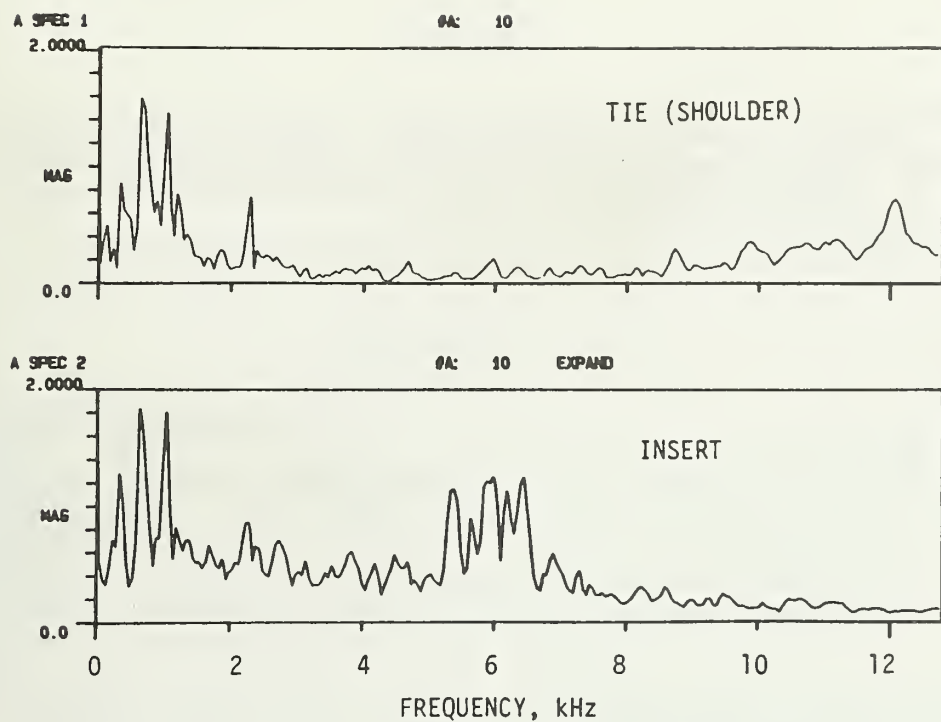
The 5-tie laboratory track was used for repeated impact load tests to explore the insert bond loss phenomenon. Drop hammer tests were conducted as summarized below:

<u>Drop Height, Inches</u>	<u>Hammer Shim Pad</u>	<u>Percentage of Tie Cracking Level</u>	<u>No. Drops</u>
12	3/8" Neoprene	52	9,500
14	3/8" Neoprene	55	5,900
18	6.5mm Ribbed Tie Pad	124	3,250
20	3/8" Neoprene	61	13,200
22	3/8" Neoprene	64	3,250
24	3/8" Neoprene	67	<u>7,900</u>
		Total:	43,000 drops

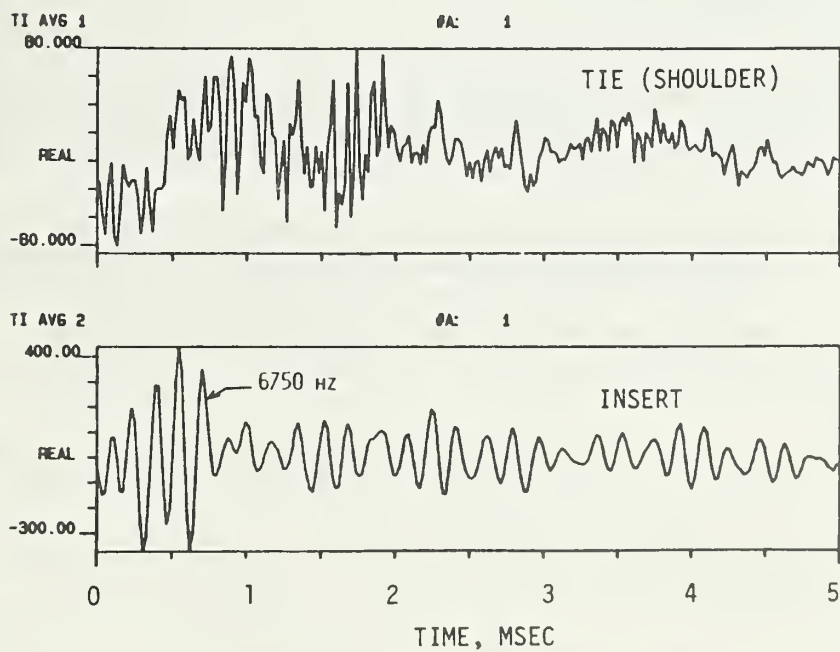
No visible damage was detected in the laboratory track during the course of this experiment. However, within the first 2000 drops (at 12 inches) some white powder was observed around the perimeter of the insert/tie shoulder interface on both the gauge and field-side inserts at the impacted rail. No additional powder accumulated after this point.

Vibration analyses of insert response to rail impact loading have shown that the insert has several modes of axial vibration (vertically oriented in the tie) in the 4 to 8 kHz frequency range. Vertical acceleration spectra for the tie surface (shoulder) and the insert are compared in Figure 5-13, where a strong response is seen at the insert between 5 and 7 Hz, but little corresponding spectral input is seen at the tie surface. These vibrations have a different "signature" for inserts on the same tie, or on different ties. Analyses of the insert design show that longitudinal compression waves will oscillate within this frequency range if the insert is either partially or totally constrained. (There are many locations within the insert that can cause reflections, which complicates the analysis.) A fully unconstrained insert will ring strongly at about 11 kHz: this has been demonstrated both analytically and experimentally.

Although insert damage was not produced in the laboratory tests, the test measurements indicate that loss of bond may occur due to the effects of high-frequency longitudinal compression waves in the insert, excited by nearby impact loads. While the amplitudes at the steel-to-concrete interface are quite small, a microscopic pulverizing action may take place that over time



(a) AUTO-SPECTRA OF VERTICAL ACCELERATIONS



(b) TIME-HISTORIES OF VERTICAL ACCELERATIONS

FIGURE 5-13. COMPARISON OF INSERT AND TIE (SHOULDER) VERTICAL ACCELERATIONS FROM IN-TRACK DROP HAMMER TESTS (STIFF EVA PADS)

will result in gross loosening of the insert. Again, the more resilient tie pad with its low-pass filter characteristic will reduce the impact energy transferred to the tie, and in turn the excitation to the insert.

5.3 Conclusions

Based on the results of these field and laboratory experiments, the following conclusions can be stated on track component dynamic performance:

- (1) Concrete tie track performance is strongly associated with the ability to withstand impact loads. Proper track design should therefore include dynamic analyses to optimize its performance.
- (2) Laboratory evaluation of track components can be accomplished with the aid of a drop hammer that simulates the magnitude and frequency content of the impact loads found in revenue service.
- (3) Component dynamic behavior should be evaluated to assure that no undesirable matching of responses takes place between components.
- (4) A dynamically optimized track structure must still withstand the abuse of the largest impact loads actually found in service. An economic trade-off exists between building stronger (and more expensive) track and maintaining wheel and rail running surface profiles in a more ideal geometric condition.
- (5) Dynamic performance (i.e., impact load response) of vehicle and track components other than concrete ties are not well known. There are ample economic reasons for needing to understand how these other components react to impact loading.

REFERENCES

1. Tuten, J. M., "Analysis of Dynamic Loads and Concrete Tie Strain From the Northeast Corridor Track", Technical Memo by Battelle's Columbus Laboratories to the Federal Railroad Administration, Improved Track Structures Research Division, Contract DOT-FR-9162, May 1981.
2. Harrison, H. and Moody, H., "Correlation Analysis of Concrete Cross Tie Track Performance", Proceedings, Second International Heavy Haul Railway Conference, Sept. 1982, Paper 82-HH-39, pp. 425-431.
3. Dean, F. E., et al, "Investigation of the Effects of Tie Pad Stiffness on the Impact Loading of Concrete Ties in the Northeast Corridor", Report No. FRA/ORD-83/05, April 1983.
4. Dean, F. E., et al, "Effect of Tie Pad Stiffness on the Impact Loading of Concrete Ties", Proc., Second International Heavy Haul Railway Conference, Sept. 1982, Paper 82-HH-41, pp. 442-458.
5. Tuten, J. M. and Harrison, H. D., "Design, Validation and Application of a Monitoring Device for Measuring Dynamic Wheel/Rail Loads", ASME Technical Paper, 1984 Winter Annual Meeting.
6. Harrison, H. D., et al, "Correlation of Concrete Tie Track Performance in Revenue Service and at the Facility for Accelerated Service Testing", Volume I A Detailed Summary, Report No. DOT/FRA/ORD-84/02.1, Final Report, August 1984.
7. Sato, Y. and Kosuge, S., "Evaluation of Rail Head Surface Configuration Viewed from Wheel Load Variation", Quarterly Reports (RTRI), Vol. 24, No. 2, 1983, pp. 68-71.
8. Newton, S. G. and Clark, R. A., "An Investigation into the Dynamic Effects on the Track of Wheelflats on Railway Vehicles", Journal Mechanical Engineering Science, IMechE, Vol. 21, No. 4, 1979, pp. 287-297.
9. Mair, R. I., "Aspects of Railroad Track Dynamics (Part I: Vertical Response)", BHP Melbourne Research Labs, Report MRL 81/3 (BHPMNM/RDC/74/017), Feb. 1974.
10. Mair, R. I., "Natural Frequency of Rail Track and Its Relationship to Rail Corrugation", Civil Engineering Transactions 1977, Inst. of Engineers, Australia, pp. 6-11.
11. Ahlbeck, D. R., "An Investigation of Impact Loads Due to Wheel Flats and Rail Joints", ASME Paper 80-WA/RT-1, 1980.
12. Jenkins, H. H., et al, "The Effect of Track and Vehicle Parameters on Wheel/Rail Vertical Dynamic Forces", Railway Engineering Journal, Vol. 3, No. 1, Jan. 1974, pp. 2-26.
13. Ahlbeck, D. R., et al "Measurements of Wheel/Rail Loads on Class 5 Track", Report No. FRA/ORD-80/19, Feb. 1980.
14. Mullen, J. D., "Rail Profile Irregularities - a study of their effects on concrete sleepered track and their removal", Proc. 5th Int. Rail Track Conference, Sept. 12-18, 1983, Newcastle, NSW, Australia.

